

AN ABSTRACT OF THE THESIS OF

Suzan M. Fadel for the degree of Doctor of Philosophy
in Civil Engineering presented on September 25, 1998.

Title: Application of the Generalized Melnikov Method to
 Weakly Damped Parametrically Excited Cross Waves
 with Surface Tension

Redacted for Privacy

Abstract approved: _ ,

Robert T. Hudspeth

The Wiggins-Holmes extension of the generalized Melnikov method (GMM) is applied to weakly damped parametrically excited cross waves with surface tension in a long rectangular wave channel in order to determine if these cross waves are chaotic. The Lagrangian density function for surface waves with surface tension is simplified by transforming the volume integrals to surface integrals and by subtracting the zero variation integrals. The Lagrangian is written in terms of the three generalized coordinates (or, equivalently the three degrees of freedom) that are the time-dependent components of the velocity potential. A generalized dissipation function is assumed to be proportional to the Stokes material derivative of the free surface. The generalized momenta are calculated from the Lagrangian and the Hamiltonian is determined from a Legendre transformation of the Lagrangian. The first order ordinary differential equations derived from the Hamiltonian are usually suitable for the application of the

GMM. However, the cross wave equations of motion must be transformed in order to obtain a suspended system for the application of the GMM. Only three canonical transformations that preserve the dynamics of the cross wave equations of motion are made because of an extension of the Herglotz algorithm to nonautonomous systems. This extension includes two distinct types of the generalized Herglotz algorithm (GHA). The system of nonlinear nonautonomous evolution equations determined from Hamilton's equations of motion of the second kind are averaged in order to obtain an autonomous system. The unperturbed system is analyzed to determine hyperbolic saddle points that are connected by heteroclinic orbits. The perturbed Hamiltonian system that includes surface tension satisfies the KAM nondegeneracy requirements; and the Melnikov integral is calculated to demonstrate that the motion is chaotic. For the perturbed dissipative system with surface tension, the Melnikov integral is identically zero implying that a higher dimensional GMM is necessary in order to demonstrate by the GMM that the motion is chaotic. However, numerical calculations of the largest Liapunov characteristic exponent demonstrate that the perturbed dissipative system with surface tension is also chaotic. A chaos diagram is computed in order to search for possible regions of the damping parameter and the Floquet parametric forcing parameter where chaotic motions may exist.

Application of the Generalized Melnikov Method to
Weakly Damped Parametrically Excited
Cross Waves with Surface Tension

by
Suzan M. Fadel

A THESIS
submitted to
Oregon State University

in partial fulfillment of
the requirements for the
degree of
Doctor of Philosophy

Completed September 25, 1998
Commencement June 1999

Doctor of Philosophy thesis of Suzan M. Fadel presented
on September 25, 1998

APPROVED:

Redacted for Privacy

Major Professor, representing Civil Engineering

Redacted for Privacy

Chair of Department of Civil, Construction, and
Environmental Engineering

Redacted for Privacy

Dean of Graduate School

I understand that my thesis will become part of the
permanent collection of Oregon State University
libraries. My signature below authorizes release of my
thesis to any reader upon request.

Redacted for Privacy

Suzan M. Fadel, Author

ACKNOWLEDGEMENTS

Deepest thanks to my professors, my family, and my friends for their support during four years of study and research at Oregon State University.

My major advisor Professor Robert T. Hudspeth encouraged and helped me to complete my research and write my dissertation.

My mathematics advisor Professor Ronald B. Guenther spent much time with me in patient and beneficial discussions.

I spent most of my time over the last four years between their offices at Graf 103 and Kidd 363. Both Professor Hudspeth and Professor Guenther supported me financially in this research.

My husband and two sons were with me and they went back home to Alexandria, Egypt. My husband continued to support me through e-mails.

My dear mother made a great sacrifice, taking care of my children and leaving my dear father alone. They both encouraged and prayed for me daily.

Words cannot express enough thanks to my professors, my family, and my friends.

TABLE OF CONTENTS

1.	Introduction	1
2.	Problem Formulation	12
2.1.	Variational Principle	12
2.2.	Decomposition of the Lagrangian Integrals	17
2.3.	Scaling and Nondimensional Parameters	19
2.4.	Trial Functions	24
2.5.	Legendre Transformation	28
2.6.	Damping Forces	30
3.	Canonical Transformations and Evolution Equations	34
3.1.	Canonical Transformations: definition and properties	34
3.2.	Poisson Brackets	35
3.3.	Generalized Herglotz Algorithm (GHA)	36
3.3.1.	GHA: Type I	36
3.3.2.	GHA: Type II	39
3.4.	Hamilton's Equations of Motion	41
3.5.	Three Canonical Transformations	42
3.5.1.	Rotation of axes	42
3.5.2.	Action/angle transformation	44
3.5.3.	Hamilton-Jacobi transformation	49
3.5.4.	Combined transformation	54
3.6.	Transformed Damping Forces	55
3.7.	Averaged System	57
4.	Application of the GMM	61
4.1.	Geometric Structure of Unperturbed Phase Space ($\alpha=0$, $\gamma=0$)	61
4.1.1.	Hyperbolic saddle points	63
4.1.2.	Dynamics on \mathcal{M}	65
4.1.3.	Heteroclinic orbits	70

TABLE OF CONTENTS, CONTINUED

4.2. Geometric Structure of Perturbed Hamiltonian Phase Space ($\alpha=0$, $\gamma>0$)	73
4.2.1. Persistence of \mathcal{M}	75
4.2.2. KAM theorem	76
4.2.3. Melnikov integral M	78
4.3. Geometric Structure of Perturbed Dissipative Phase Space ($\alpha>0$, $\gamma>0$)	80
4.3.1. Persistence of \mathcal{M}	83
4.3.2. Averaging method	84
4.3.3. Melnikov integral M	88
4.3.4. Liapunov characteristic exponents .	90
4.4. Comparison with Data	95
4.5. Conclusions	99
5. Recommendations for Further Study	103
Bibliography	105
Appendices	111

LIST OF FIGURES

FIGURE	PAGE
1. Stability diagrams of the linear Mathieu equation at primary resonance ($N=1$). (a) without dissipation (1.1) (b) with dissipation (1.3)	3
2. Definition sketch of the rectangular wave channel, showing the fluid domain out to an arbitrary length $x'=\ell'$ down the channel	14
3. Motion of a phase space point for an integrable Hamiltonian system with two degrees of freedom (4.6). (a) Invariant tori in a three dimensional constant energy space $E = \bar{E}$ (after Rasband, 1990). (b) The flow on a two-dimensional torus on \mathcal{M} for $H(P_1, P_2) = \bar{E}$ (after Lichtenberg & Lieberman, 1992)	68
4. Three-dimensional unperturbed $\alpha=\gamma=0$ heteroclinic manifold \mathcal{H} (after Bowline et al., in press) . . .	69
5. The unperturbed $\alpha=\gamma=0$ reduced four-dimensional phase space $(q, p, Q_1, Q_2) \in T^1 \times \mathbb{R}^1 \times T^2$ (P_1 and P_2 are constants)	72
6. Numerical calculation of the largest Liapunov characteristic exponent (after Benettin et al., 1976) Where $d_0=1$, $x=\psi$, $y=\psi+\delta\psi$, $\tau = 0.1$ seconds	94
7. Chaos diagram for the regions in the parameter space (v, ϵ) where chaotic motion may exist	95
8. Stability diagram for mode 1 cross-waves. Numbers refer to the experiment run numbers for mode 1 cross waves (circles) and no cross-waves (triangles) (after Bowline et al., in press)	96

LIST OF FIGURES, CONTINUED

FIGURE	PAGE
9. Stability diagram for mode 2 cross-waves. Numbers refer to the experiment run numbers for mode 2 cross waves (circles) and no cross-waves (triangles) (after Bowline et al., in press)	97
10. Stability diagram for mode 4 cross-waves. Numbers refer to the experiment run numbers for mode 4 cross waves (circles) and no cross-waves (triangles) (after Bowline et al., in press)	98

LIST OF APPENDICES

APPENDIX	PAGE
A. Dimensional Wavemaker Boundary-Value Problem . . .	112
B. Dimensional Linearized Boundary-Value Problem . .	113
C. Coefficients used in (2.13), (2.16), (2.26), and (3.41)	119
D. Nonautonomous Hamiltonian Components	120
E. Calculation of the Melnikov Integral	122
Component I_1	122
Component I_2	122
Component I_3	123
F. A Mathematica Program for Calculating the Largest Liapunov Exponent	125
G. Nomenclature	127

To the mother of my kids, Omar and Amr.

Thank you Mama.

Application of the Generalized Melnikov Method to
Weakly Damped Parametrically Excited
Cross Waves with Surface Tension

1. Introduction

A long rectangular wave channel with a horizontal flat bottom, two rigid vertical side walls and a wavemaker generates progressive waves that dissipate on a sloping beach. In addition to these directly forced longitudinal progressive waves with wavemaker frequency ω'_p , two types of transverse waves may occur; viz.,

- (1) sloshing waves that are directly excited by the wavemaker (Barnard *et al.*, 1977, Kit *et al.*, 1987, and Shemer & Kit, 1988), and
- (2) cross waves that are parametrically excited by the progressive waves at the subharmonic of the wavemaker frequency (Garrett, 1970, Jones, 1984, Lichter & Chen, 1987, Shemer & Lichter, 1987, Miles, 1988, Shemer & Kit, 1989, Underhill *et al.*, 1991, and Bowline *et al.*, in press).

Parametrically excited standing cross waves that oscillate in a direction transverse to the wavemaker forcing with crests perpendicular to the wavemaker are analyzed by the generalized Melnikov method (GMM). In general, cross waves oscillate at half the frequency of the wavemaker forcing (or, equivalently, the progressive wave) $\omega'_c = \omega'_p/2$ although other instability frequencies may occur. Eigenvalues based on the channel width determines the wavelengths $L'_c = 2(\text{channel width})/n$ of possible cross wave modes where n = the mode number and is equal to the number of half-wavelengths across the channel (*vide* (Bl1c), Appendix B). Energy is transferred from the directly forced longitudinal progressive waves to the cross waves through

spatial mean motion of the free surface and their growth is due to the rate of working of the wavemaker against the transverse stresses associated with the cross waves. Garrett (1970) was the first to show that the mechanism for excitation of (transverse) cross waves is a parametric resonance. Miles (1984) has shown that the motion of cross waves in an inviscid fluid is formally equivalent to a parametrically excited pendulum.

The parametrically excited pendulum described by Berge, et al. (1984) is analogous to the generation of subharmonic resonant cross waves. The motion of a parametrically excited pendulum is governed by the linear Mathieu equation (Miles & Henderson, 1990, and Norris, 1994) according to

$$\frac{d^2\theta}{dt^2} + \omega_0^2 (1 + h \cos 2\omega t) \theta = 0, \quad 0 < h < 1 \quad (1.1)$$

where h = a small parameter, 2ω = the parametric excitation frequency, ω_0 = the natural frequency of the pendulum in the absence of the parametric excitation $h=0$. Hamilton's equations of motion of the parametrically excited pendulum are given by

$$\frac{d\theta}{dt} = p; \quad \frac{dp}{dt} = -\omega_0^2 (1 + P) \theta; \quad P = h \cos 2\omega t \quad (1.2a-c)$$

that may be obtained from the Hamiltonian

$$H(p, \theta) = H_0(p, \theta) + H_h(P, \theta) = \frac{p^2 + \omega_0^2 \theta^2}{2} + \frac{\omega_0^2}{2} [P \theta^2] \quad (1.2d)$$

where $H_0(p, \theta)$ and $H_h(P, \theta)$ are the free oscillations and the Floquet parametric forcing components of the Hamiltonian, respectively. The Floquet parametric forcing Hamiltonian component H_h will be identified later in the

cross wave Hamiltonian (vide §3). Parametric resonance occurs in a bandwidth about $\omega_0 = N\omega$, where N is an integer. The primary resonance occurs at $N = 1$. An instability, often called subharmonic, due to resonance occurs for some range of ω when $h > 2|1 - (\omega/\omega_0)^2|$. In the parameter space defined by ω/ω_0 as the abscissa and h as the ordinate, the regions of instability correspond to shaded sectors of width h^N whose vertices are located at $h = 0$ and $\omega/\omega_0 = 1/N$. The boundaries between the stable and unstable regions are called neutral stability curves or transition curves (Jordan & Smith, 1987). The primary resonance of $N = 1$ shown in Figure 1a has the largest zone of instability

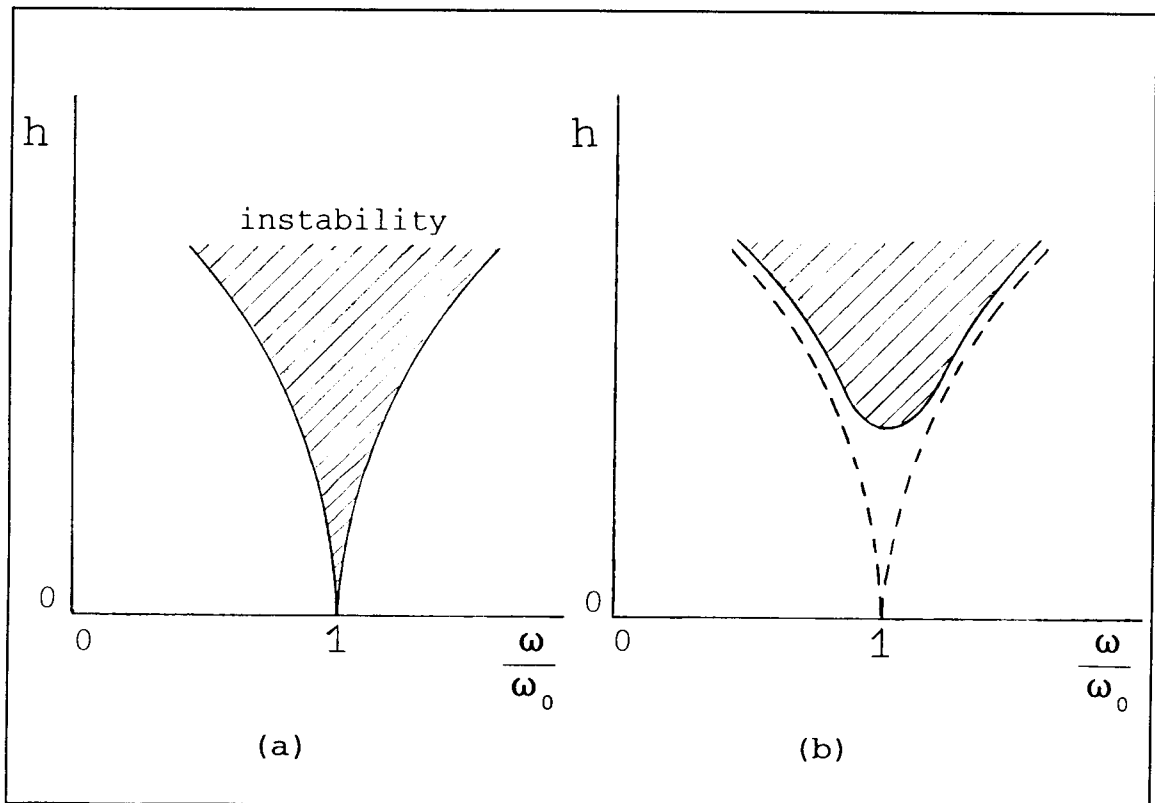


Figure 1. Stability diagrams of the linear Mathieu equation at primary resonance ($N = 1$). (a) without dissipation (1.1), (b) with dissipation (1.3).

and is of the most practical interest (Bogoliubov & Mitropolsky, 1961). From the Floquet theory (Arnold, 1983), the linear Mathieu equation (1.1) has no stable solutions inside the shaded sectors of the parameter space $(\omega/\omega_0, h)$; and outside these shaded sectors both of the solutions are stable (Hale, 1967).

In the presence of weak dissipation δ , where $0 < \delta \ll \omega_0$, the Mathieu equation (1.1) becomes

$$\frac{d^2\theta}{dt^2} + \delta \frac{d\theta}{dt} + \omega_0^2 (1 + h \cos 2\omega t) \theta = 0 \quad (1.3)$$

and the instability occurs for $h > 2 \left[\left(1 - \omega^2/\omega_0^2 \right)^2 + \omega^2 \delta^2/\omega_0^4 \right]$. Consequently, the vertices of the shaded sectors are no longer intersecting the horizontal axis of $h=0$ as shown in Figure 1b. Moreover, the regions of instability of the damped Mathieu equation (1.3) are entirely contained in the instability sectors of the undamped Mathieu equation (1.1). A finite parametric excitation threshold h is now needed for instability to occur as shown in Figure 1b for the primary resonance of $\omega = \omega_0$.

The detailed nature of subharmonic parametric forcing leading to cross wave generation in a rectangular channel has been investigated both theoretically and experimentally, by Garrett (1970), Mahony (1972), Barnard & Pritchard (1972), and Jones (1984). These studies concentrated mainly on the linear and nonlinear growth rate for this type of instability.

Jones (1984) was the first to derive the inviscid model equation valid to third order in the ordering parameter ε as well as the appropriate boundary conditions at the wavemaker. An important result of Jones' work is that only the order $O(\varepsilon)$ self-interactions of the cross waves and the interaction of the progressive waves with the

cross waves contribute to resonance effects. The order $O(\epsilon)$ self-interaction of progressive waves do not contribute to resonance.

Lichter & Shemer (1986) analyzed the development of cross wave patterns along the tank when the wavemaker was operated at moderate to high amplitudes. The qualitative nature of the wave fields was found to depend strongly on the forcing amplitude. At small to moderate amplitudes of the forcing, no cross wave developed and the area in the vicinity of the wavemaker was dominated by a plane progressive wave at the forcing frequency.

Kit *et al.* (1987) conclude that dissipation has to be incorporated in the model in order to provide agreement between the numerical results and the experimental observations. While this work was on sloshing waves, their conclusion apply to the cross waves as well (Lichter, 1987, and Kit & Shemer, 1989).

Lichter & Chen (1987) prove that the evolution equation governing the cross waves is nonlinear Schrodinger equation with a homogeneous boundary condition at the wavemaker. With the inclusion of an empirically determined damping coefficient along the tank, their numerical results show good agreement with experimental data.

Shemer & Lichter (1987) observed four different wave regions in the vicinity of the wavemaker when operated at moderate to high amplitudes. Neutral stability curves were determined experimentally and served to define the range of the forcing amplitudes where cross waves occurred.

Lichter (1987) gave few simple expressions that determine the relative contribution of the free surface, side walls, and bottom damping in the evolution of viscous cross waves.

Miles (1988) and Miles & Becker (1988) apply a variational formulation for cross waves in short and long

rectangular channels. They incorporate weak linear dissipation by introducing additional terms in the LHS of Hamilton's equations of motion. Miles' analysis includes the nonlinear interaction between the motion of the wave maker and the cross wave to second order and self-interaction of cross waves to third order.

Kit & Shemer (1989) investigated the influence of the dissipation along the rectangular wave channel and at the wavemaker, on neutral stability curves of cross waves.

Shemer & Kit (1989) performed both experimental and numerical studies of cross waves in rectangular channels. Dissipation was incorporated in their model equation and in the wavemaker boundary condition following the ideas outlined by Shemer & Kit (1988) for the closely related phenomenon of nonlinear sloshing waves. The relative importance of dissipation at the side walls of the channel increased quickly with the increasing of the mode number. At low amplitude of the wavemaker forcing side-wall dissipation was more pronounced.

Underhill et al. (1991) investigated cross waves and found three prominent frequencies present: a primary subharmonic and two slow temporal modulations. The stability diagrams were divided precisely into regions where cross wave motion is periodic, quasiperiodic, and chaotic. Quasiperiodic or conditionally periodic motion may be defined as the flow on the surface of a torus and it consists of two or more incommensurate frequencies.

There is no widely accepted definition for chaotic motion. From a practical point of view, chaotic motion may be defined as a bounded steady state behavior that is neither a fixed point, periodic, nor quasiperiodic (Parker & Chua, 1989). A dynamical system exhibiting chaotic behavior evolves in a deterministic way, but long-term prediction of the system's state is impossible because the

uncertainty in determining its initial state grows exponentially with time (Wolf, 1986). Most chaotic systems exhibit sensitive dependence on initial conditions. In general, two time-dependent solutions with slightly different initial conditions grow apart at an exponential rate and the differences in the initial conditions are manifested at a later time by significantly different dynamical states.

There are various theoretical criteria for testing or diagnosing the chaotic behavior of a dynamical system. One common criterion for chaotic behavior is a method based on the search for horseshoe maps and homoclinic/heteroclinic orbits in mathematical models of dynamical systems. This mathematical technique, called the Melnikov method, gives a local criterion for transverse intersection of stable and unstable manifolds of the perturbed system and chaotic motion near the unperturbed (undamped and unforced) homoclinic/heteroclinic orbits. In general, the Melnikov method does not signal the appearance of strange attractors (that represents persistent chaotic behavior over a global domain of phase space). The Melnikov method requires that the dynamical system be described in terms of a set of first order ordinary differential equations of the phase space variables and that the unperturbed (undamped and unforced) system possesses homoclinic/heteroclinic orbits connecting hyperbolic saddle points. The Melnikov method measures the distance between stable and unstable manifolds of the perturbed system from the unperturbed homoclinic/heteroclinic orbits. When there are multiple transverse intersections of the manifolds, the Melnikov integral yields simple zeros that indicate the presence of Smale horseshoes and chaotic motion. A general review on this method may be found in Moon (1992) and Abraham & Shaw (1992). A more detailed background on homoclinic/

heteroclinic orbits and the Melnikov method may be found in Melnikov (1963), Guckenheimer & Holmes (1983), and Wiggins (1988 & 1990).

The original work of Melnikov (1963) that was applied to only a one degree of freedom system has been extended by Wiggins & Holmes (1987), Wiggins (1988), and Wiggins (1990) to include higher dimensional systems. This extension may be referred to as the generalized Melnikov method or the GMM. Wiggins (1988) identified three dynamical systems I, II, and III that may be analyzed by the GMM.

The GMM has been applied to numerous mechanical systems and has been successfully applied to a fluid continuum by Holmes (1986), Allen *et al.* (1991), and Bowline *et al.* (in press).

Holmes (1986) applies the GMM to surface waves in a cylindrical basin excited by vertical oscillations of the basin and found chaos.

Allen *et al.* (1991) apply the GMM to quasi-geostrophic flow over a variable topography and also found chaos.

Bowline *et al.* (in press) apply the GMM to search for the chaotic behavior of parametrically excited cross waves in a long wave channel and found chaos. They performed an experimental study of cross waves and observed a simultaneous generation of primary-resonance ($\omega'_p : \omega'_c = 2:1$) and secondary-resonance ($\omega'_p : \omega'_c = 1:1$) cross waves.

The research by Bowline *et al.* (in press) is extended to include both surface tension and weak dissipation to the mathematical model of cross waves in a long rectangular wave channel. The surface tension is incorporated in the Luke (1967) Lagrangian formulation of the problem following Becker & Miles (1992). A generalized Hamilton's principle is applied to obtain the boundary value problem. A generalized dissipation function that is proportional to the time rate of change of the free surface elevation is

incorporated so that the dissipation will appear correctly in the dynamic free surface boundary condition. In order to apply the GMM, the Hamiltonian function is transformed by three successive canonical transformations that are based on the Herglotz algorithm. The Herglotz algorithm is extended to nonautonomous systems; and two types of the generalized Herglotz algorithm (GHA) are given. The GHA will be applied to injectively transform the Hamilton's equations of motion to a system that may be analyzed by the GMM. Without dissipation, the equations of motion are of the form identified by Wiggins (1988) as System III. With dissipation, the equations of motion are System I but the GMM failed to detect chaos.

The Liapunov characteristic exponents represent an alternative criteria for diagnosing the chaotic behavior of a dynamical system. They measure the mean rate of exponential divergence of nearby trajectories. One positive Liapunov characteristic exponent indicates chaos. Reviews of the Liapunov characteristic exponents are given by Wolf (1986) and by Lichtenberg & Lieberman (1992). The largest Liapunov characteristic exponent is employed by many investigators to test for the chaotic dynamics of parametrically excited surface waves including Umeki & Kambe (1989), Kambe & Umeki (1990), and Tsai *et al.* (1990). The largest Liapunov characteristic exponent is numerically determined for the perturbed dissipative system (System I) when the GMM failed to predict chaos.

The following is a brief review of the contents of the subsequent sections.

Section two is devoted to the variational formulation of the problem. The Lagrangian for a free surface wave with surface tension is introduced in §2.1 following Becker & Miles (1992). In §2.2 the Lagrangian is simplified by transforming the volume integrals to surface integrals and

by subtracting the zero variation integrals. A scaling procedure is carried out in §2.3 to obtain the scaling parameters required to evaluate the chaotic behavior. In §2.4 the wavemaker displacement, the velocity potential, and the free surface elevation are specified. The Lagrangian is written in terms of the generalized coordinates that are the time-dependent components of the cross wave and the progressive wave velocity potentials. In §2.5 the generalized momenta are calculated from the Lagrangian and the Hamiltonian is determined by applying the Legendre transformation of the Lagrangian. Finally, in §2.6 the generalized damping forces corresponding to the set of generalized coordinates are determined.

Section three is devoted to the canonical transformations and the determination of the evolution equations. In §3.1 and §3.2, some properties of canonical transformations and one of the common tests that may be employed to confirm the canonical character of a transformation, that is Poisson brackets are given. The Herglotz algorithm is extended in §3.3 for nonautonomous systems and two types of the GHA are given. The Hamilton's equations of motion of the second type is introduced in §3.4 and the equations of motion before and after a canonical transformation are given. Three canonical transformations are computed in §3.5 using the GHA. The transformed Hamiltonian, the transformed damping forces and the averaged system are computed in §3.5, §3.6, and §3.7, respectively.

Section four is devoted to the application of the GMM. Firstly, the unperturbed (unforced and undamped) system is analyzed. The hyperbolic saddle points and heteroclinic orbits are computed in §4.1. Secondly, the perturbed Hamiltonian system with surface tension is analyzed in §4.2. The KAM theorem requirement and the Melnikov integral

are evaluated. Thirdly, the perturbed dissipative system with surface tension is investigated using the GMM and the largest Liapunov exponent is numerically determined in §4.3. In §4.4 a comparison with experimental data by Bowline *et al.* (in press) shows good agreement with the present theoretical analysis. Finally, §4.5 introduces some conclusions.

section five provides some recommendations for further studies on the chaotic dynamics of parametrically excited standing cross waves.

2. Problem Formulation

All dependent and independent dimensional variables are denoted by a superscript prime to distinguish them from nondimensional unprimed variables. The fluid is assumed to be incompressible and inviscid and the flow to be irrotational. The dimensional fluid particle velocities \mathbf{u}' and the dimensional total pressure in the fluid P' are computed from

$$\mathbf{u}' = -\bar{\nabla}'\phi' \quad ; \quad \frac{P'}{\rho'} = -g'z' + \phi'_{t'} - \frac{1}{2} |\bar{\nabla}'\phi'|^2 \quad ; \quad (2.1, 2.2)$$

where ϕ' = a dimensional velocity potential; ρ' = the fluid mass density; g' = the gravitational acceleration; $\bar{\nabla}'$ = the three-dimensional gradient operator; and the subscript t' denotes the partial derivative with respect to time. The Bernoulli constant is assumed to be incorporated into the velocity potential (Landau & Lifshitz, 1987). The fluid domain is the long rectangular wave channel shown in Figure 2 that extends from the wavemaker S'_{χ} ; $x' = \chi(z', t')$ to an arbitrary cross-section at a distance $x' = \ell'$ where the length ℓ' is assumed to be integer multiple of progressive wave lengths L'_p .

2.1. Variational Principle

The Lagrangian \mathcal{L}' for a free surface wave with surface tension is (Becker & Miles, 1992)

$$\mathcal{Q}' = \int_{V'(t')} \left[\frac{1}{2} |\bar{\nabla}' \phi'|^2 - \phi'_{t'} + g' z' \right] dV' + T' \int_{S'_{\eta'}} \frac{(\zeta' - 1)}{\zeta'} dS'_{\eta'} ; \quad (2.3a)$$

where η' is the free-surface displacement, and where

$$dS'_{\eta'} = \zeta' dx' dy' ; \quad \zeta' = \left[1 + |\bar{\nabla}' \eta'|^2 \right]^{\frac{1}{2}} . \quad (2.3b, c)$$

The positive definite kinematic surface tension T' is the ratio of the conventional surface tension to the fluid mass density. The fluid domain $V'(t')$ is bounded by the following six surface boundaries: the wavemaker S'_{χ} ; $x' = \chi'(z', t')$, the free surface S'_{η} ; $z' = \eta'(x', y'; t)$, the horizontal bottom S'_h ; $z' = -h'$, the two vertical sides $S'_{\pm b}$; $y' = \pm b'$, and the far field vertical surface S'_{ℓ} ; $x' = \ell'$.

Hamilton's principle. If the system is in a configuration V'_1 at time t'_1 and in a configuration V'_2 at time t'_2 , the path that the system follows from configuration V'_1 to configuration V'_2 will be the one for which

$$\delta \int_{t'_1}^{t'_2} \mathcal{Q}' dt' + \int_{t'_1}^{t'_2} F' \left(\frac{D\eta'}{Dt'} \right) dt' = 0 ; \quad (2.4a)$$

The first integral in (2.4a) is the action integral of the Lagrangian (Luke, 1967). The generalized dissipation function per unit mass density $F'(D\eta'/Dt')$ is given by

$$F' \left(\frac{D\eta'}{Dt'} \right) = -\alpha \sqrt{\frac{g'}{\kappa'}} \int_{S'_{\eta'}} \frac{D\eta'}{Dt'} \frac{\delta \eta'}{\zeta'} dS'_{\eta'} ; \quad (2.4b)$$

where α = a dimensionless damping parameter and κ' = the cross wave wavenumber (vide §1), and where $D\eta'/Dt'$ = the Stokes material derivative of the free surface

$$\frac{D\eta'}{Dt'} = \frac{\partial \eta'}{\partial t'} - \bar{\nabla}'\phi' \cdot \bar{\nabla}'\eta' \quad (2.4c)$$

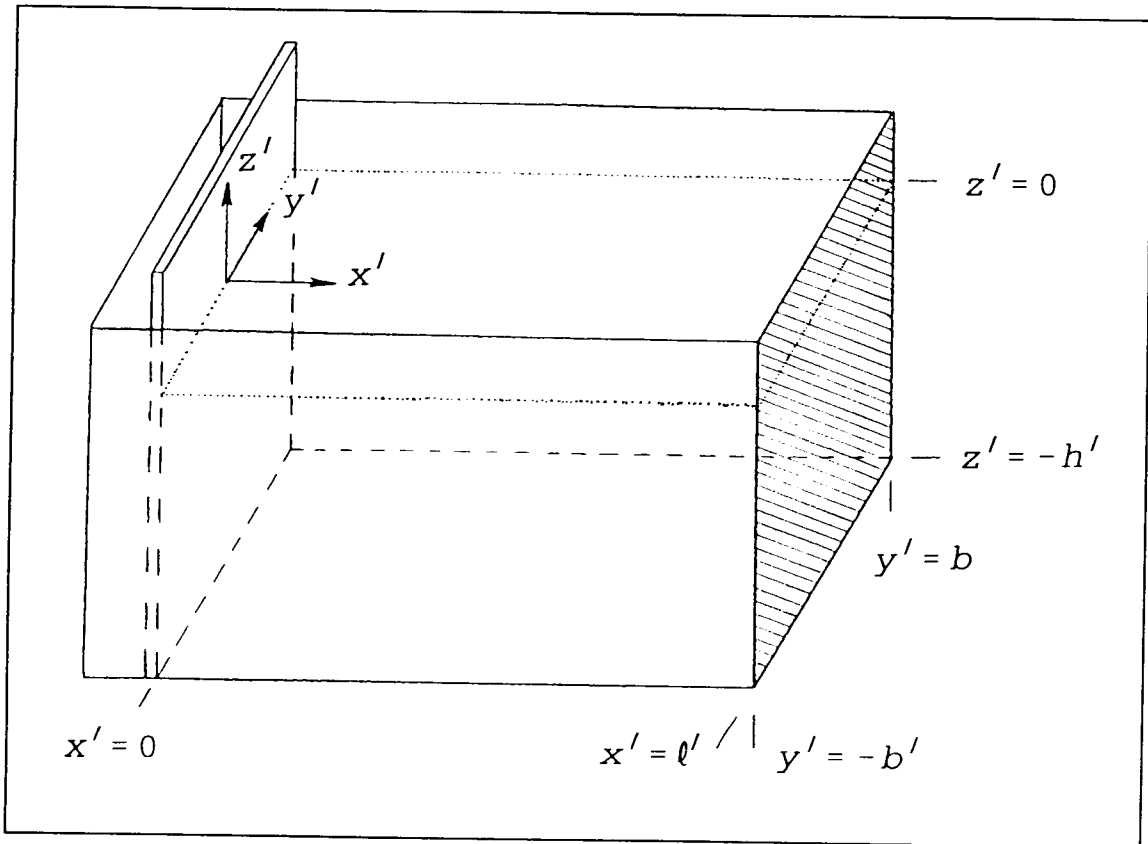


Figure 2. Definition sketch of the rectangular wave channel, showing the fluid domain out to an arbitrary length $x' = \ell'$ down the channel.

The dimensional boundary-value-problem may be obtained by requiring that the independent variation of ϕ' and η' vanish at the arbitrary temporal values t_1' and t_2' in

(2.4a) (Appendix A; Luke, 1967; Whitham, 1974; or Becker & Miles, 1992). The first variation of the Lagrangian \mathcal{L}'

(2.3a) is given by

$$\begin{aligned}
 \delta \mathcal{L}' &= \delta \int_{-h'-b'x'}^{\eta'} \int_{-b'x'}^{b'} \int \left(\frac{1}{2} |\bar{\nabla}' \phi'|^2 - \phi'_{t'} + g' z' \right) dx' dy' dz' + T' \delta \int_{-b'x'}^{b'} \int_{-b'x'}^{b'} (\zeta' - 1) dx' dy' \\
 &= \int_{-h'-b'x'}^{\eta'} \int_{-b'x'}^{b'} \int \left(\bar{\nabla}' \phi' \cdot \bar{\nabla}' (\delta \phi') - (\delta \phi')_{t'} \right) dx' dy' dz' + \int_{-b'x'}^{b'} \int_{-b'x'}^{b'} \left(\frac{1}{2} |\bar{\nabla}' \phi'|^2 - \phi'_{t'} + g' z' \right)_{z'=\eta'} \delta \eta' dx' dy' \\
 &\quad + T' \int_{-b'x'}^{b'} \int_{-b'x'}^{b'} \zeta'^{(-1)} (\bar{\nabla}' \eta' \cdot \bar{\nabla}' \delta \eta') dx' dy'
 \end{aligned} \tag{2.5}$$

where the differential surface $dS'_{\eta'}$ in (2.3a) has been replaced by the horizontal projection from (2.3b). The following identities will be used repeatedly (cf. Hildebrand §6.9, 1976):

1) the first form of Green's theorem,

$$\int_{V'} (\psi' \bar{\nabla}'^2 \phi' + \bar{\nabla}' \phi' \cdot \bar{\nabla}' \psi') dV' = \int_{S'} \psi' (\bar{\nabla}' \phi' \cdot \hat{n}) dS' ; \tag{2.6a}$$

2) Liebniz's rule,

$$\int_{V'(t')} \psi'_{t'} dV' = \frac{\partial}{\partial t'} \int_{V'(t')} \psi' dV' - \int_{S'} \psi' (\bar{\mathbf{U}}' \cdot \hat{n}) dS' ; \tag{2.6b}$$

3) differentiation formula,

$$\bar{\mathbf{F}}' \cdot \bar{\nabla}' G' = \bar{\nabla}' \cdot (G' \bar{\mathbf{F}}') - (\bar{\nabla}' \cdot \bar{\mathbf{F}}') G' ; \tag{2.6c}$$

4) Gauss's divergence theorem,

$$\int_{S'} \bar{\nabla}' \cdot (G' \bar{\mathbf{F}}') dS' = \int_{\partial S'} (\bar{\mathbf{F}}' \cdot \hat{n}) G' d\mathcal{S}' ; \tag{2.6d}$$

where \hat{n} is the outward unit normal of the fluid boundary. The identity (2.6d) may be used to transform either volume integrals to surface integrals or surface integrals to line integrals. Therefore, dS' in (2.6d) may be either a differential volume or surface and $d\mathcal{S}'$ may be either a differential surface or line, respectively. The volume integral in (2.5) may be transformed using the identities (2.6a) and (2.6b) by substituting $\psi' = \delta\phi'$. The first surface integral in (2.5) is the LHS of the dynamical free surface boundary condition (A3). The second surface integral in (2.5) may be transformed using the identities (2.6c) and (2.6d) through the substitution $\bar{\mathbf{F}}' = \zeta'^{(-1)} \bar{\nabla}' \eta'$, and $G' = \delta\eta'$. These transformations reduce the first

variation of the Lagrangian (2.5) to

$$\begin{aligned} \delta\mathcal{L}' + \frac{\partial}{\partial t'} \int_{V'(t')} \delta\phi' dV' &= \int_{-b'\chi'_{\eta'}}^{b'\chi'_{\eta'}} \int_{t'}^{t'} \left[\frac{1}{2} |\bar{\nabla}'\phi'|^2 - \phi'_{t'} + g'\eta' - T'\bar{\nabla}' \cdot \left(\zeta'^{(-1)} \bar{\nabla}' \eta' \right) \right]_{z'=\eta'} \delta\eta' dx' dy' \\ &- \int_{V'(t')} (\bar{\nabla}^2 \phi') \delta\phi' dV' + \int_{S'} (\phi'_n + \bar{\mathbf{u}}'_{s'} \cdot \hat{\mathbf{n}}_{s'}) \delta\phi' dS'_{s'} + T' \int_{\partial S'_{\eta'}} \zeta'^{(-1)} \eta'_n \delta\eta' d\mathcal{S}'_{\eta'} \end{aligned} \quad (2.7a)$$

where the subscript n denotes a normal derivative; viz.,

$$\eta'_n = \bar{\nabla}' \eta' \cdot \hat{\mathbf{n}} \quad , \quad \phi'_n = \bar{\nabla}' \phi' \cdot \hat{\mathbf{n}} \quad (2.7b, c)$$

The differential surfaces $dS'_{s'}$; the outward unit normal

$\hat{\mathbf{n}}_{s'}$; and the boundary motion $\bar{\mathbf{u}}'_{s'} \cdot \hat{\mathbf{n}}_{s'}$ are given by the following:

$$S'_{\eta'}: dS'_{\eta'} = \zeta' dx' dy'; \quad \hat{\mathbf{n}}_{\eta'} = \frac{1}{\zeta'} \left(-\eta'_{x'}, -\eta'_{y'}, 1 \right); \quad \bar{\mathbf{u}}'_{\eta'} \cdot \hat{\mathbf{n}}_{\eta'} = \frac{\eta'_{t'}}{\zeta'} \quad (2.8a-c)$$

$$S'_{\chi'}: dS'_{\chi'} = \sqrt{1 + \chi'^2_{z'}} dy' dz'; \quad \hat{\mathbf{n}}_{\chi'} = \frac{(-1, 0, \chi'_{z'})}{\sqrt{1 + \chi'^2_{z'}}}; \quad \bar{\mathbf{u}}'_{\chi'} \cdot \hat{\mathbf{n}}_{\chi'} = \frac{-\chi'_{t'}}{\sqrt{1 + \chi'^2_{z'}}} \quad (2.8d-f)$$

The geometric quantity $\bar{\nabla}' \cdot (\zeta'^{(-1)} \bar{\nabla}' \eta')$ in (2.7a) represents the total curvature of the free surface (Wehausen & Laitone (3.5), 1960) and may be linearized by using the binomial expansion as follows (Benjamin & Scott, 1979):

$$\bar{\nabla}' \cdot (\zeta'^{(-1)} \bar{\nabla}' \eta') = \bar{\nabla}'^2 \eta' + O(|\bar{\nabla}' \eta'|^2) \quad (2.9)$$

The order $O(\cdot)$ residual contains other products as well but only the leading term is given. This approximation may be justified by the scaling presented below (§2.3). Requiring that the last integral on the RHS of (2.7a) vanish implies either the natural contact line condition $\eta'_n = 0$ (A6a,b) or the edge constraint $\eta' = 0$ that may be more realistic for some fluid domains (*cf.* Benjamin & Scott, 1979).

2.2. Decomposition of the Lagrangian Integrals

A Lagrangian that is equivalent to (2.3) and that is more convenient for computations may be derived by transforming the volume integral in (2.3a) as follows. The first and the second terms in the volume integrand will be transformed by substituting $\psi' = \phi'$ into the identities (2.6a,b); the third term in the volume integrand will be transformed by substituting $g'z' = \bar{\nabla}' \cdot (\bar{\mathbf{F}}' G')$ into the identity (2.6d), where $\bar{\mathbf{F}}' = z'^2 \hat{\mathbf{k}}$ and $G' = g'/2$. Following these transformations, the Lagrangian (2.3) reduces to

$$\begin{aligned}
L' &= \mathcal{L}' + \frac{\partial}{\partial t'} \int_{V'} \Phi' dV' + g' h'^2 b' [\ell' - \chi'(-h', t')] - \frac{1}{2} \int_{-b'-h'}^{b'} \int_{\chi'}^{\eta'} (g' z'^2 \chi'_{z'})_{x'=\chi'} dz' dy' \\
&= -\frac{1}{2} \int_{V'} \Phi' \bar{\nabla}^2 \Phi' dV' + \int_{S'} \left(\frac{1}{2} \Phi'_n + \bar{\mathbf{U}}'_{s'} \cdot \hat{\mathbf{n}}_{s'} \right) \Phi' dS' + \frac{1}{2} \int_{-b'\chi'_{\eta'}}^{b'} \int_{\chi'_{\eta'}}^{\ell'} g' \eta'^2 dx' dy' \\
&\quad + T' \int_{-b'\chi'_{\eta'}}^{b'} \int_{\chi'_{\eta'}}^{\ell'} (\zeta' - 1) dx' dy'
\end{aligned} \tag{2.10}$$

where $\chi'_{\eta'} = \chi'(z' = \eta', t')$; $\eta'_{\chi'} = \eta'(x' = \chi', y', t')$; and $\eta'_{\ell'} = \eta'(x' = \ell', y', t')$. The difference $[L' - \mathcal{L}']$ in (2.10) makes a null contribution to the variation of the action integral of the Lagrangian and this implies that the Lagrangian L' satisfies Hamilton's principle (2.4) (Miles, 1988). Substituting (2.8a-f), (A2), (A4a,b), and (A5) into the Lagrangian (2.10) and grouping the terms according to the surfaces over which each term is integrated, the Lagrangian (2.10) may be decomposed into the following integrals:

$$L' = L'_{V'} + L'_{\chi'} + L'_{\ell'} + L'_{\eta'} + L'_{T'} \tag{2.11a}$$

where

$$L'_{V'} = -\frac{1}{2} \int_{V'} \Phi' \bar{\nabla}^2 \Phi' dV' \tag{2.11b}$$

$$L'_{\chi'} = -\frac{1}{2} \int_{-b'-h'}^{b'} \int_{\chi'}^{\eta'} [\Phi' \chi'_{t'}]_{x'=\chi'} dz' dy' \tag{2.11c}$$

$$L'_{\ell'} = -\frac{1}{2} \int_{-b'-h'}^{b'} \int_{\chi'}^{\eta'} [\Phi' \Phi'_{x'}]_{x'=\ell'} dz' dy' \tag{2.11d}$$

$$L'_{\eta'} = \frac{1}{2} \int_{-b'}^{b'} \int_{\chi'_{\eta'}}^{\ell'} \left[\phi' \eta'_{t'} + g' \eta'^2 \right]_{z'=\eta'} dx' dy' \quad (2.11e)$$

$$L'_{T'} = T' \int_{-b'}^{b'} \int_{\chi'_{\eta'}}^{\ell'} (\zeta' - 1) dx' dy' \approx \frac{T'}{2} \int_{-b'}^{b'} \int_{\chi'_{\eta'}}^{\ell'} |\bar{\nabla}' \eta'|^2 dx' dy' \quad (2.11f)$$

The approximation (2.11f) is the result of substituting the linearized approximation to the total curvature of the free surface (2.9). The volume integral (2.11b) is identically equal to zero by (A1) so that the decomposition of the integrals is reduced to only surface integrals over the free surface η' , the wavemaker surface χ' , and the far field boundary surface ℓ' . In order to proceed further with the Hamiltonian formulation, the Lagrangian must be expressed in terms of generalized coordinates that may be either the field variable η' or ϕ' . The velocity potential ϕ' is chosen as the field variable and η' will be expressed in terms of ϕ' by using the free surface boundary conditions (A2, A3) and the contact line condition (A6a,b).

2.3. *Scaling and Nondimensional Parameters*

The velocity potential ϕ' and the free surface displacement η' are assumed to be linear sum of a progressive wave component (subscript p) that is independent of y' and a cross wave component (subscript c) that is independent of x' as follows:

$$\phi'(x', y', z', t') = \phi'_p(x', z', t') + \phi'_c(y', z', t') \quad (2.12a)$$

$$\eta'(x', y', t') = \eta'_p(x', t') + \eta'_c(y', t') \quad (2.12b)$$

The dimensional (primed) variables are related to the nondimensional (unprimed) variables by the following scales:

$$x' = \frac{x}{k'} ; \quad y' = \frac{y}{\kappa'} ; \quad z' = \frac{z}{\kappa'} ; \quad t' = \frac{t}{\sqrt{g' \kappa'}} \quad (2.13a-d)$$

$$h = \kappa' h' ; \quad \xi = k' \ell' ; \quad b = \kappa' b' \quad (2.13e-g)$$

$$\phi'_p = \phi_p a'_p \sqrt{\frac{g'}{k'}} ; \quad \phi'_c = \phi_c a'_c \sqrt{\frac{g'}{\kappa'}} \quad (2.13h, i)$$

$$\eta'_p = a'_p \eta_p ; \quad \eta'_c = a'_c \eta_c ; \quad \chi' = a'_w \chi ; \quad L' = \frac{L a_c'^2 g'}{k' \kappa'} \quad (2.13j-m)$$

where a'_w = the amplitude of the wavemaker displacement; k' and a'_p = the wavenumber and amplitude of the progressive wave, respectively; and κ' and a'_c = the wavenumber and amplitude of the cross wave, respectively. The progressive wave frequency ω'_p is related to the progressive wavenumber k' by the deep water dispersion relationship $\omega_p'^2 = g' k' \tau_\lambda$ where $\tau_\lambda = 1 + (\tau/\lambda^4)$. The cross wave frequency is related to the cross wavenumber by the deep water dispersion relationship $\omega_c'^2 = g' \kappa'$ where $\kappa'_\tau = \kappa' (1 + \tau)$. The progressive wave period and wavelength are given by $T'_p = 2\pi/\omega'_p$ and $L'_p = 2\pi/k'$, respectively. The cross wave period and wavelength are given by $T'_c = 2\pi/\omega'_c$ and $L'_c = 2\pi/\kappa'$, respectively. The scalings (2.13) yield the following non-dimensional parameters:

$$\varepsilon = \kappa' a'_c ; \quad \beta = \omega'_c / \omega'_p ; \quad \gamma = k' a'_w \quad (2.14a-c)$$

$$\tau = T' \kappa'^{1/2} / g' ; \quad \lambda = \sqrt{\kappa' / k'} ; \quad \Gamma = a'_p / a'_c \quad (2.14d, f)$$

The dimensionless velocity potential $\phi(x, y, z, t)$ and free surface displacement $\eta(x, y, t)$ in (2.12) are now given by

$$\phi(x, y, z, t) = \phi_c(y, z, t) + \Gamma \lambda \phi_p(x, z, t) \quad (2.15a)$$

$$\eta(x, y, t) = \eta_c(y, t) + \Gamma \eta_p(x, t) \quad (2.15b)$$

The scaled boundary value problem for the dimensionless velocity potential $\phi(x, y, z, t)$ and the dimensionless free surface elevation $\eta(x, y, t)$ for the irrotational flow of an incompressible, inviscid fluid confined to the rectangular wave tank shown in Figure 2 is:

$$\frac{1}{\lambda^4} \phi_{xx} + \phi_{yy} + \phi_{zz} = 0 ; \quad \gamma \chi \leq x \leq \xi, y \leq |b|, -h \leq z \leq \varepsilon \eta \quad (2.16a)$$

$$\phi_z = -\tau_1 \eta_t + \varepsilon \left(\frac{1}{\lambda^4} \phi_x \eta_x + \phi_y \eta_y \right) ; \quad z = \varepsilon \eta, \gamma \chi \leq x \leq \xi, y \leq |b| \quad (2.16b)$$

$$\frac{\varepsilon}{2} \left(\frac{1}{\lambda^4} \phi_x^2 + \phi_y^2 + \phi_z^2 \right) - \tau_1 \phi_t + \eta = \tau \left(\frac{1}{\lambda^4} \eta_{xx} + \eta_{yy} \right) - \alpha \phi_z ; \quad \begin{cases} \gamma \chi \leq x \leq \xi, \\ y \leq |b|, z = \varepsilon \eta \end{cases} \quad (2.16c)$$

$$\bar{\nabla} \phi \cdot \hat{n} = 0 ; \quad \begin{cases} y = |b|, -h \leq z \leq \varepsilon \eta, \gamma \chi \leq x \leq \xi \\ z = -h, y \leq |b|, \gamma \chi \leq x \leq \xi \end{cases} \quad (2.16d, e)$$

$$\phi_x = -\frac{\gamma}{\varepsilon} \lambda^4 \tau_1 \chi_t + \gamma \lambda^4 \phi_z \chi_z ; \quad x = \gamma \chi, y \leq |b|, -h \leq z \leq \varepsilon \eta \quad (2.16f)$$

$$\bar{\nabla}\eta \cdot \hat{n} = 0 \quad ; \quad \begin{cases} x = \gamma\chi, & y \leq |b|, & -h \leq z \leq \varepsilon\eta \\ y = |b|, & \gamma\chi \leq x \leq \xi, & -h \leq z \leq \varepsilon\eta \end{cases} \quad (2.16g,h)$$

together with the appropriate radiation condition; where $\tau_1 = \sqrt{1+\tau}$ and $\kappa_\tau = \kappa(1+\tau)$ (Appendix C). The subscripts x , y , z , and t denote partial differentiations. The free surface curvature in the first term on the RHS in (2.16c) requires more information about the free surface elevation at the boundaries; and the contact line condition (2.16g,h) (or, alternatively, the edge constraint) provides the required dynamical constraint. The nondimensional Lagrangian L may now be decomposed into the following dimensionless integrals:

$$L = L_\chi + L_\xi + L_\eta + L_\tau \quad (2.17a)$$

where

$$L_\chi = -\frac{\gamma}{2\varepsilon} \int_{-b}^b \int_{-h}^{\varepsilon\eta_\chi} \left(\tau_1 \phi \chi_t \right)_{x=\gamma\chi} dz dy \quad (2.17b)$$

$$L_\xi = -\frac{1}{2\lambda^4} \int_{-b}^b \int_{-h}^{\varepsilon\eta_\xi} \left(\phi \phi_x \right)_{x=\xi} dz dy \quad (2.17c)$$

$$L_\eta = \frac{1}{2} \int_{-b}^b \int_{\gamma\chi_\eta}^{\xi} \left(\tau_1 \phi \eta_t + \eta^2 \right)_{z=\varepsilon\eta} dx dy \quad (2.17d)$$

$$L_\tau = \frac{\tau}{2} \int_{-b}^b \int_{\gamma\chi_\eta}^{\xi} \left(\frac{1}{\lambda^4} \eta_x^2 + \eta_y^2 \right) dx dy \quad (2.17e)$$

where $\eta_\chi = \eta(x=\gamma\chi, y; t)$, $\eta_\xi = \eta(x=\xi, y; t)$, and $\chi_\eta = \chi(z=\varepsilon\eta; t)$. The wavemaker integral (2.17b) and the free-surface integral (2.17d) will be approximated by (Miles, 1988)

$$\int_{-h}^{\varepsilon\eta} [\cdot] dz \approx \int_{-h}^0 [\cdot] dz + \varepsilon\eta [\cdot]_{z=0} + O(\varepsilon^2) ; \quad (2.18a)$$

$$\int_{\gamma\chi}^{\xi} [\cdot] dx \approx \int_0^{\xi} [\cdot] dx - \gamma\chi [\cdot]_{x=0} + O(\gamma^2) ; \quad (2.18b)$$

in order to posit solutions by separation of variables. The perturbation (wavemaker forcing) parameter γ is smaller than the Floquet parametric forcing (ordering) parameter ε because experiments demonstrate that the standing cross wave amplitude becomes larger than the wavemaker forcing amplitude as $t \rightarrow \infty$. The parameter ordering is, therefore,

$$0 < \gamma^2 < \varepsilon\gamma < \varepsilon^2 < \gamma < \varepsilon < 1 \quad \text{or} \quad 0 < \frac{\gamma^2}{\varepsilon} < \gamma < \frac{\gamma}{\varepsilon} < 1 \quad (2.19a,b)$$

The higher order terms that will be neglected are $O(\varepsilon^2)$, $O(\varepsilon\gamma)$, and $O(\gamma^2)$; but terms $O(\gamma/\varepsilon)$ will be retained. Ignoring these higher order terms, the nondimensional Lagrangian integrals (2.17a-e) are approximated by:

$$\begin{aligned} L_\chi = & -\frac{\gamma\tau_1}{2\varepsilon} \int_{-b}^b \int_{-h}^0 \left[\left(\phi_c + \Gamma\lambda\phi_p \right) \chi_t \right]_{x=0} dz dy \\ & + \int_{-b}^b \left[\varepsilon \chi_t \left(\eta_c + \Gamma\eta_p \right) \left(\phi_c + \Gamma\lambda\phi_p \right) \right]_{x,z=0} dy + O(\varepsilon^2) \end{aligned} \quad (2.20a)$$

$$\begin{aligned} L_\xi = & -\frac{\Gamma\lambda}{2\lambda^4} \int_{-b}^b \int_{-h}^0 \left[\phi_{px} \left(\phi_c + \Gamma\lambda\phi_p \right) \right]_{x=\xi} dz dy \\ & + \int_{-b}^b \left[\varepsilon \phi_{px} \left(\eta_c + \Gamma\eta_p \right) \left(\phi_c + \Gamma\lambda\phi_p \right) \right]_{x=\xi, z=0} dy + O(\varepsilon^2) \end{aligned} \quad (2.20b)$$

$$\begin{aligned}
L_\eta = & \frac{1}{2} \int_{-b}^b \int_0^\xi \left\{ \tau_1 (\eta_c + \Gamma \eta_p)_t \left[(\phi_c + \Gamma \lambda \phi_p) + \epsilon (\eta_c + \Gamma \eta_p) (\phi_c + \Gamma \lambda \phi_p)_z \right] + (\eta_c + \Gamma \eta_p)^2 \right\}_{z=0} dx dy \\
& - \frac{\gamma}{2} \int_{-b}^b \left\{ \chi \left[\tau_1 (\phi_c + \Gamma \lambda \phi_p) (\eta_c + \Gamma \eta_p)_t + (\eta_c + \Gamma \eta_p)^2 \right] \right\}_{x,z=0} dy + O(\epsilon^2)
\end{aligned} \tag{2.20c}$$

$$\begin{aligned}
L_\tau = & \frac{\tau}{2} \int_{-b}^b \int_0^\xi \left[\frac{\Gamma^2}{\lambda^4} \eta_{p_x}^2 + \eta_{c_y}^2 \right] dx dy \\
& - \int_{-b}^b \left[\gamma \chi \left(\frac{\Gamma^2}{\lambda^4} \eta_{p_x}^2 + \eta_{c_y}^2 \right) \right]_{x,z=0} dy + O(\gamma \epsilon)
\end{aligned} \tag{2.20d}$$

2.4. Trial Functions

The wave maker motion, the velocity potentials, and the free surface elevations are now to be specified. The wavemaker forcing is specified as

$$\chi = f(z) \sin \frac{t}{\beta} \begin{cases} f(z) = 1 + \frac{z}{h} & \text{for a full draft hinge,} \\ f(z) = 1 & \text{for a full draft piston.} \end{cases} \tag{2.21a,b}$$

The wavemaker shape function $f(z)$ is independent of the cross tank dimension y ; consequently, no transverse (sloshing) waves may be generated by the wavemaker motion (2.21). Because the wavemaker displacement was scaled by the wavemaker amplitude a'_w measured at the still water level $z = 0$, $f(z=0) = 1$ from (2.21). A generic planar wavemaker function is given by Hudspeth and Sulisz (1992). The cross wave potential ϕ_c will be approximated by a linear deep water standing wave; and the progressive wave potential ϕ_p will be approximated by a linear deep water traveling wave. As the chaos is assumed to be temporal

rather than spatial, the time dependencies of the potentials will be the unknown variables. These dimensionless deep water velocity potentials are (Appendix B; vide Eagleson & Dean, p.19, 1966):

$$\phi_c(y, z; t) = q(t) \cos(y-b) \exp[z] ; \quad (2.22a)$$

$$\phi_p(x, z; t) = [Q_1(t) \cos x + Q_2(t) \sin x] \exp[z/\lambda^2] ; \quad (2.22b)$$

where the variables $q(t)$, $Q_1(t)$, and $Q_2(t)$ are the generalized coordinates (or, equivalently, the degrees of freedom). The free-surface displacement η is a solution to the linearized inhomogeneous boundary value problem given by

$$\mathcal{L}^\eta \eta = [\mathcal{L}_p^\eta \eta_p - f_p] + [\mathcal{L}_c^\eta \eta_c - f_c] \equiv 0 \quad (2.23a)$$

$$\mathcal{L}_p^\eta \eta_p - f_p = 0 ; \quad \mathcal{L}_c^\eta \eta_c - f_c = 0 \quad (2.23b, c)$$

$$\eta_{p_x} = 0 ; \quad x=0 , \quad \eta_{c_y} = 0 ; \quad y=|b| \quad (2.23d, e)$$

where

$$\mathcal{L}_p^\eta \eta_p = \frac{\tau}{\lambda^4} \eta_{p_{xx}} - \eta_p , \quad f_p = \alpha \lambda \phi_{p_z} - \tau_1 \lambda \phi_{p_t} ; \quad z=0 \quad (2.23f, g)$$

$$\mathcal{L}_c^\eta \eta_c = \tau \eta_{c_{yy}} - \eta_c , \quad f_c = \alpha \phi_{c_z} - \tau_1 \phi_{c_t} ; \quad z=0 \quad (2.23h, i)$$

where $\tau_1 = \sqrt{1+\tau}$ (Appendix C). The general solution to (2.23c) following the substitution of (2.22a) is an homogeneous solution η_h^c and an inhomogeneous particular solution η_i^c given by

$$\begin{aligned}
\eta_c &= \eta_h^c + \eta_i^c \\
&= A \cosh\left(\frac{y-b}{\sqrt{\tau}}\right) + B \sinh\left(\frac{y-b}{\sqrt{\tau}}\right) + \frac{1}{\tau_1^2} \left(-q\alpha + \tau_1 \dot{q}\right) \cos(y-b)
\end{aligned} \tag{2.24a}$$

The homogeneous boundary conditions (2.23e) require that

$A = B = 0$ at $y = \pm b$ and (2.24a) reduces to only η_i^c ; i.e.,

$$\eta_c = \frac{1}{\tau_1^2} \left(-q\alpha + \tau_1 \dot{q}\right) \cos(y-b) \tag{2.24b}$$

The progressive wave free surface displacement η_p is determined far from the wavemaker. The general solution to (2.23b) following the substitution of (2.22b) is an homogeneous solution η_h^p and an inhomogeneous particular solution η_i^p given by

$$\begin{aligned}
\eta_p &= \eta_h^p + \eta_i^p \\
&= C \exp\left[-\frac{\lambda^2 x}{\sqrt{\tau}}\right] + D \exp\left[\frac{\lambda^2 x}{\sqrt{\tau}}\right] \\
&\quad + \left(\frac{-Q_1 \alpha + \lambda^2 \tau_1 \dot{Q}_1}{\lambda \tau_\lambda}\right) \cos x + \left(\frac{-Q_2 \alpha + \lambda^2 \tau_1 \dot{Q}_2}{\lambda \tau_\lambda}\right) \sin x
\end{aligned} \tag{2.25a}$$

where $\tau_\lambda = 1 + (\tau/\lambda^4)$ (Appendix C). For the evanescent eigenmodes to be bounded as $x \rightarrow +\xi$, $D = 0$. The homogeneous contact line condition (2.23d) requires that

$$C = \frac{\sqrt{\tau}}{\lambda^2} \left(\frac{-Q_2 \alpha + \lambda^2 \tau_1 \dot{Q}_2}{\lambda \tau_\lambda} \right); \tag{2.25b}$$

and the progressive wave free-surface displacement η_p reduces to

$$\eta_p = \left(\frac{-Q_1 \alpha + \lambda^2 \tau_1 \dot{Q}_1}{\lambda \tau_\lambda} \right) \cos x + \left(\frac{-Q_2 \alpha + \lambda^2 \tau_1 \dot{Q}_2}{\lambda \tau_\lambda} \right) \left(\sin x + \frac{\sqrt{\tau}}{\lambda^2} \exp \left[-\frac{\lambda^2}{\sqrt{\tau}} x \right] \right) \quad (2.25c)$$

All of the spatial integrals in (2.20a-d) may now be evaluated since the spatial dependencies are known. All $O(\varepsilon)$ progressive wave self-interaction terms (ϕ_p or η_p) will be ignored (*vide* §1; or Jones, 1984). It is convenient to rewrite the Lagrangian by grouping the integrals according to their order rather than the surface over which each term is integrated. The integral ordering in (2.20a-d) will be: L_0 that are all $O(1)$ integrals; L_ε that are all $O(\varepsilon)$ integrals; and L_γ that are all $O(\gamma)$ integrals that are the result of the wavemaker forcing. Substituting the trial functions (2.21), (2.22), (2.24b), and (2.25c); then setting $\alpha=0$ the surface integrals in the Lagrangian (2.20a-d) become

$$L = L_0 + L_\varepsilon + L_\gamma + O(\varepsilon^2, \varepsilon\gamma, \gamma^2) ; \quad (2.26a)$$

where

$$L_0 = -\frac{b\Gamma^2}{2} \left[\xi(Q_1^2 + Q_2^2) + Q_1 Q_2 \right] + \frac{b\tau_1^2 \Gamma^2}{2\lambda^2 \tau_\lambda^2} \left[\xi \lambda^4 \tau_\lambda (\dot{Q}_1^2 + \dot{Q}_2^2) + 4\tau \dot{Q}_1 \dot{Q}_2 \right] - \frac{b\xi}{2} (q^2 - \dot{q}^2) \quad (2.26b)$$

$$L_\varepsilon = -\frac{\varepsilon b \Gamma \tau_1 \tau}{2\lambda^3 \tau_\lambda} q^2 \dot{Q}_2 - \frac{\varepsilon b \Gamma}{2\tau_1 \lambda^3} q \dot{q} Q_2 \quad (2.26c)$$

$$\begin{aligned}
L_Y = & -\gamma b \cos\left(\frac{t}{\beta}\right) \left(f_1 \frac{\Gamma \lambda \tau_1 Q_1}{\epsilon \beta} + \frac{\Gamma^2 \tau_1^2}{\beta \tau_\lambda} Q_1 \left(\lambda^2 \dot{Q}_1 + \sqrt{\tau} \dot{Q}_2 \right) + \frac{q \dot{q}}{2\beta} \right) \\
& + \gamma b \sin\left(\frac{t}{\beta}\right) \left(\Gamma^2 Q_1^2 - \frac{\Gamma^2 \tau_1^2}{\lambda^2 \tau_\lambda^2} \left(\lambda^4 \dot{Q}_1^2 + \lambda^2 \sqrt{\tau} \dot{Q}_1 \dot{Q}_2 + \tau \dot{Q}_2^2 \right) + \frac{-\dot{q}^2 + q^2}{2} \right)
\end{aligned}
\tag{2.26d}$$

The coefficient f_1 in (2.26d) is a function of the wavemaker shape function $f(z)$ (2.21a,b) and is given in Appendix C. The Lagrangian components L_0 , L_ϵ , and L_Y represent the free oscillations, the Floquet parametric forcing of the cross wave by the progressive wave (Jones, 1984), and the 100% nonautonomous perturbed (wavemaker forcing) components, respectively.

2.5. Legendre Transformation

The Legendre transformation of the Lagrangian $L(\mathbf{q}, \dot{\mathbf{q}}, t)$ with respect to the generalized velocities $\dot{\mathbf{q}} = (\dot{q}, \dot{Q}_1, \dot{Q}_2)$ generates the Hamiltonian according to (Lichtenberg & Lieberman, 1992)

$$H = p \dot{q} + P_1 \dot{Q}_1 + P_2 \dot{Q}_2 - L \tag{2.27}$$

where $\mathbf{p} = (p, P_1, P_2)$ is the set of generalized momenta corresponding to the set of generalized coordinates $\mathbf{q} = (q, Q_1, Q_2)$. The generalized momenta are computed from the free oscillations and the Floquet parametric forcing components of the Lagrangian function $(L_0 + L_\epsilon)$ (Goldstein, 1980) according to

$$p_i = \frac{\partial (L_0 + L_\epsilon)}{\partial \dot{q}_i} ; \quad i = 1, 2, 3 \tag{2.28a}$$

$$p_1 = p = b \xi \dot{q} - \frac{\epsilon b \Gamma}{2 \tau_1 \lambda^3} q Q_2 \quad (2.28b)$$

$$p_2 = P_1 = \frac{b \tau_1^2 \Gamma^2 \lambda^2}{\tau_\lambda} \left(\xi \dot{Q}_1 + \frac{2 \tau}{\lambda^4 \tau_\lambda} \dot{Q}_2 \right) \quad (2.28c)$$

$$p_3 = P_2 = - \frac{\epsilon b \tau_1 \Gamma \tau}{2 \lambda^3 \tau_\lambda} q^2 + \frac{b \tau_1^2 \Gamma^2 \lambda^2}{\tau_\lambda} \left(\xi \dot{Q}_2 + \frac{2 \tau}{\lambda^4 \tau_\lambda} \dot{Q}_1 \right) \quad (2.28d)$$

Inverting (2.28) for \dot{q}_i yields

$$\dot{q} = \frac{p}{b \xi} + \frac{\epsilon \Gamma q Q_2}{2 \tau_1 \xi \lambda^3} \quad (2.29a)$$

$$\dot{Q}_1 = \frac{\lambda^4 \tau_\lambda P_1 - \frac{2 \tau}{\xi} P_2}{b \tau_1^2 \Gamma^2 \lambda^6 \xi} - \frac{\epsilon \tau^2 q^2}{\Gamma \lambda^9 \xi^2 \tau_1 \tau_\lambda} \quad (2.29b)$$

$$\dot{Q}_2 = \frac{\lambda^4 \tau_\lambda P_2 - \frac{2 \tau}{\xi} P_1}{b \xi \tau_1^2 \Gamma^2 \lambda^6} + \frac{\epsilon \tau q^2}{2 \Gamma \xi \lambda^5 \tau_1} \quad (2.29c)$$

The parameter ξ that denotes length down the channel will now be used as an ordering parameter since $\xi \gg 1$. This approximation by order is both a way of simplifying the Hamiltonian (2.27) and of applying the long channel assumption. This approximation is used only for determining the order of the coefficient for each variable grouping and not to scale the different variable combinations. Substituting (2.29) and (2.26) into (2.27) yields the following Hamiltonian:

$$H(\mathbf{q}, \mathbf{p}, t) = H_0(\mathbf{q}, \mathbf{p}) + H_\epsilon(\mathbf{q}, \mathbf{p}) + H_\gamma(\mathbf{q}, \mathbf{p}, t) + O(\epsilon^2, \epsilon \gamma, \gamma^2) ; \quad (2.30a)$$

where

$$H_0 = \frac{b \Gamma^2}{2} \left(\xi (Q_1^2 + Q_2^2) + Q_1 Q_2 \right) + \frac{1}{2} b \xi q^2 + \frac{p^2}{2 b \xi} + \frac{(P_1^2 + P_2^2)}{2 b \beta^2 \Gamma^2 \xi} - \frac{2 \tau P_1 P_2}{b \tau_1^2 \Gamma^2 \lambda^6 \xi^2} \quad (2.30b)$$

$$H_\epsilon = \frac{\epsilon \Gamma}{2 \tau_1 \xi \lambda^3} q p Q_2 + \frac{\epsilon \tau}{2 \tau_1 \Gamma \xi \lambda^5} q^2 P_2 - \frac{\epsilon \tau^2}{\tau_1 \Gamma \xi^2 \lambda^9 \tau_\lambda} q^2 P_1 \quad (2.30c)$$

$$H_\gamma = \gamma \cos\left(\frac{t}{\beta}\right) \left(f_1 \frac{b \Gamma \lambda \tau_1 Q_1}{\epsilon \beta} + \frac{Q_1 (\lambda^2 P_1 + \sqrt{\tau} P_2)}{\beta \xi \lambda^2} \right. \\ \left. - \frac{2 \tau Q_1 (\lambda^2 P_2 + \sqrt{\tau} P_1)}{\beta \xi^2 \lambda^6 \tau_\lambda} + \frac{p q}{2 \beta \xi} \right) \\ - \gamma \sin\left(\frac{t}{\beta}\right) \left(b \Gamma^2 Q_1^2 - \frac{(\lambda^2 P_1 + \sqrt{\tau} P_2)^2}{b \tau_1^2 \Gamma^2 \xi^2 \lambda^6} + \frac{1}{2} b q^2 - \frac{p^2}{2 b \xi^2} \right) \quad (2.30d)$$

The $H_0(\mathbf{q}, \mathbf{p}) + H_\epsilon(\mathbf{q}, \mathbf{p})$ components represent the free oscillations and the Floquet parametric forcing of the cross wave by the progressive wave (vide §1, and Jones, 1984). The perturbed (wavemaker forcing) $H_\gamma(\mathbf{q}, \mathbf{p}, t)$ terms are 100% nonautonomous and will not survive the averaging theorem that is required for Wiggins-Holmes extension of the generalized Melnikov method (GMM) (vide §3). All of $H_\epsilon(\mathbf{q}, \mathbf{p})$ terms are of $O(\epsilon)$ with the long channel parameter ξ in the denominator. If $\xi \rightarrow \infty$ were assumed, all $O(\epsilon)$ terms would vanish. Because the $H_\epsilon(\mathbf{q}, \mathbf{p})$ terms represent the Floquet parametric forcing of the cross wave by the progressive wave, allowing $H_\epsilon(\mathbf{q}, \mathbf{p})$ to vanish would remove all possibility of finding chaos in the system because nonlinear oscillations of the cross waves are required for a homoclinic/heteroclinic orbit to form in the phase plane (Wiggins, 1988).

2.6. Damping Forces

The scaled Hamilton's principle (2.4a) may be written as (Guenther & Schwerdtfeger, 1985)

$$\delta \int_{t_1}^{t_2} \mathcal{L} dt = \int_{t_1}^{t_2} \sum_{i=1}^3 D_i \delta q_i dt \quad (2.31)$$

where $\mathbf{D} = (D_1, D_2, D_3)$ is a set of generalized components of the damping force corresponding to the set of generalized coordinates $\mathbf{q} = (q, Q_1, Q_2)$. Substituting dS'_η from (2.3b) and $D\eta'/Dt'$ from (2.4c) and (A2) and applying the scales in (2.13) to the variables in (2.4a) yields the scaled variation of the action integral of the Lagrangian given by

$$\delta \int_{t_1}^{t_2} \mathcal{L} dt = - \int_{t_1}^{t_2} \int_{-b}^b \int_0^\xi (\alpha \phi_z \delta \eta) dx dy dt \quad (2.32)$$

Equating the variation of the action integral of the Lagrangian in both (2.31) and (2.32) gives

$$\int_{t_1}^{t_2} \sum_{i=1}^3 D_i \delta q_i dt = - \int_{t_1}^{t_2} \int_{-b}^b \int_0^\xi \alpha \phi_z \delta \eta dx dy dt \quad (2.33a)$$

where

$$\delta \eta = \sum_{i=1}^3 \left(\frac{\partial \eta}{\partial q_i} \delta q_i + \frac{\partial \eta}{\partial \dot{q}_i} \delta \dot{q}_i \right) \quad (2.33b)$$

Integrating the $\delta \dot{q}_i$ term in (2.33b) by parts with respect to time t and noting that δq vanishes at the arbitrary temporal values t_1 and t_2 reduces (2.33a) to

$$D_i = \alpha \int_{-b}^b \int_0^\xi \left[-\phi_z \frac{\partial \eta}{\partial q_i} + \frac{\partial}{\partial t} \left(\phi_z \frac{\partial \eta}{\partial \dot{q}_i} \right) \right] dx dy ; \quad i = 1, 2, 3 \quad (2.34)$$

Substituting the scaled velocity potential $\phi = \phi_c + \Gamma \lambda \phi_p$ from (2.22a,b) and the scaled free surface displacement $\eta = \eta_c + \Gamma \eta_p$ from (2.24b) and (2.25c) yields the following damping forces:

$$D_1 = \frac{b \alpha \xi}{\tau_1} \left(\dot{q} + \frac{\alpha}{\tau_1} q \right) \quad (2.35a)$$

$$D_2 = \frac{b \alpha \xi \tau_1 \Gamma^2}{\tau_\lambda} \left(\dot{Q}_1 + \frac{\alpha}{\tau_1 \lambda^2} Q_1 \right) \quad (2.35b)$$

$$D_3 = \frac{2 b \alpha \xi \tau_1 \tau \Gamma^2}{\lambda^4 \tau_\lambda^2} \left[\frac{\lambda^4 \tau_\lambda}{2 \tau} \left(\dot{Q}_2 + \frac{\alpha}{\tau_1 \lambda^2} Q_2 \right) + \frac{1}{\xi} \left(\dot{Q}_1 + \frac{\alpha}{\tau_1 \lambda^2} Q_1 \right) \right] \quad (2.35c)$$

Substituting (2.29) into (2.35) yields the damping forces expressed in terms of the canonical variables (q, p)

$$D_1 = \left(\frac{\alpha}{\tau_1} \right) p + \left(\frac{\alpha \varepsilon b \Gamma}{2 \tau_1^2 \lambda^3} \right) q Q_2 + \left(\frac{\alpha^2 b \xi}{\tau_1^2} \right) q \quad (2.36a)$$

$$D_2 = \left(\frac{\alpha}{\lambda^2 \tau_1} \right) P_1 - \left(\frac{2 \alpha \tau}{\xi \lambda^6 \tau_1 \tau_\lambda} \right) P_2 - \left(\frac{\alpha \varepsilon b \Gamma \tau^2}{\lambda^9 \xi \tau_\lambda^2} \right) q^2 + \left(\frac{\alpha^2 b \xi \Gamma^2}{\lambda^2 \tau_\lambda} \right) Q_1 \quad (2.36b)$$

$$D_3 = \left(\frac{\alpha}{\tau_1 \lambda^2} \right) P_2 + \left(\frac{\alpha \varepsilon b \Gamma \tau}{2 \lambda^5 \tau_\lambda} \right) q^2 + \left(\frac{2 \alpha^2 b \tau \Gamma^2}{\lambda^6 \tau_\lambda^2} \right) Q_1 + \left(\frac{\alpha^2 b \xi \Gamma^2}{\lambda^2 \tau_\lambda} \right) Q_2 \quad (2.36c)$$

The parameter ξ denotes a dimensionless length down the channel and is used as an ordering parameter because $\xi \gg 1$. This approximation by order is a way of both simplifying

the damping forces (2.36) and of applying the long channel assumption. This approximation is used only for determining the order of the coefficient for each variable grouping and not to scale the different variable combinations.

3. Canonical Transformations and Evolution Equations

In Hamiltonian systems, significant simplifications may be obtained using canonical transformations that preserve the dynamics of the evolution equations (Goldstein, 1980). Holmes (1986) used this property to evaluate chaotic waves in a cylindrical basin by applying two canonical transformations and obtained a simplified system of equations. It may occasionally be obvious how to choose some of the transformed variables as the new canonical variables (e.g., action-angle); but it is not always easy to determine the remaining new variables so that the resulting transformation is canonical. In a canonical transformation from the set (q, p) to the set (Q, P) , the dynamical state of the system may be defined in terms of the new set of variables (Q, P) . Because the canonical transformation destroys the distinction between coordinates and momenta, the set of variables Q may no longer be restricted to sets that define the configuration of the system as did the original set of coordinates q (Desloge, 1982).

3.1. Canonical Transformations: definition and properties

A time-dependent transformation $(q, p) \Rightarrow (Q, P)$ where

$$Q_i = Q_i(\mathbf{q}, \mathbf{p}, t), \quad P_i = P_i(\mathbf{q}, \mathbf{p}, t) \quad ; \quad i = 1, 2, \dots, N \quad (3.1a, b)$$

is canonical if and only if there exists a generating function $F(\mathbf{u}, \mathbf{U}, t)$ such that (Desloge, p.794, 1982)

$$dF(\mathbf{u}, \mathbf{U}, t) = \sum_{i=1}^N \left(v_i du_i - V_i dU_i \right) \quad (3.2a)$$

where

$$\begin{vmatrix} \frac{\partial^2 F}{\partial u_1 \partial U_1} & \cdot & \cdot & \cdot & \frac{\partial^2 F}{\partial u_1 \partial U_N} \\ \cdot & \cdot & \frac{\partial^2 F}{\partial u_i \partial U_j} & \cdot & \cdot \\ \frac{\partial^2 F}{\partial u_N \partial U_1} & \cdot & \cdot & \cdot & \frac{\partial^2 F}{\partial u_N \partial U_N} \end{vmatrix} \neq 0 \quad (3.2b)$$

and where the combinations of $2N$ new and old variables are

$$u_i, v_i = \begin{cases} q_i, p_i \\ p_i, -q_i \end{cases}, \quad U_i, V_i = \begin{cases} Q_i, P_i \\ P_i, -Q_i \end{cases}; \quad i = 1, 2, \dots, N \quad (3.2c-f)$$

Conditions (3.2) represent a generalized definition for a canonical transformation (Desloge, 1982). Canonical transformations have the following properties (Goldstein, p396, 1980):

- (1) If the transformed variables $(Q(q, p), P(q, p))$ are canonical, then the inverse transformed variables $(q(Q, P), p(Q, P))$ exist and are also canonical.
- (2) Two successive canonical transformations define a transformation that is also canonical.

3.2. Poisson Brackets

The Poisson bracket is one of several posterior verifications that a transformation is canonical (Goldstein, p397, 1980). If R_j, R_k are any two members of the transformed set of $2N$ variables

$\mathbf{Q}, \mathbf{P} = Q_1, \dots, Q_N; P_1, \dots, P_N$; the Poisson bracket for the canonical transformation (3.1) is defined as

$$[R_j, R_k]_{\mathfrak{P}} = \sum_{i=1}^N \left[\frac{\partial R_j}{\partial q_i} \frac{\partial R_k}{\partial p_i} - \frac{\partial R_j}{\partial p_i} \frac{\partial R_k}{\partial q_i} \right] \quad (3.3)$$

The transformation (3.1) is canonical if and only if the Poisson brackets satisfy the following conditions:

$$[Q_i, Q_j]_{\mathfrak{P}} = 0 ; \quad [Q_i, P_j]_{\mathfrak{P}} = \delta_{ij} ; \quad [P_i, P_j]_{\mathfrak{P}} = 0 \quad (3.4a-c)$$

where δ_{ij} = Kronecker delta.

3.3. Generalized Herglotz Algorithm (GHA)

The Herglotz algorithm (Guenther, et al., 1996) may be generalized by: (1) including time t as a parameter; and (2) defining a generating function by (3.2a) with a non-zero determinant of second derivatives with respect to \mathbf{u} , \mathbf{U} defined in (3.2b). The GHA transforms a set of $2N$ variables (\mathbf{u}, \mathbf{v}) to a set of $2N$ new variables (\mathbf{U}, \mathbf{V}) by choosing N of the new variables U_i and then computes the remaining N new variables V_i uniquely from the chosen U_i so that the transformation $(\mathbf{u}, \mathbf{v}) \Rightarrow (\mathbf{U}, \mathbf{V})$ is canonical. The variables U_i are chosen so that a desired simplification of the Hamiltonian may be achieved. The old (u_i, v_i) and new (U_i, V_i) variables may be any of the four combinations in (3.2c-f). The transformation $(\mathbf{u}, \mathbf{v}) \Rightarrow (\mathbf{U}, \mathbf{V})$ may be shown to be canonical by the Poisson bracket conditions (3.4a-c).

Two types of the GHA may be employed. Type I equates N new variables to old ones $U_i(\mathbf{u}, \mathbf{v}, t)$; and Type II equates N old variables to new ones $u_i = u_i(\mathbf{U}, \mathbf{V}, t)$. In both cases, however, the N new variables are to be chosen. Each type will be discussed separately below and are given by (3.5) and (3.6), respectively.

3.3.1. GHA: Type I

Equate N new variables to the old variables

$$U_i = U_i(\mathbf{u}, \mathbf{v}, t) ; \quad i = 1, 2, \dots, N \quad (3.5a)$$

such that the Poisson bracket (3.3) satisfies

$$[U_i, U_j]_{\mathbf{uv}} = 0 \quad ; \quad i, j = 1, 2, \dots, N \quad (3.5b)$$

and the determinant

$$\begin{vmatrix} \frac{\partial U_1}{\partial v_1} & \cdot & \cdot & \cdot & \frac{\partial U_1}{\partial v_N} \\ \cdot & \cdot & \frac{\partial U_i}{\partial v_j} & \cdot & \cdot \\ \frac{\partial U_N}{\partial v_1} & \cdot & \cdot & \cdot & \frac{\partial U_N}{\partial v_N} \end{vmatrix} \neq 0 \quad (3.5c)$$

Equate N Herglotz auxiliary functions $X_i(\mathbf{u}, \mathbf{v})$ to absolute value of the ratios of the old variables in either of the following forms:

$$X_i = X_i(\mathbf{u}, \mathbf{v}) = \begin{cases} |u_i/v_i| \\ |v_i/u_i| \end{cases} \quad ; \quad i = 1, 2, \dots, N \quad (3.5d, e)$$

such that the Jacobian of the chosen new variables \mathbf{U} and the auxiliary functions \mathbf{X} is nonzero; i.e.,

$$\frac{\partial(\mathbf{U}, \mathbf{X})}{\partial(\mathbf{u}, \mathbf{v})} \neq 0 \quad (3.5f)$$

Other forms for the Herglotz auxiliary functions \mathbf{X} (3.5d,e) that satisfy the nonzero Jacobian condition (3.5f) may also be used. Solve (3.5d or e) for $v_i = v_i(\mathbf{u}, \mathbf{X})$; substitute $v_i(\mathbf{u}, \mathbf{X})$ into (3.5a) and invert (3.5a) to obtain

$$u_i = u_i(\mathbf{U}, \mathbf{X}, t) \quad ; \quad i = 1, 2, \dots, N \quad (3.5g)$$

Compute the generating function $F(\mathbf{u}, \mathbf{U}, t)$ in (3.2a) from

$$dF(\mathbf{u}(\mathbf{U}, \mathbf{X}, t), \mathbf{U}, t) = \sum_{i=1}^N \left(v_i du_i - V_i dU_i \right) \quad (3.5h)$$

by expanding to obtain

$$\sum_{i=1}^N \left(\frac{\partial F}{\partial X_i} dX_i + \frac{\partial F}{\partial U_i} dU_i \right) = \sum_{i=1}^N \left(\sum_{j=1}^N v_j \frac{\partial u_j}{\partial X_i} dX_i + \sum_{j=1}^N v_j \frac{\partial u_j}{\partial U_i} dU_i - v_i dU_i \right) \quad (3.5i)$$

Equate the coefficients of like differentials on both sides of (3.5i) to find: 1) the generating function $F(\mathbf{u}, \mathbf{U}, t)$ from the indefinite integral

$$F(\mathbf{u}, \mathbf{U}, t) = \sum_{i=1}^N \int^{X_i} \sum_{j=1}^N v_j \frac{\partial u_j}{\partial X_i'} dX_i' + C(\mathbf{U}, t) \quad (3.5j)$$

and 2) the remaining N new variables $V_i(\mathbf{u}, \mathbf{v}, t)$ from

$$V_i(\mathbf{u}, \mathbf{v}, t) = \sum_{j=1}^N v_j \frac{\partial u_j}{\partial U_i} - \frac{\partial F}{\partial U_i} ; \quad i = 1, 2, \dots, N \quad (3.5k)$$

where the integration constant $C(\mathbf{U}, t)$ in (3.5j) is an arbitrary additive function of time and \mathbf{U} that may be neglected. The $2N$ old (u_i, v_i) and new (U_i, V_i) variables may be any of the four combinations in (3.2c-f). The transformation given by (3.5a) and (3.5k) may be shown to be canonical by the Poisson bracket conditions (3.4a-c). In order to determine the transformed Hamiltonian in terms of the new variables (\mathbf{U}, \mathbf{V}) , the inverse canonical transformation $(\mathbf{u}(\mathbf{U}, \mathbf{V}, t), \mathbf{v}(\mathbf{U}, \mathbf{V}, t))$ must be computed and the new Hamiltonian $K(\mathbf{Q}, \mathbf{P}, t)$ is given by

$$K(\mathbf{Q}, \mathbf{P}, t) = H(\mathbf{q}(\mathbf{Q}, \mathbf{P}, t), \mathbf{p}(\mathbf{Q}, \mathbf{P}, t), t) + \frac{\partial F(\mathbf{u}, \mathbf{U}, t)}{\partial t} \quad (3.5l)$$

where $F(\mathbf{u}, \mathbf{U}, t)$ is the generating function (3.5j) for the canonical transformation $(\mathbf{U}(\mathbf{u}, \mathbf{v}, t), \mathbf{V}(\mathbf{u}, \mathbf{v}, t))$.

3.3.2. GHA: Type II

Equate N old variables to the chosen new variables

$$u_i = u_i(\mathbf{U}, \mathbf{V}, t) \quad ; \quad i = 1, 2, \dots, N \quad (3.6a)$$

such that the Poisson bracket (3.3) satisfies

$$[u_i, u_j]_{\mathbf{UV}} = 0 \quad ; \quad i, j = 1, 2, \dots, N \quad (3.6b)$$

and the determinant

$$\begin{vmatrix} \frac{\partial u_1}{\partial V_1} & \cdot & \cdot & \cdot & \frac{\partial u_1}{\partial V_N} \\ \cdot & \cdot & \frac{\partial u_i}{\partial V_j} & \cdot & \cdot \\ \frac{\partial u_N}{\partial V_1} & \cdot & \cdot & \cdot & \frac{\partial u_N}{\partial V_N} \end{vmatrix} \neq 0 \quad (3.6c)$$

Equate N Herglotz auxiliary functions $X_i(\mathbf{U}, \mathbf{V})$ to absolute value of the ratios of the new variables in either of the following forms:

$$X_i = X_i(\mathbf{U}, \mathbf{V}) = \begin{cases} |U_i/V_i| \\ |V_i/U_i| \end{cases} \quad ; \quad i = 1, 2, \dots, N \quad (3.6d, e)$$

such that the Jacobian of the chosen old variables \mathbf{u} and the auxiliary functions \mathbf{X} is nonzero; i.e.,

$$\frac{\partial(\mathbf{u}, \mathbf{X})}{\partial(\mathbf{U}, \mathbf{V})} \neq 0 \quad (3.6f)$$

Other forms for the Herglotz auxiliary functions \mathbf{X} (3.6d,e) that satisfy the nonzero Jacobian condition (3.6f) may also be used. Solve (3.6d or e) for $V_i = V_i(\mathbf{U}, \mathbf{X})$; substitute $V_i(\mathbf{U}, \mathbf{X})$ into (3.6a) and invert (3.6a) to obtain

$$U_i = U_i(\mathbf{u}, \mathbf{X}, t) \quad ; \quad i = 1, 2, \dots, N \quad (3.6g)$$

Compute the generating function $F(\mathbf{u}, \mathbf{U}, t)$ in (3.2a) from

$$dF(\mathbf{u}, \mathbf{U}(\mathbf{u}, \mathbf{x}, t), t) = \sum_{i=1}^N \left(V_i dU_i - v_i du_i \right) \quad (3.6h)$$

by expanding to obtain

$$\sum_{i=1}^N \left(\frac{\partial F}{\partial X_i} dX_i + \frac{\partial F}{\partial u_i} du_i \right) = \sum_{i=1}^N \left(\sum_{j=1}^N V_j \frac{\partial U_j}{\partial X_i} dX_i + \sum_{j=1}^N V_j \frac{\partial U_j}{\partial u_i} du_i - v_i du_i \right) \quad (3.6i)$$

Equate the coefficients of like differentials on both sides of (3.6i) to find: 1) the generating function $F(\mathbf{u}, \mathbf{U}, t)$ from the indefinite integral

$$F(\mathbf{u}, \mathbf{U}, t) = \sum_{i=1}^N \int^{X_i} \sum_{j=1}^N V_j \frac{\partial U_j}{\partial X_i'} dX_i' + C(\mathbf{u}, t) \quad (3.6j)$$

and 2) the remaining N old variables $v_i(\mathbf{U}, \mathbf{V}, t)$ from

$$v_i(\mathbf{U}, \mathbf{V}, t) = \sum_{j=1}^N V_j \frac{\partial U_j}{\partial u_i} - \frac{\partial F}{\partial u_i} ; \quad i = 1, 2, \dots, N \quad (3.6k)$$

where the integration constant $C(u, t)$ in (3.6j) is an arbitrary additive function of time and \mathbf{u} that may be neglected. The $2N$ old (u_i, v_i) and new (U_i, V_i) variables may be any of the four combinations in (3.2c-f). The transformation given by (3.6a) and (3.6k) may be shown to be canonical by the Poisson bracket conditions (3.4a-c). The transformed Hamiltonian $K(\mathbf{Q}, \mathbf{P}, t)$ in terms of the new variables is given by

$$K(\mathbf{Q}, \mathbf{P}, t) = H(\mathbf{q}(\mathbf{Q}, \mathbf{P}, t), \mathbf{p}(\mathbf{Q}, \mathbf{P}, t), t) - \frac{\partial F(\mathbf{u}, \mathbf{U}, t)}{\partial t} \quad (3.6l)$$

where $F(\mathbf{u}, \mathbf{U}, t)$ is the generating function for the canonical transformation $(\mathbf{u}(\mathbf{U}, \mathbf{V}, t), \mathbf{v}(\mathbf{U}, \mathbf{V}, t))$.

3.4. Hamilton's Equations of Motion

Following the Legendre transformation (2.27), the dynamics of a damped dynamical system may be determined from Hamilton's equations of motion of the second kind (Scheck, 1990) according to

$$\dot{q}_i = \frac{\partial H}{\partial p_i} \quad ; \quad \dot{p}_i = -\frac{\partial H}{\partial q_i} - D_i \quad ; \quad i = 1, 2, \dots, N \quad (3.7a, b)$$

where $D(\mathbf{q}, \mathbf{p})$ is a set of generalized components of the damping force that are computed from the set of generalized coordinates \mathbf{q} . If a canonical transformation $\mathbf{Q} = \mathbf{Q}(\mathbf{q}, \mathbf{p}, t)$, $\mathbf{P} = \mathbf{P}(\mathbf{q}, \mathbf{p}, t)$ is obtained with a generating function $F(\mathbf{u}, \mathbf{U}, t)$ using the GHA-Type I, then the Hamiltonian K for the new set of variables is given by (3.5l) according to

$$K(\mathbf{Q}, \mathbf{P}, t) = H[\mathbf{q}(\mathbf{Q}, \mathbf{P}, t), \mathbf{p}(\mathbf{Q}, \mathbf{P}, t), t] + \frac{\partial F(\mathbf{u}, \mathbf{U}, t)}{\partial t} \quad (3.7c)$$

where u_i and U_i may be any of the four combinations in (3.2c-f). The transformed Hamilton's equations of motion (3.7a,b) are

$$\dot{Q}_i = \frac{\partial K}{\partial P_i} + \sum_{j=1}^N \tilde{D}_j \frac{\partial q_j}{\partial P_i} \quad ; \quad i = 1, 2, \dots, N \quad (3.7d)$$

$$\dot{P}_i = -\frac{\partial K}{\partial Q_i} - \sum_{j=1}^N \tilde{D}_j \frac{\partial q_j}{\partial Q_i} \quad ; \quad i = 1, 2, \dots, N \quad (3.7e)$$

where \tilde{D} is the transformed set of generalized components of the damping force

$$\tilde{D}_i(Q, P, t) = D_i[\mathbf{q}(Q, P, t), \mathbf{p}(Q, P, t)] ; \quad i = 1, 2, \dots, N \quad (3.7f)$$

After each canonical transformation, the damping force components may be introduced into all of the $2N$ evolution equations (3.7d,e) if q_j is a function of both Q and P .

3.5. Three Canonical Transformations

In order to apply the GMM to the dynamical system (3.7d,e), suitable canonical transformations must be found that will first simplify the $O(1)$ terms H_0 (2.30b); second simplify the $O(\varepsilon)$ terms H_ε (3.20c); and third suspend the $O(\gamma)$ terms H_γ (3.20d). In order to achieve this sequence, the GHA will be applied to two of the following three canonical transformations. Because the rotation of axes transformation (vide (3.8) below) is well-known (Goldstein, p146, 1980), the GHA will not be employed for that transformation even though it is still applicable. Each transformation will be discussed separately below and are given by (3.8), (3.18), and (3.21&28), respectively.

3.5.1. Rotation of axes $(\mathbf{q}, \mathbf{p}) \Rightarrow (\tilde{\mathbf{q}}, \tilde{\mathbf{p}})$

The Hamiltonian component H_0 in (2.30b) contains the cross-product terms $Q_1 Q_2$ and $P_1 P_2$ that may be removed by a rotation of axes transformation. The new canonical variables and the transformed Hamiltonian components are denoted by tildes. The rotation transformations are

$$q = \tilde{q} \quad p = \tilde{p} \quad (3.8a, b)$$

$$Q_1 = \tilde{Q}_1 \cos \theta + \tilde{Q}_2 \sin \theta \quad P_1 = \tilde{P}_1 \cos \theta + \tilde{P}_2 \sin \theta \quad (3.8c, d)$$

$$Q_2 = \tilde{Q}_2 \cos \theta - \tilde{Q}_1 \sin \theta \quad P_2 = \tilde{P}_2 \cos \theta - \tilde{P}_1 \sin \theta \quad (3.8e, f)$$

that are canonical because the Poisson bracket conditions (3.4a-c) are satisfied; viz.,

$$[q_i, q_j]_{\tilde{q}\tilde{p}} = 0 ; \quad [q_i, p_j]_{\tilde{q}\tilde{p}} = \delta_{ij} ; \quad [p_i, p_j]_{\tilde{q}\tilde{p}} = 0 \quad (3.9a-c)$$

The angle $\theta = \pi/4$ will eliminate the cross-product terms $\tilde{Q}_1 \tilde{Q}_2$ and $\tilde{P}_1 \tilde{P}_2$ in the Hamiltonian component H_0 in (2.30b).

The transformed Hamiltonian $\tilde{H}(\tilde{\mathbf{q}}, \tilde{\mathbf{p}}, t)$ may be computed by substituting (3.8) into (2.30) with $\theta = \pi/4$ and is given in component form by

$$H \Rightarrow \tilde{H} = \tilde{H}_0 + \tilde{H}_\varepsilon + \tilde{H}_\gamma(t) + O(\varepsilon^2, \varepsilon\gamma, \gamma^2) \quad (3.10a)$$

where

$$\begin{aligned} \tilde{H}_0 = & \left[\frac{b\xi}{2} \tilde{q}^2 + \frac{\tilde{p}^2}{2b\xi} \right] + \left[\frac{b\Gamma^2\xi}{2} \tilde{Q}_1^2 + \frac{\tilde{P}_1^2}{2b\beta^2\Gamma^2\xi} \right] + \left[\frac{b\Gamma^2\xi}{2} \tilde{Q}_2^2 + \frac{\tilde{P}_2^2}{2b\beta^2\Gamma^2\xi} \right] \\ & + \left[\frac{b\Gamma^2}{4} (\tilde{Q}_2^2 - \tilde{Q}_1^2) + \frac{\tau(\tilde{P}_1^2 - \tilde{P}_2^2)}{b\tau_1^2\Gamma^2\lambda^6\xi^2} \right] \end{aligned} \quad (3.10b)$$

$$\tilde{H}_\varepsilon = \frac{\varepsilon\Gamma}{2\sqrt{2}\tau_1\xi\lambda^3} \tilde{q}\tilde{p}(\tilde{Q}_2 - \tilde{Q}_1) - \frac{\varepsilon\tau(2\tau + \xi\lambda^4\tau_\lambda)}{2\sqrt{2}\tau_1\Gamma\xi^2\lambda^9\tau_\lambda} \tilde{q}^2\tilde{P}_1 + \frac{\varepsilon\tau(-2\tau + \xi\lambda^4\tau_\lambda)}{2\sqrt{2}\tau_1\Gamma\xi^2\lambda^9\tau_\lambda} \tilde{q}^2\tilde{P}_2 \quad (3.10c)$$

$$\begin{aligned}
\tilde{H}_\gamma = \gamma \cos\left(\frac{t}{\beta}\right) & \left(f_1 \frac{b\Gamma\lambda\tau_1(\tilde{Q}_1 + \tilde{Q}_2)}{\sqrt{2}\epsilon\beta} + \frac{(\tilde{Q}_1 + \tilde{Q}_2)\left((\lambda^2 - \sqrt{\tau})\tilde{P}_1 + (\lambda^2 + \sqrt{\tau})\tilde{P}_2\right)}{2\beta\xi\lambda^2} \right. \\
& \left. - \frac{\tau(\tilde{Q}_1 + \tilde{Q}_2)\left((\lambda^2 + \sqrt{\tau})\tilde{P}_2 + (-\lambda^2 + \sqrt{\tau})\tilde{P}_1\right)}{\beta\xi^2\lambda^6\tau_\lambda} + \frac{\tilde{p}\tilde{q}}{2\beta\xi} \right) \\
- \gamma \sin\left(\frac{t}{\beta}\right) & \left(\frac{b\Gamma^2}{2}(\tilde{Q}_1 + \tilde{Q}_2)^2 - \frac{\left((\lambda^2 - \sqrt{\tau})\tilde{P}_1 + (\lambda^2 + \sqrt{\tau})\tilde{P}_2\right)^2}{2b\tau_1^2\Gamma^2\xi^2\lambda^6} + \frac{1}{2}b\tilde{q}^2 - \frac{\tilde{p}^2}{2b\xi^2} \right)
\end{aligned} \tag{3.10d}$$

All of the terms that are proportional to the dimensionless surface tension parameter τ in (3.10) are of order $O(\xi^{-2})$. The coordinate-dependent \tilde{q} terms are of higher order of magnitude $O(\xi)$ than the momenta-dependent \tilde{p} terms. The Hamiltonian component \tilde{H}_ϵ in (3.10c) contains all the Floquet parametric forcing of the cross wave by the progressive wave (vide (1.2)). The 100% nonautonomous perturbed (wavemaker forcing) component \tilde{H}_γ in (3.10d) contains only one term that is dependent of the wavemaker shape function f_1 (Appendix C) and will not survive the averaging theorem that is required for the GMM. The free oscillations component \tilde{H}_0 in (3.10b) motivates the next canonical transformation to action-angle. The first three energy brackets in (3.10b) will be used to choose the action set of the new canonical variables (vide (3.11) below).

3.5.2. Action/angle transformation $(\tilde{q}, \tilde{p}) \Rightarrow (\hat{q}, \hat{p})$

The first three bracketed terms in the free oscillations component \tilde{H}_0 in (3.10b) are chosen to be the new action canonical variables $\hat{p}(\tilde{q}, \tilde{p})$. This transformation

is an application of the GHA-Type I (3.5) with $N = 3$ and $(u, U) = (\tilde{\mathbf{p}}, \hat{\mathbf{p}})$. The first three energy brackets in \tilde{H}_0 in (3.10b) are chosen to be the three new canonical variables $\hat{\mathbf{p}}(\tilde{\mathbf{q}}, \tilde{\mathbf{p}})$ according to

$$\hat{p} = \frac{b\xi}{2} \tilde{q}^2 + \frac{\tilde{p}^2}{2b\xi} \quad (3.11a)$$

$$\hat{p}_1 = \frac{b\Gamma^2\xi}{2} \tilde{Q}_1^2 + \frac{\tilde{P}_1^2}{2b\beta^2\Gamma^2\xi} \quad (3.11b)$$

$$\hat{p}_2 = \frac{b\Gamma^2\xi}{2} \tilde{Q}_2^2 + \frac{\tilde{P}_2^2}{2b\beta^2\Gamma^2\xi} \quad (3.11c)$$

that satisfy the Poisson brackets (3.5b) given by

$$[\hat{p}_i, \hat{p}_j]_{\tilde{\mathbf{q}}\tilde{\mathbf{p}}} = 0 \quad ; \quad i, j = 1, 2, 3 \quad (3.12a)$$

and the non-zero determinant (3.5c) given by

$$\begin{vmatrix} \frac{\partial \hat{p}}{\partial \tilde{q}} & \frac{\partial \hat{p}}{\partial \tilde{Q}_1} & \frac{\partial \hat{p}}{\partial \tilde{Q}_2} \\ \frac{\partial \hat{p}_1}{\partial \tilde{q}} & \frac{\partial \hat{p}_1}{\partial \tilde{Q}_1} & \frac{\partial \hat{p}_1}{\partial \tilde{Q}_2} \\ \frac{\partial \hat{p}_2}{\partial \tilde{q}} & \frac{\partial \hat{p}_2}{\partial \tilde{Q}_1} & \frac{\partial \hat{p}_2}{\partial \tilde{Q}_2} \end{vmatrix} = b^3 \Gamma^4 \xi^3 q Q_1 Q_2 \neq 0 \quad (3.12b)$$

The Herglotz auxiliary functions $X_i = X_i(\tilde{\mathbf{p}}, \tilde{\mathbf{q}})$ are chosen in the ratio form (3.5e) to be

$$X_1 = \tilde{q}/\tilde{p} \quad ; \quad X_2 = \tilde{Q}_1/\tilde{P}_1 \quad ; \quad X_3 = \tilde{Q}_2/\tilde{P}_2 \quad (3.13a-c)$$

that satisfy the nonzero Jacobian condition (3.5f)

$$\frac{\partial(\hat{\mathbf{p}}, \mathbf{x})}{\partial(\tilde{\mathbf{q}}, \tilde{\mathbf{p}})} = - \frac{(\tilde{P}_1^2 + b^2 \Gamma^4 \beta^2 \xi^2 \tilde{Q}_1^2)}{b^3 \beta^4 \Gamma^4 \xi^3 (\tilde{p} \tilde{P}_1 \tilde{P}_2)^2} (\tilde{P}_2^2 + b^2 \Gamma^4 \beta^2 \xi^2 \tilde{Q}_2^2) (\tilde{p}^2 + b^2 \xi^2 \tilde{q}^2) \neq 0 \quad (3.14)$$

Solving (3.13) for $\tilde{q}_i = \tilde{q}_i(\tilde{\mathbf{p}}, \mathbf{x})$; substituting $\tilde{q}_i(\tilde{\mathbf{p}}, \mathbf{x})$ into (3.11); and finally inverting (3.11) gives the following three new positive definite canonical action variables $\tilde{\mathbf{p}}(\mathbf{x}, \hat{\mathbf{p}})$:

$$\tilde{p} = \sqrt{\frac{2b\xi\hat{p}}{1+b^2\xi^2X_1^2}}, \quad \tilde{p}_1 = \sqrt{\frac{2b\xi\beta^2\Gamma^2\hat{p}_1}{1+b^2\xi^2\beta^2\Gamma^4X_2^2}}, \quad \tilde{p}_2 = \sqrt{\frac{2b\xi\beta^2\Gamma^2\hat{p}_2}{1+b^2\xi^2\beta^2\Gamma^4X_3^2}} \quad (3.15a-c)$$

Substituting $(u_i, v_i) = (\tilde{p}_i, -\tilde{q}_i)$ into (3.5j) gives the generating function F for the canonical transformation $(\tilde{\mathbf{q}}, \tilde{\mathbf{p}}) \Rightarrow (\hat{\mathbf{q}}, \hat{\mathbf{p}})$ from the following indefinite integral:

$$F(\tilde{\mathbf{p}}(\hat{\mathbf{p}}, \mathbf{x}), \hat{\mathbf{p}}) = - \sum_{i=1}^3 \int^{X_i} \left(\tilde{q} \frac{\partial \tilde{p}}{\partial X_i'} + \tilde{Q}_1 \frac{\partial \tilde{p}_1}{\partial X_i'} + \tilde{Q}_2 \frac{\partial \tilde{p}_2}{\partial X_i'} \right) dX_i' \\ = \left[\begin{aligned} & - \frac{b\xi\hat{p}X_1}{1+b^2\xi^2X_1^2} + \hat{p} \tan^{-1}(b\xi X_1) \\ & - \frac{b\xi\Gamma^2\beta^2\hat{p}_1X_2}{1+b^2\beta^2\xi^2\Gamma^4X_2^2} + \beta\hat{p}_1 \tan^{-1}(b\xi\beta\Gamma^2X_2) \\ & - \frac{b\xi\Gamma^2\beta^2\hat{p}_2X_3}{1+b^2\beta^2\xi^2\Gamma^4X_3^2} + \beta\hat{p}_2 \tan^{-1}(b\xi\beta\Gamma^2X_3) \end{aligned} \right] \quad (3.16)$$

where the arbitrary function of time has been dropped. Substitute $(u_i, v_i) = (\tilde{p}_i, -\tilde{q}_i)$; $V_i = -\hat{q}_i$ and (3.16) into (3.5k) to obtain the remaining set of three new angle variables $\hat{\mathbf{q}}(\tilde{\mathbf{q}}(\hat{\mathbf{p}}, \mathbf{x}), \tilde{\mathbf{p}}(\hat{\mathbf{p}}, \mathbf{x}))$ from

$$\hat{q}_i = \sum_{j=1}^3 \tilde{q}_j \frac{\partial \tilde{p}_j}{\partial \hat{p}_i} + \frac{\partial F}{\partial \hat{p}_i} ; \quad i = 1, 2, 3 \quad (3.17a)$$

where

$$\hat{q} = \text{Tan}^{-1} (b\xi X_1) \quad (3.17b)$$

$$\hat{Q}_1 = \beta \text{Tan}^{-1} (b\beta\xi\Gamma^2 X_2) \quad (3.17c)$$

$$\hat{Q}_2 = \beta \text{Tan}^{-1} (b\beta\xi\Gamma^2 X_3) \quad (3.17d)$$

Substitute $X_i = X_i(\tilde{\mathbf{p}}, \tilde{\mathbf{q}})$ from (3.13) into (3.17); then invert both (3.11) and (3.17) for $(\tilde{\mathbf{q}}(\hat{\mathbf{q}}, \hat{\mathbf{p}}), \tilde{\mathbf{p}}(\hat{\mathbf{q}}, \hat{\mathbf{p}}))$ to obtain the canonical transformation to action/angle variables given by the following:

$$\tilde{q} = \sqrt{\frac{2\hat{p}}{b\xi}} \sin \hat{q} \quad \tilde{p} = \sqrt{2b\xi\hat{p}} \cos \hat{q} \quad (3.18a, b)$$

$$\tilde{Q}_1 = \sqrt{\frac{2\hat{P}_1}{b\xi\Gamma^2}} \sin\left(\frac{\hat{Q}_1}{\beta}\right) \quad \tilde{P}_1 = \Gamma\beta\sqrt{2b\xi\hat{P}_1} \cos\left(\frac{\hat{Q}_1}{\beta}\right) \quad (3.18c, d)$$

$$\tilde{Q}_2 = \sqrt{\frac{2\hat{P}_2}{b\xi\Gamma^2}} \sin\left(\frac{\hat{Q}_2}{\beta}\right) \quad \tilde{P}_2 = \Gamma\beta\sqrt{2b\xi\hat{P}_2} \cos\left(\frac{\hat{Q}_2}{\beta}\right) \quad (3.18e, f)$$

where the action variables $\hat{\mathbf{p}} = (\hat{p}, \hat{P}_1, \hat{P}_2)$ are positive definite. This transformation may be confirmed to be canonical by the Poisson bracket conditions (3.4a-c) given by

$$[\tilde{q}_i, \tilde{q}_j]_{\text{ap}} = 0 ; \quad [\tilde{q}_i, \tilde{p}_j]_{\text{ap}} = \delta_{ij} ; \quad [\tilde{p}_i, \tilde{p}_j]_{\text{ap}} = 0 \quad (3.19a-c)$$

The transformed Hamiltonian $\hat{H}(\hat{\mathbf{q}}, \hat{\mathbf{p}}, t)$ may be computed by substituting (3.18) into (3.10) and is given in component form by

$$\tilde{H} \Rightarrow \hat{H} = \hat{H}_0 + \hat{H}_\varepsilon + \hat{H}_\gamma(t) + O(\varepsilon^2, \varepsilon\gamma, \gamma^2) \quad (3.20a)$$

where

$$\begin{aligned}
\hat{H}_0 = & \left[\hat{p} + \hat{p}_1 + \hat{p}_2 \right] + \left(\frac{2\beta^2\tau}{\lambda^6\xi\tau_1^2} \right) \hat{p}_1 \cos^2 \left(\frac{\hat{Q}_1}{\beta} \right) - \left(\frac{2\beta^2\tau}{\lambda^6\xi\tau_1^2} \right) \hat{p}_2 \cos^2 \left(\frac{\hat{Q}_2}{\beta} \right) \\
& - \left(\frac{\hat{p}_1}{2\xi} \right) \sin^2 \left(\frac{\hat{Q}_1}{\beta} \right) + \left(\frac{\hat{p}_2}{2\xi} \right) \sin^2 \left(\frac{\hat{Q}_2}{\beta} \right)
\end{aligned} \tag{3.20b}$$

$$\begin{aligned}
\hat{H}_e = & \frac{\varepsilon \hat{p} \sin(2\hat{Q})}{2\sqrt{b\xi^3}\lambda^3\tau_1} \left[\sqrt{\hat{p}_2} \sin \left(\frac{\hat{Q}_2}{\beta} \right) - \sqrt{\hat{p}_1} \sin \left(\frac{\hat{Q}_1}{\beta} \right) \right] \\
& - \frac{\varepsilon \beta \tau \hat{p} \sin^2 \hat{Q}}{\sqrt{b\xi^5}\lambda^9\tau_1\tau_\lambda} \left[(2\tau + \xi\lambda^4\tau_\lambda) \sqrt{\hat{p}_1} \cos \left(\frac{\hat{Q}_1}{\beta} \right) + (2\tau - \xi\lambda^4\tau_\lambda) \sqrt{\hat{p}_2} \cos \left(\frac{\hat{Q}_2}{\beta} \right) \right] \\
= & \frac{\varepsilon \hat{p}}{4\sqrt{b\xi^3}\lambda^3\tau_1} \left\{ \sqrt{\hat{p}_2} \left[\cos \left(2\hat{Q} - \frac{\hat{Q}_2}{\beta} \right) - \cos \left(2\hat{Q} + \frac{\hat{Q}_2}{\beta} \right) \right] \right. \\
& \left. - \sqrt{\hat{p}_1} \left[\cos \left(2\hat{Q} - \frac{\hat{Q}_1}{\beta} \right) - \cos \left(2\hat{Q} + \frac{\hat{Q}_1}{\beta} \right) \right] \right\} - \frac{\varepsilon \beta \tau \hat{p}}{2\sqrt{b\xi^5}\lambda^9\tau_1\tau_\lambda} \\
& \left\{ (2\tau + \xi\lambda^4\tau_\lambda) \sqrt{\hat{p}_1} \left[\cos \left(\frac{\hat{Q}_1}{\beta} \right) - \frac{1}{2} \cos \left(2\hat{Q} + \frac{\hat{Q}_1}{\beta} \right) - \frac{1}{2} \cos \left(2\hat{Q} - \frac{\hat{Q}_1}{\beta} \right) \right] \right. \\
& \left. + (2\tau - \xi\lambda^4\tau_\lambda) \sqrt{\hat{p}_2} \left[\cos \left(\frac{\hat{Q}_2}{\beta} \right) - \frac{1}{2} \cos \left(2\hat{Q} + \frac{\hat{Q}_2}{\beta} \right) - \frac{1}{2} \cos \left(2\hat{Q} - \frac{\hat{Q}_2}{\beta} \right) \right] \right\}
\end{aligned} \tag{3.20c}$$

$$\begin{aligned}
\hat{H}_\gamma = \gamma \cos\left(\frac{t}{\beta}\right) & \left[\left(\sqrt{\hat{P}_1} \sin\left(\frac{\hat{Q}_1}{\beta}\right) + \sqrt{\hat{P}_2} \sin\left(\frac{\hat{Q}_2}{\beta}\right) \right) \left[\frac{\sqrt{B} \lambda f_1 \tau_1}{\beta \epsilon \sqrt{\xi}} + \right. \right. \\
& \frac{(\lambda^2 - \sqrt{\tau}) (2\tau + \xi \lambda^4 \tau_\lambda)}{\lambda^6 \xi^2 \tau_\lambda} \sqrt{\hat{P}_1} \cos\left(\frac{\hat{Q}_1}{\beta}\right) + \\
& \left. \left. \frac{(\lambda^2 + \sqrt{\tau}) (-2\tau + \xi \lambda^4 \tau_\lambda)}{\lambda^6 \xi^2 \tau_\lambda} \sqrt{\hat{P}_2} \cos\left(\frac{\hat{Q}_2}{\beta}\right) \right] + \frac{\hat{p} \sin(2\hat{q})}{2\beta\xi} \right] \\
- \frac{\gamma}{\xi} \sin\left(\frac{t}{\beta}\right) & \left[\frac{-\beta^2}{\lambda^6 \tau_1^2} \left[(\lambda^2 - \sqrt{\tau}) \sqrt{\hat{P}_1} \cos\left(\frac{\hat{Q}_1}{\beta}\right) + (\lambda^2 + \sqrt{\tau}) \sqrt{\hat{P}_2} \cos\left(\frac{\hat{Q}_2}{\beta}\right) \right]^2 \right. \\
& \left. + \left[\sqrt{\hat{P}_1} \sin\left(\frac{\hat{Q}_1}{\beta}\right) + \sqrt{\hat{P}_2} \sin\left(\frac{\hat{Q}_2}{\beta}\right) \right]^2 + \hat{p} (\sin^2 \hat{q} - \cos^2 \hat{q}) \right]
\end{aligned} \tag{3.20d}$$

The free oscillations component \hat{H}_0 in (3.20b) and the Floquet parametric forcing component \hat{H}_ϵ in (3.20c) depend on the canonical variables (\hat{q}, \hat{p}) . The perturbed (wavemaker forcing) component \hat{H}_γ in (3.20d) is 100% nonautonomous and will not survive the averaging theorem that is required for the GMM. The dependency of \hat{H}_ϵ on (\hat{Q}_1, \hat{Q}_2) and some of the nonautonomous terms in \hat{H}_γ may be suspended by applying the next nonautonomous canonical transformation.

3.5.3. Hamilton-Jacobi transformation $(\hat{q}, \hat{p}) \Rightarrow (q, p)$

The main objectives of this final canonical transformation are to obtain a completely integrable unperturbed Hamiltonian system where \hat{Q}_1 and \hat{Q}_2 are cyclic coordinates and to suspend some of the nonautonomous terms in \hat{H}_γ in order to apply the GMM. This transformation will include near resonance cases by defining a detuning

parameter that transforms the first bracketed $O(1)$ term in (3.20b) $[\hat{p} + \hat{p}_1 + \hat{p}_2]$ to be $O(\epsilon)$ (Holmes, 1986). This transformation is an application of the GHA-Type II (3.6), with $N = 3$ and $(u, U) = (\hat{\mathbf{q}}, \mathbf{p})$. In order to eliminate \hat{Q}_1 and \hat{Q}_2 from the autonomous Hamiltonian component \hat{H}_ϵ (3.20c), the following nonautonomous transformations for $\hat{\mathbf{q}}(\mathbf{q}, t)$ in (3.6a) are chosen:

$$\hat{q} = \frac{t}{2\beta} + q + Q_1 \quad (3.21a)$$

$$\hat{Q}_1 = t + 2\beta Q_1 \quad (3.21b)$$

$$\hat{Q}_2 = 3t + 2\beta (q + Q_1 + Q_2) \quad (3.21c)$$

that satisfy the Poisson brackets (3.6b) given by

$$[\hat{q}_i, \hat{q}_j]_{\mathbf{qp}} = 0 \quad ; \quad i, j = 1, 2, 3 \quad (3.22a)$$

and the non-zero determinant (3.6c) given by

$$\begin{vmatrix} \frac{\partial \hat{q}}{\partial q} & \frac{\partial \hat{q}}{\partial Q_1} & \frac{\partial \hat{q}}{\partial Q_2} \\ \frac{\partial \hat{Q}_1}{\partial q} & \frac{\partial \hat{Q}_1}{\partial Q_1} & \frac{\partial \hat{Q}_1}{\partial Q_2} \\ \frac{\partial \hat{Q}_2}{\partial q} & \frac{\partial \hat{Q}_2}{\partial Q_1} & \frac{\partial \hat{Q}_2}{\partial Q_2} \end{vmatrix} = 4\beta^2 \neq 0 \quad (3.22b)$$

The Herglotz auxiliary functions $X_i = X_i(\mathbf{p}, \mathbf{q})$ are chosen in the ratio form (3.6d) to be

$$X_1 = p/q \quad ; \quad X_2 = P_1/Q_1 \quad ; \quad X_3 = P_2/Q_2 \quad (3.23a-c)$$

that satisfy the nonzero Jacobian condition (3.6f)

$$\frac{\partial(\hat{\mathbf{q}}, \mathbf{x})}{\partial(\mathbf{q}, \mathbf{p})} = \frac{4\beta^2}{qQ_1Q_2} \neq 0 \quad (3.24)$$

Solving (3.23) for $q_i = q_i(\mathbf{p}, \mathbf{x})$; substituting $q_i(\mathbf{p}, \mathbf{x})$ into (3.21); and finally inverting (3.21) gives $\mathbf{p}(\hat{\mathbf{q}}, \mathbf{x}, t)$ as

$$p = \frac{X_1}{2\beta} (2\beta \hat{q} - \hat{Q}_1), \quad P_1 = \frac{-X_2}{2\beta} (t - \hat{Q}_1), \quad P_2 = \frac{-X_3}{2\beta} (2t + 2\beta \hat{q} - \hat{Q}_2) \quad (3.25a-c)$$

Substituting $(U_i, V_i) = (p_i, -q_i)$ into (3.6j) will give the generating function F for the nonautonomous canonical transformation $(\hat{\mathbf{q}}, \hat{\mathbf{p}}) \Rightarrow (\mathbf{q}, \mathbf{p})$ from the following indefinite integral:

$$\begin{aligned} F(\hat{\mathbf{q}}, \mathbf{p}(\hat{\mathbf{q}}, \mathbf{x}, t), t) &= - \sum_{i=1}^3 \int^{x_i} \left[q \frac{\partial p}{\partial X_i'} + Q_1 \frac{\partial P_1}{\partial X_i'} + Q_2 \frac{\partial P_2}{\partial X_i'} \right] dX_i' \\ &= \frac{-1}{4\beta^2} \left[X_1 (2\beta \hat{q} - \hat{Q}_1)^2 + X_2 (t - \hat{Q}_1)^2 + X_3 (2t + 2\beta \hat{q} - \hat{Q}_2)^2 \right] \end{aligned} \quad (3.26)$$

where the arbitrary function of time and $\hat{\mathbf{q}}$ has been dropped. Substitute $(U_i, V_i) = (p_i, -q_i)$; $v_i = \hat{p}_i$ and (3.26) into (3.6k) to obtain the remaining set of three old variables $\hat{\mathbf{p}}(\mathbf{p}(\hat{\mathbf{q}}, \mathbf{x}, t), \mathbf{q}(\hat{\mathbf{q}}, t))$ from

$$\hat{p}_i = - \sum_{j=1}^3 q_j \frac{\partial p_j}{\partial \hat{q}_i} - \frac{\partial F}{\partial \hat{q}_i} \quad ; \quad i = 1, 2, 3 \quad (3.27a)$$

where

$$\hat{p} = \frac{1}{2\beta} \left[(2\beta \hat{q} - \hat{Q}_1) X_1 + (2t + 2\beta \hat{q} - \hat{Q}_2) X_3 \right] \quad (3.27b)$$

$$\hat{P}_1 = \frac{-1}{4\beta^2} \left[(2\beta \hat{q} - \hat{Q}_1) X_1 + (t - \hat{Q}_1) X_2 \right] \quad (3.27c)$$

$$\hat{P}_2 = \frac{-1}{4\beta^2} (2t + 2\beta \hat{q} - \hat{Q}_2) X_3 \quad (3.27d)$$

Substitute (3.25) for X_i into (3.27b-d) to obtain $\hat{\mathbf{p}}(\mathbf{p})$

$$\hat{p} = p - P_2 \quad (3.28a)$$

$$\hat{P}_1 = \frac{1}{2\beta} (P_1 - p) \quad (3.28b)$$

$$\hat{P}_2 = \frac{1}{2\beta} P_2 \quad (3.28c)$$

Since the action variables (3.28) must be nonnegative the condition on the new variables \mathbf{p} is

$$P_1 \geq p \geq P_2 > 0 \quad (3.28d)$$

The transformations (3.21) and (3.28) may be confirmed to be canonical by the Poisson bracket conditions (3.4a-c) given by

$$[\hat{q}_i, \hat{q}_j]_{\mathbf{qp}} = 0 ; \quad [\hat{q}_i, \hat{p}_j]_{\mathbf{qp}} = \delta_{ij} ; \quad [\hat{p}_i, \hat{p}_j]_{\mathbf{qp}} = 0 \quad (3.29a-c)$$

The first bracketed $O(1)$ term in (3.20b) $[\hat{p} + \hat{P}_1 + \hat{P}_2]$ will be transformed using (3.28) to

$$[\hat{p} + \hat{P}_1 + \hat{P}_2] = \left(1 - \frac{1}{2\beta} \right) (p - P_2) + \frac{P_1}{2\beta} \quad (3.30a)$$

The primary Floquet resonance condition is, approximately, (Holmes, 1986)

$$2 \omega'_c \approx \omega'_p \quad (3.30b)$$

so that

$$2 \omega'_c - \omega'_p = O(\epsilon) \quad (3.30c)$$

A detuning parameter Ω may now be defined as

$$\left(1 - \frac{\omega'_p}{2 \omega'_c}\right) = \left(1 - \frac{1}{2\beta}\right) = \epsilon \Omega \quad (3.30d)$$

where $\Omega = O(1)$ is the detuning parameter that defines the primary parametric Floquet resonance $\omega'_p : \omega'_c = 2:1$.

Substituting $\mathbf{q}(\hat{\mathbf{q}}, t)$ from (3.21) and $X_i = X_i(\mathbf{p}, \mathbf{q})$ from

(3.23) into (3.26) yields the following generating function in terms of $(\hat{\mathbf{q}}, \mathbf{p}, t)$:

$$F(\hat{\mathbf{q}}, \mathbf{p}, t) = p(-\hat{q} + \frac{1}{2\beta} \hat{Q}_1) + \frac{1}{2\beta} P_1(t - \hat{Q}_1) + \frac{1}{2\beta} P_2(2t + 2\beta \hat{q} - \hat{Q}_2) \quad (3.31)$$

The transformed Hamiltonian $H(\mathbf{q}, \mathbf{p}, t)$ may be computed by substituting (3.20), (3.21), (3.28), (3.30d) and (3.31) into (3.6l) and is given in component form for the autonomous and the nonautonomous terms by

$$\hat{H} - \frac{\partial F}{\partial t} \Rightarrow H = H_0 + H_0(t) + H_\epsilon + H_\epsilon(t) + H_\gamma + H_\gamma(t) + O(\epsilon^2, \epsilon\gamma, \gamma^2) \quad (3.32a)$$

where the autonomous Hamiltonian components are

$$H_0 = \left(-\frac{1}{8\beta\xi} + \frac{\beta\tau}{2\xi\lambda^6\tau_1^2}\right) (P_1 - p) + \left(-\frac{1}{\beta} + \frac{1}{8\beta\xi} - \frac{\beta\tau}{2\xi\lambda^6\tau_1^2}\right) P_2 \quad (3.32b)$$

$$H_{\epsilon} = \epsilon \Omega (p - P_2) + \frac{\epsilon (p - P_2) \sqrt{P_1 - p}}{4 \sqrt{2b\beta} \xi^5 \lambda^9 \tau_1 \tau_{\lambda}} \left[\left(2\beta \tau^2 - \xi \lambda^4 \tau_{\lambda} (\lambda^2 - \beta \tau) \right) \cos(2q) \right] \quad (3.32c)$$

$$H_{\gamma} = \left(\frac{\gamma \sqrt{b} f_1 \lambda \tau_1}{2 \epsilon \sqrt{2\xi} \beta^3} \right) \sqrt{P_1 - p} \sin(2Q_1) + \gamma \left(\frac{2\beta - 1}{4\beta\xi} \right) (P_2 - p) \sin 2(q + Q_1) \quad (3.32d)$$

and where the nonautonomous Hamiltonian components $H_0(t)$, $H_{\epsilon}(t)$, and $H_{\gamma}(t)$ are given in Appendix D by (D1), (D2), and (D3), respectively. The free oscillations component H_0 in (3.32b) depends only on the canonical variables \mathbf{p} . The Floquet parametric forcing component H_{ϵ} in (3.32c) is independent of the canonical variables Q_1 or Q_2 . The autonomous perturbed (wavemaker forcing) component H_{γ} in (3.32d) will survive the averaging theorem that is required for the GMM.

3.5.4. Combined transformation $(\mathbf{q}_{orig}, \mathbf{p}_{orig}) \Rightarrow (\mathbf{q}, \mathbf{p})$

The original canonical variables following the Legendre transformation are designated as $(\mathbf{q}_{orig}, \mathbf{p}_{orig})$ and may be expressed as functions of the final transformed canonical variables (\mathbf{q}, \mathbf{p}) by successive substitutions of the transformed variables (3.18), and (3.21,28) into (3.8); i.e.,

$$q_{orig} = \sqrt{\frac{2}{b\xi}} \sqrt{p - P_2} \sin\left(q + Q_1 + \frac{t}{2\beta}\right) \quad (3.33a)$$

$$p_{orig} = \sqrt{2b\xi} \sqrt{p - P_2} \cos\left(q + Q_1 + \frac{t}{2\beta}\right) \quad (3.33b)$$

$$Q_{1orig} = \frac{1}{\Gamma \sqrt{2b\beta\xi}} \left[\sqrt{P_1 - p} \sin \left(2Q_1 + \frac{t}{\beta} \right) + \sqrt{P_2} \sin \left(2(q + Q_1 + Q_2) + \frac{3t}{\beta} \right) \right] \quad (3.33c)$$

$$P_{1orig} = \Gamma \sqrt{\frac{b\beta\xi}{2}} \left[\sqrt{P_1 - p} \cos \left(2Q_1 + \frac{t}{\beta} \right) + \sqrt{P_2} \cos \left(2(q + Q_1 + Q_2) + \frac{3t}{\beta} \right) \right] \quad (3.33d)$$

$$Q_{2orig} = \frac{1}{\Gamma \sqrt{2b\beta\xi}} \left[-\sqrt{P_1 - p} \sin \left(2Q_1 + \frac{t}{\beta} \right) + \sqrt{P_2} \sin \left(2(q + Q_1 + Q_2) + \frac{3t}{\beta} \right) \right] \quad (3.33e)$$

$$P_{2orig} = \Gamma \sqrt{\frac{b\beta\xi}{2}} \left[-\sqrt{P_1 - p} \cos \left(2Q_1 + \frac{t}{\beta} \right) + \sqrt{P_2} \cos \left(2(q + Q_1 + Q_2) + \frac{3t}{\beta} \right) \right] \quad (3.33f)$$

The combined transformation $(\mathbf{q}_{orig}, \mathbf{p}_{orig}) \Rightarrow (\mathbf{q}, \mathbf{p})$ in (3.33) represents a canonical transformation by property (2) in §3.1. The combined transformation (3.33) may be used to obtain the transformed set of generalized components of the damping force $\tilde{\mathbf{D}}(\mathbf{q}, \mathbf{p}, t)$ and the transformed Hamilton's equations of motion (vide 3.35 and 3.36 below).

3.6. Transformed Damping Forces $\tilde{\mathbf{D}}(\mathbf{q}, \mathbf{p}, t)$

The damping forces (2.36) rewritten in terms of the original canonical variables designated as $(\mathbf{q}_{orig}, \mathbf{p}_{orig})$ are

$$D_1 = \left(\frac{\alpha}{\tau_1} \right) p_{orig} + \left(\frac{\alpha \varepsilon b \Gamma}{2 \tau_1^2 \lambda^3} \right) q_{orig} Q_{2orig} + \left(\frac{\alpha^2 b \xi}{\tau_1^2} \right) q_{orig} \quad (3.34a)$$

$$D_2 = \left(\frac{\alpha}{\lambda^2 \tau_1} \right) P_{1orig} - \left(\frac{2 \alpha \tau}{\xi \lambda^6 \tau_1 \tau_\lambda} \right) P_{2orig} - \left(\frac{\alpha \varepsilon b \Gamma \tau^2}{\lambda^9 \xi \tau_\lambda^2} \right) Q_{orig}^2 + \left(\frac{\alpha^2 b \xi \Gamma^2}{\lambda^2 \tau_\lambda} \right) Q_{1orig} \quad (3.34b)$$

$$D_3 = \left(\frac{\alpha}{\tau_1 \lambda^2} \right) P_{2_{orig}} + \left(\frac{\alpha \varepsilon b \Gamma \tau}{2 \lambda^5 \tau_\lambda} \right) q_{orig}^2 + \left(\frac{2 \alpha^2 b \tau \Gamma^2}{\lambda^6 \tau_\lambda^2} \right) Q_{1_{orig}} + \left(\frac{\alpha^2 b \xi \Gamma^2}{\lambda^2 \tau_\lambda} \right) Q_{2_{orig}} \quad (3.34c)$$

Substituting the combined canonical transformation (3.33) into the damping forces (3.34) yields the following transformed damping forces as functions of the final transformed canonical variables (q, p):

$$\begin{aligned} \tilde{D}_1 = & \frac{\sqrt{2b\xi}\alpha}{\tau_1} \sqrt{p-P_2} \cos\left(q+Q_1+\frac{t}{2\beta}\right) + \frac{\sqrt{2b\xi}\alpha^2}{\tau_1^2} \sqrt{p-P_2} \sin\left(q+Q_1+\frac{t}{2\beta}\right) \\ & + \frac{\varepsilon\alpha}{2\lambda^3\xi\sqrt{\beta}\tau_1^2} \sqrt{p-P_2} \sin\left(q+Q_1+\frac{t}{2\beta}\right) \left[\sqrt{P_2} \sin\left(2(q+Q_1+Q_2)+\frac{3t}{\beta}\right) \right. \\ & \quad \left. - \sqrt{P_1-p} \sin\left(2Q_1+\frac{t}{\beta}\right) \right] \end{aligned} \quad (3.35a)$$

$$\begin{aligned} \tilde{D}_2 = & \left(\frac{\sqrt{b\beta}\alpha\Gamma(2\tau+\lambda^4\xi\tau_\lambda)}{\tau_1\tau_\lambda\lambda^6\sqrt{2\xi}} \right) \sqrt{P_1-p} \cos\left(2Q_1+\frac{t}{\beta}\right) \\ & + \left(\frac{\sqrt{b\beta}\alpha\Gamma(-2\tau+\lambda^4\xi\tau_\lambda)}{\tau_1\tau_\lambda\lambda^6\sqrt{2\xi}} \right) \sqrt{P_2} \cos\left(2(q+Q_1+Q_2)+\frac{3t}{\beta}\right) \\ & - \frac{2\Gamma\varepsilon\alpha\tau^2}{\lambda^9\xi^2\tau_\lambda^2} (p-P_2) \sin^2\left(q+Q_1+\frac{t}{2\beta}\right) + \frac{\alpha^2\Gamma\sqrt{b\xi}}{\lambda^2\tau_\lambda\sqrt{2\beta}} \sqrt{P_1-p} \sin\left(2Q_1+\frac{t}{\beta}\right) \\ & + \frac{\alpha^2\Gamma\sqrt{b\xi}}{\lambda^2\tau_\lambda\sqrt{2\beta}} \sqrt{P_2} \sin\left(2(q+Q_1+Q_2)+\frac{3t}{\beta}\right) \end{aligned} \quad (3.35b)$$

$$\begin{aligned}
\tilde{D}_3 = & \left(\frac{\alpha \Gamma \sqrt{B} \beta \xi}{\sqrt{2} \lambda^2 \tau_1} \right) \left[-\sqrt{P_1 - P} \cos \left(2 Q_1 + \frac{t}{\beta} \right) + \sqrt{P_2} \cos \left(2 (q + Q_1 + Q_2) + \frac{3t}{\beta} \right) \right] \\
& + \left(\frac{\varepsilon \alpha \Gamma \tau}{\lambda^5 \xi \tau_\lambda} \right) (p - P_2) \sin^2 \left(q + Q_1 + \frac{t}{2\beta} \right) \\
& + \left(\frac{\alpha^2 \Gamma \sqrt{B} (2\tau - \lambda^4 \xi \tau_\lambda)}{\lambda^6 \tau_\lambda^2 \sqrt{2} \beta \xi} \right) \sqrt{P_1 - P} \sin \left(2 Q_1 + \frac{t}{\beta} \right) \\
& + \left(\frac{\alpha^2 \Gamma \sqrt{B} (2\tau + \lambda^4 \xi \tau_\lambda)}{\lambda^6 \tau_\lambda^2 \sqrt{2} \beta \xi} \right) \sqrt{P_2} \sin \left(2 (q + Q_1 + Q_2) + \frac{3t}{\beta} \right)
\end{aligned} \tag{3.35c}$$

that are 100% nonautonomous.

3.7. Averaged System

The transformed Hamilton's equations of motion (3.7d,e) rewritten in terms of the original ($\mathbf{q}_{orig}, \mathbf{p}_{orig}$) and the final (\mathbf{q}, \mathbf{p}) canonical variables are

$$\dot{q}_i = \frac{\partial H}{\partial p_i} + \sum_{j=1}^3 \tilde{D}_j \frac{\partial (q_{orig})_j}{\partial p_i} ; \quad i = 1, 2, 3 \tag{3.36a}$$

$$\dot{p}_i = -\frac{\partial H}{\partial q_i} - \sum_{j=1}^3 \tilde{D}_j \frac{\partial (q_{orig})_j}{\partial q_i} ; \quad i = 1, 2, 3 \tag{3.36b}$$

where $H(\mathbf{q}, \mathbf{p}, t)$ and $\tilde{\mathbf{D}}(\mathbf{q}, \mathbf{p}, t)$ = the transformed Hamiltonian and the transformed damping forces as functions of the final transformed canonical variables (\mathbf{q}, \mathbf{p}), respectively. Because it is difficult to analyze the full nonlinear non-autonomous system, an averaging method may be applied to obtain an autonomous system (Umeki & Kambe, 1989).

Following Holmes (1986), the averaged system of first order

ordinary differential equations may be determined by averaging the Hamiltonian $H(\mathbf{q}, \mathbf{p}, t)$ in (3.32a) where the summation expressions on the RHS of (3.36) are designated as

$$\sum_{\partial p_i} = \sum_{j=1}^3 \tilde{D}_j \frac{\partial (q_{orig})_j}{\partial p_i}, \quad \sum_{\partial q_i} = \sum_{j=1}^3 \tilde{D}_j \frac{\partial (q_{orig})_j}{\partial q_i} ; \quad i = 1, 2, 3$$

(3.37a, b)

The Hamiltonian $H(\mathbf{q}, \mathbf{p}, t)$ in (3.32a) averaged over the dimensionless cross wave period 2π (vide §2.3) is given by the following:

$$\begin{aligned} \langle H \rangle &= H_0(p, P_1, P_2) + H_e(q, p, P_1, P_2) + H_\gamma(q, p, P_1, P_2, Q_1) \\ &= \left(-\frac{1}{8\beta\xi} + \frac{\beta\tau}{2\xi\lambda^6\tau_1^2} \right) (P_1 - p) + \left(-\frac{1}{\beta} + \frac{1}{8\beta\xi} - \frac{\beta\tau}{2\xi\lambda^6\tau_1^2} \right) P_2 \\ &\quad + \varepsilon \left[\Omega(p - P_2) + \frac{(p - P_2)\sqrt{P_1 - p}}{4\sqrt{2b\beta\xi^5\lambda^9\tau_1\tau_\lambda}} \left[(2\beta\tau^2 - \xi\lambda^4\tau_\lambda(\lambda^2 - \beta\tau)) \cos(2q) \right] \right] \\ &\quad + \gamma \left[\left(\frac{\sqrt{b}f_1\lambda\tau_1}{2\varepsilon\sqrt{2\xi\beta^3}} \right) \sqrt{P_1 - p} \sin(2Q_1) + \left(\frac{2\beta - 1}{4\beta\xi} \right) (P_2 - p) \sin 2(q + Q_1) \right] \end{aligned}$$

(3.38)

Substituting the transformed damping forces (3.35) and the combined transformation (3.33) into (3.37) and then averaging over the dimensionless cross wave period 2π (vide §2.3) lead to

$$\begin{aligned} \langle \sum_{\partial p} \rangle = & -\alpha \varepsilon \frac{\lambda^6 \xi \tau_\lambda^2 (P_1 - p) + \tau \tau_1^2 (2\tau + \lambda^4 \xi \tau_\lambda) (P_2 - p)}{8\sqrt{2b\beta \xi^5 \lambda^9 \tau_1^2 \tau_\lambda^2 \sqrt{P_1 - p}}} \sin 2q \\ & + \frac{\alpha^2}{4} \left(\frac{2}{\tau_1^2} + \frac{\tau - \lambda^4 \xi \tau_\lambda}{\beta \lambda^6 \xi \tau_\lambda^2} \right) \end{aligned} \quad (3.39a)$$

$$\langle \sum_{\partial p_1} \rangle = \frac{\alpha^2 (-\tau + \lambda^4 \xi \tau_\lambda)}{4\beta \lambda^6 \xi \tau_\lambda^2} + \alpha \varepsilon \frac{\tau (2\tau + \lambda^4 \xi \tau_\lambda) (P_2 - p)}{8\sqrt{2b\beta \xi^5 \lambda^9 \tau_\lambda^2 \sqrt{P_1 - p}}} \sin 2q \quad (3.39b)$$

$$\langle \sum_{\partial p_2} \rangle = \frac{\alpha^2}{4} \left(\frac{-2}{\tau_1^2} + \frac{\tau + \lambda^4 \xi \tau_\lambda}{\beta \lambda^6 \xi \tau_\lambda^2} \right) + \alpha \varepsilon \frac{\sqrt{P_1 - p}}{8\sqrt{2b\beta \xi^3 \lambda^3 \tau_1^2}} \sin 2q \quad (3.39c)$$

and

$$\langle \sum_{\partial q} \rangle = \frac{\alpha}{\tau_1} p - \frac{\alpha (\tau + \lambda^4 \xi \tau_\lambda (\lambda^2 - 1))}{\lambda^6 \xi \tau_1 \tau_\lambda} P_2 - \alpha \varepsilon \frac{\sqrt{P_1 - p} (p - P_2)}{4\sqrt{2b\beta \xi^3 \lambda^3 \tau_1^2}} \cos 2q \quad (3.40a)$$

$$\langle \sum_{\partial Q_1} \rangle = \alpha \frac{(4\lambda^2 - 1)(p - P_2) + P_1}{2\lambda^2 \tau_1} + \frac{\alpha \varepsilon (\tau \tau_1^2 - \lambda^2 \tau_\lambda) (p - P_2)}{2\sqrt{2b\beta \xi^3 \lambda^5 \tau_\lambda \tau_1^2}} \sqrt{P_1 - p} \cos 2q \quad (3.40b)$$

$$\langle \sum_{\partial Q_2} \rangle = \frac{\alpha (-\tau + \lambda^4 \xi \tau_\lambda)}{\lambda^6 \xi \tau_1 \tau_\lambda} P_2 \quad (3.40c)$$

Substituting (3.38), (3.39), and (3.40) into (3.36) yields the following averaged system of first order ordinary differential equations:

$$\begin{aligned} \dot{q} = & -a_1 + \varepsilon \Omega + \varepsilon a_3 \frac{2P_1 + P_2 - 3p}{\sqrt{P_1 - p}} \cos[2q] - \gamma c_1 \frac{\sin[2Q_1]}{\varepsilon \sqrt{P_1 - p}} \\ & - \gamma c_2 \sin[2(q + Q_1)] + \alpha^2 d_1 - \alpha \varepsilon \left[\frac{d_2 (P_1 - p) + d_3 (P_2 - p)}{\sqrt{P_1 - p}} \right] \sin[2q] \end{aligned} \quad (3.41a)$$

$$\begin{aligned} \dot{p} = & 4 \varepsilon a_3 \sqrt{P_1 - p} (p - P_2) \sin[2q] - 2 \gamma c_2 (P_2 - p) \cos[2(q + Q_1)] \\ & + \alpha d_4 P_2 - \frac{\alpha}{\tau_1} p + 2 \alpha \varepsilon d_2 \sqrt{P_1 - p} (p - P_2) \cos[2q] \end{aligned} \quad (3.41b)$$

$$\begin{aligned} \dot{P}_1 = & - \frac{4 \gamma}{\varepsilon} c_1 \sqrt{P_1 - p} \cos[2Q_1] - 2 \gamma c_2 (P_2 - p) \cos[2(q + Q_1)] \\ & + \alpha \frac{(4 \lambda^2 - 1) (P_2 - p) - P_1}{2 \lambda^2 \tau_1} - \alpha \varepsilon d_5 \sqrt{P_1 - p} (p - P_2) \cos[2q] \end{aligned} \quad (3.41c)$$

$$\dot{P}_2 = \alpha P_2 \left(\frac{\tau - \lambda^4 \xi \tau_\lambda}{\lambda^6 \xi \tau_1 \tau_\lambda} \right) \quad (3.41d)$$

$$\begin{aligned} \dot{Q}_1 = & a_1 + \varepsilon a_3 \frac{(p - P_2)}{\sqrt{P_1 - p}} \cos[2q] + \gamma c_1 \frac{\sin[2Q_1]}{\varepsilon \sqrt{P_1 - p}} \\ & + \alpha^2 d_6 + \alpha \varepsilon d_3 \frac{P_2 - p}{\sqrt{P_1 - p}} \sin[2q] \end{aligned} \quad (3.41e)$$

$$\begin{aligned} \dot{Q}_2 = & a_2 - \varepsilon \Omega - 2 \varepsilon a_3 \sqrt{P_1 - p} \cos[2q] + \gamma c_2 \sin[2(q + Q_1)] \\ & + \alpha^2 d_7 + \alpha \varepsilon d_2 \sqrt{P_1 - p} \sin[2q] \end{aligned} \quad (3.41f)$$

where the coefficients a_i , c_i , and d_i are summarized in Appendix C. The RHS of (3.41) are independent of the variable Q_2 ; and the condition (3.28d) on the final canonical transformed variable p becomes $P_1 > p \geq P_2 > 0$.

4. Application of the GMM

The GMM provides the necessary conditions for the occurrence of chaos in three classes of perturbed dynamical systems specified as I, II, and III in Wiggins (p.336, 1988). The GMM determines the existence of transverse homoclinic points; *i.e.*, transverse intersections between the stable and unstable manifolds to any invariant sets of the perturbed system given the existence of a homoclinic/heteroclinic orbit to a hyperbolic invariant manifold in the unperturbed (undamped $\alpha=0$ and unperturbed $\gamma=0$) system. The unperturbed system $\alpha=\gamma=0$ is analyzed in §4.1. The GMM will be applied to two classes of perturbed systems. The GMM predicts chaos in §4.2 for the perturbed Hamiltonian system $\alpha=0$, $\gamma>0$ that is System III. The GMM fails to predict chaos in §4.3 for the perturbed dissipative system $\alpha>0$, $\gamma>0$ that is System I.

4.1. Geometric Structure of Unperturbed Phase Space ($\alpha=0, \gamma=0$)

The unperturbed vector field $(\dot{\mathbf{q}}, \dot{\mathbf{p}})$ may be obtained by setting the perturbation (wavemaker forcing) parameter $\gamma=0$ and dissipation $\alpha=0$ in the evolution equations (3.41) and is given by

$$\dot{q} = -a_1 + \varepsilon \Omega + \varepsilon a_3 \frac{2P_1 + P_2 - 3p}{\sqrt{P_1 - p}} \cos(2q) \quad (4.1a)$$

$$\dot{p} = 4 \varepsilon a_3 \sqrt{P_1 - p} (p - P_2) \sin(2q) \quad (4.1b)$$

$$\dot{P}_1 = 0 \quad (4.1c)$$

$$\dot{P}_2 = 0 \quad (4.1d)$$

$$\dot{Q}_1 = a_1 + \varepsilon a_3 \frac{(p - P_2)}{\sqrt{P_1 - p}} \cos(2q) \quad (4.1e)$$

$$\dot{Q}_2 = a_2 - \varepsilon \Omega - 2\varepsilon a_3 \sqrt{P_1 - p} \cos(2q) \quad (4.1f)$$

where the coefficients a_1, a_2 and a_3 are defined in Appendix C and are functions of the following dimensionless parameters: the long channel parameter ξ (2.13f), the frequency ratio parameter β (2.14b), the surface tension parameter τ (2.14d), and the wave-length ratio parameter λ (2.14e). The unperturbed vector field $\alpha=\gamma=0$ (4.1) has the form of a three degrees of freedom Hamiltonian system with $(q, p, P_1, P_2, Q_1, Q_2) \in \mathbb{T}^1 \times \mathbb{R}^1 \times \mathbb{R}^2 \times \mathbb{T}^2$. An important consequence of the Hamilton-Jacobi canonical transformation (§3.5c) is that the unperturbed Floquet Hamiltonian

$$\langle H \rangle (\gamma=0) = H_0(p, P_1, P_2) + H_\varepsilon(q, p, P_1, P_2) \quad (4.2)$$

is independent of the variables Q_1 and Q_2 , where $\langle H \rangle$ is given by (3.38); and that the condition (3.28d) on the canonical variables p is $P_1 > p \geq P_2 > 0$.

4.1.1. Hyperbolic saddle points

For every $(P_1, P_2) \in \mathbb{R}^2$, the (q-p) components of the unperturbed vector field $\alpha=\gamma=0$ (4.1) possess an hyperbolic saddle point that varies smoothly with P_1 and P_2 . Solving (4.1b) for p_0 from

$$4 \varepsilon a_3 \sqrt{P_1 - P_0} (p_0 - P_2) \sin(2q_0) = 0 \quad (4.3a)$$

gives

$$p_0(P_2) = P_2 \quad ; \quad 2q_0 \neq n\pi \quad ; \quad n = 0, 1, \dots \quad (4.3b, c)$$

Substituting (4.3b) into (4.1a) and solving for q_0 from

$$-a_1 + \varepsilon \Omega + \varepsilon a_3 \frac{2P_1 + P_2 - 3P_2}{\sqrt{P_1 - P_2}} \cos(2q_0) = 0 \quad (4.3d)$$

gives

$$q_0(P_1, P_2) = \frac{1}{2} \cos^{-1} \left(\frac{a_1 - \varepsilon \Omega}{2 \varepsilon a_3 \sqrt{P_1 - P_2}} \right) \quad (4.3e)$$

where

$$P_1 \geq P_2 + \left(\frac{a_1 - \varepsilon \Omega}{2 \varepsilon a_3} \right)^2 \quad (4.3f)$$

The fixed point (q_0, p_0) (4.3e, b) represents a hyperbolic saddle point provided that the determinant

$$\left| \begin{array}{cc} \frac{\partial \dot{q}}{\partial q} & \frac{\partial \dot{q}}{\partial p} \\ \frac{\partial \dot{p}}{\partial q} & \frac{\partial \dot{p}}{\partial p} \end{array} \right|_{(q=q_0, p=p_0)} = 4 \left[(a_1 - \varepsilon \Omega)^2 - 4 (P_1 - P_2) \varepsilon^2 a_3^2 \right] < 0 \quad (4.3g)$$

is negative and where (\dot{q}, \dot{p}) are given by (4.1a,b). The symmetry properties of Hamiltonian systems require that, if e is an eigenvalue of the determinant (4.3g), then so is $-e$. This implies that the stable and the unstable manifolds of the hyperbolic saddle point (q_0, p_0) (4.3e,b) have equal dimensions (Abraham & Marsden, 1978). In the full six-dimensional phase space $(q, p, P_1, P_2, Q_1, Q_2) \in T^1 \times \mathbb{R}^1 \times \mathbb{R}^2 \times T^2$, the unperturbed system $\alpha = \gamma = 0$ has a four-dimensional $(\mathbb{R}^2 \times T^2)$ normally hyperbolic invariant manifold (with boundary $\partial \mathcal{M}$) given by the union of the hyperbolic saddle points (q_0, p_0) in (3.4d,b) according to

$$\mathcal{M} = \{(q, p, P_1, P_2, Q_1, Q_2) \in T^1 \times \mathbb{R}^1 \times \mathbb{R}^2 \times T^2 \mid q = q_0(P_1, P_2); p = p_0(P_2)\} \quad (4.4)$$

The normally hyperbolic invariant manifold \mathcal{M} has five-dimensional $(\mathbb{R}^1 \times \mathbb{R}^2 \times T^2)$ stable manifold $W^s(\mathcal{M})$ and unstable manifold $W^u(\mathcal{M})$ that coincide along the five-dimensional heteroclinic manifold

$$\mathcal{H} = W^s(\mathcal{M}) \cap W^u(\mathcal{M}) = \mathcal{M} \quad (4.5)$$

where $W^s(\mathcal{M})$ and $W^u(\mathcal{M})$ are the set of initial conditions that approach the hyperbolic saddle points on \mathcal{M} as $t \rightarrow \pm\infty$ under the action of the unperturbed flow (Wiggins, p.354, 1988). The unperturbed locally stable and unstable manifolds of the normally hyperbolic invariant manifold \mathcal{M} may be denoted as $W_{loc}^s(\mathcal{M})$ and $W_{loc}^u(\mathcal{M})$, respectively.

Because $\dot{P}_1 = \dot{P}_2 = 0$ by (4.1c,d), no trajectories may cross the boundary of the normally hyperbolic invariant manifold $\partial\mathcal{M}$. However, in the perturbed system (§4.2,3) \dot{P}_1 and \dot{P}_2 may not be zero; and, therefore, trajectories may cross the boundary $\partial\mathcal{M}$.

4.1.2. Dynamics on \mathcal{M}

The unperturbed vector field $\alpha=\gamma=0$ (4.1) restricted to the normally hyperbolic invariant manifold \mathcal{M} (4.4) may be determined by substituting $q = q_0$ (4.3e) and $p = p_0$ (4.3b) into (4.1c-f) according to

$$\dot{P}_1 = 0 ; \quad \dot{P}_2 = 0 \quad (4.6a,b)$$

$$\dot{Q}_1 = a_1 \quad (4.6c)$$

$$\dot{Q}_2 = a_2 - a_1 \quad (4.6d)$$

where the coefficients a_1 and a_2 are defined in Appendix C. The unperturbed vector field $\alpha=\gamma=0$ restricted to \mathcal{M} (4.6) has the form of a two degrees of freedom (*i.e.*, four-dimensional phase space $(T^1 \times \mathbb{R}^1 \times T^2)$) completely integrable Hamiltonian system with the Hamiltonian given by the level energy surfaces

$$H(P_1, P_2) = \langle H \rangle (q = q_0, p = p_0; \gamma = 0) = a_1 P_1 + (a_2 - a_1) P_2 = E \quad (4.7)$$

where $\langle H \rangle$ is given by (3.38); E is a constant energy set of the system; and P_1 and P_2 are the two constants (or integrals) of motion (Hao, 1990 and Helleman, 1980). The constant energy E allows the phase space motion to be

reduced from four dimensions ($\mathbb{R}^2 \times \mathbb{T}^2$) to three dimensions. The constancy of P_1 and P_2 by (4.6a,b) or by (4.1c,d) allows a further reduction to a one dimensional surface in the three-dimensional constant energy space. On the one-dimensional surface, the angular motion is parameterized by the two frequencies associated with each degree of freedom from (4.6c,d) according to

$$\sigma_1 = a_1 \quad (4.8a)$$

$$\sigma_2 = a_2 - a_1 \quad (4.8b)$$

where the coefficients a_1 and a_2 are defined in Appendix C. The angular components of the motion on the normally hyperbolic invariant manifold \mathcal{M} (4.4) may be determined by integrating (4.6c,d) and are given by

$$Q_1(t) = a_1 t + Q_1(0) \quad (4.9a)$$

$$Q_2(t) = (a_2 - a_1) t + Q_2(0) \quad (4.9b)$$

Consequently, the normally hyperbolic invariant manifold \mathcal{M} (4.4) has the structure of a two-parameter (P_1, P_2) family of two-dimensional tori. For a fixed $P_1 = \bar{P}_1$ and $P_2 = \bar{P}_2$, a corresponding two-dimensional torus on \mathcal{M} , shown in Figure 3 may be denoted as

$$\Upsilon(\bar{P}_1, \bar{P}_2) = \left\{ (q, p, P_1, P_2, Q_1, Q_2) \in \mathbb{T}^1 \times \mathbb{R}^1 \times \mathbb{R}^2 \times \mathbb{T}^2 \ni q = q_0(\bar{P}_1, \bar{P}_2); \right. \\ \left. p = p_0(\bar{P}_2); P_1 = \bar{P}_1; P_2 = \bar{P}_2 \right\} \quad (4.10)$$

where the hyperbolic saddle points $q_0(P_1, P_2)$ and $p_0(P_2)$ are given by (4.3e,b). Each two-dimensional torus $\Upsilon(\bar{P}_1, \bar{P}_2) \subset \mathcal{M}$ (4.10) is invariant; i.e., any trajectory starting at a point on the surface of the torus remains on the surface.

For a constant energy value $E = \bar{E}$, say, the corresponding level energy surface (4.7) may be represented in the three-dimensional constant energy space as a family of concentric tori as shown in Figure 3. The (P_1, P_2) -variables measure the radii of the circular cross section and the minimum ring of the torus shown in Figure 3. The angular (Q_1, Q_2) -variables measure the two angles of a point on the surface of the torus as shown in Figure 3. Choosing $E = \bar{E}$ and fixing the value of P_1 also fixes the value of P_2 by (4.7). Because both frequencies of motion (4.8) are independent of P_1 or P_2 , they do not change from one concentric torus to another concentric torus. The motion on the surface of the invariant torus $\Upsilon(\bar{P}_1, \bar{P}_2) \subset \mathcal{M}$ is quasiperiodic (or conditionally periodic) (Lichtenberg & Lieberman, p.22, 1992). If the frequency ratio

$$\frac{\sigma_1}{\sigma_2} = \frac{a_1}{a_2 - a_1} \quad (4.11)$$

is a rational number, the motion on the surface of the two-dimensional invariant torus degenerates into a periodic trajectory of one-dimension that closes on itself; and the torus may be referred to as a resonant torus. In general, the frequency ratio (4.11) is an irrational number and the motion on the surface of the two-dimensional invariant torus may no longer be periodic; *i.e.*, trajectories wind densely on the surface of the torus and never close on themselves; and the torus may be referred to as a nonresonant torus (Arnold, Appendix 8, 1978). The two-dimensional nonresonant invariant torus $\Upsilon(\bar{P}_1, \bar{P}_2) \subset \mathcal{M}$ has a three-dimensional $(\mathbb{R}^1 \times \mathbb{T}^2)$ stable manifold $W^s(\Upsilon(\bar{P}_1, \bar{P}_2))$ and unstable manifold $W^u(\Upsilon(\bar{P}_1, \bar{P}_2))$ that coincide along the

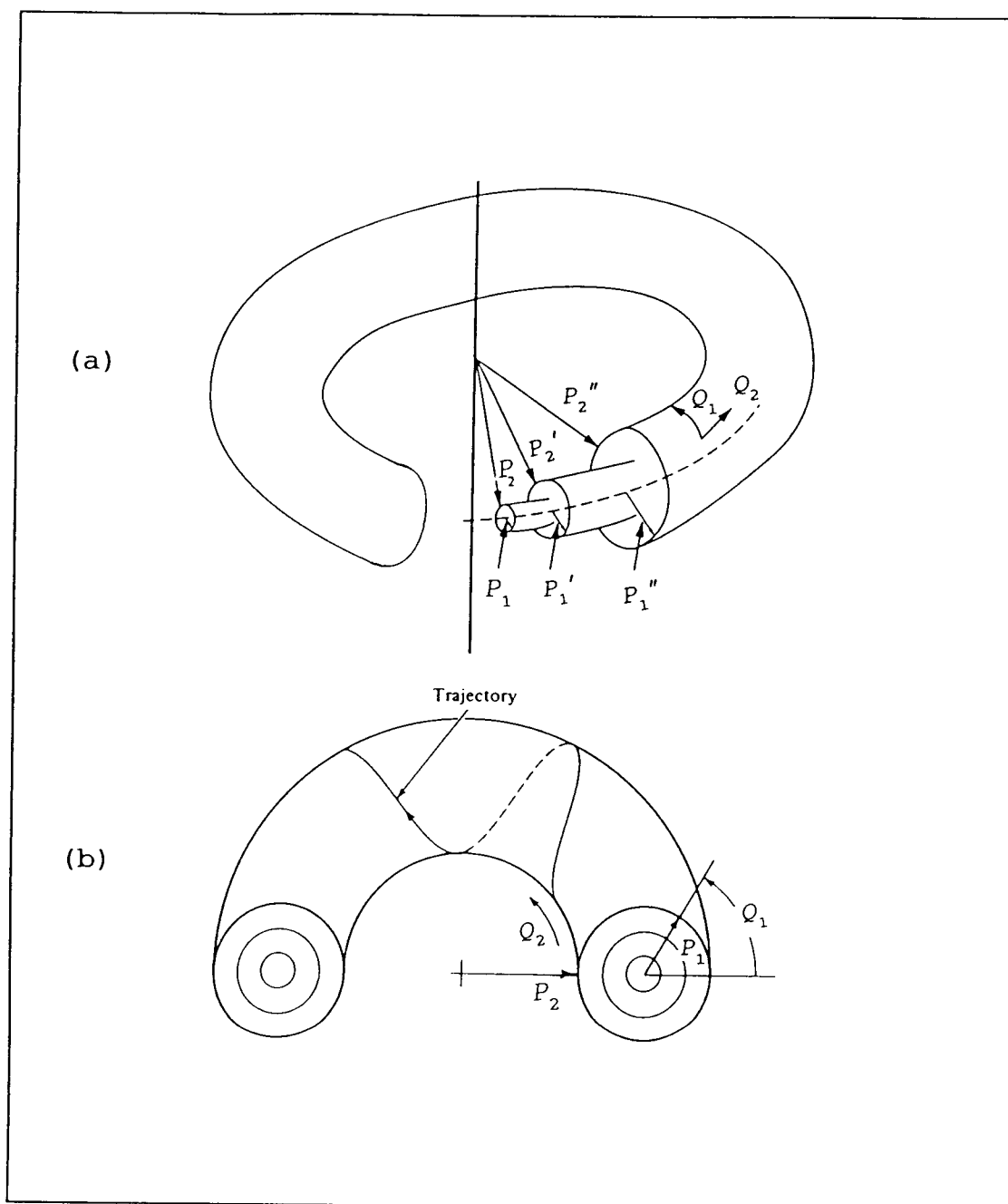


Figure 3. Motion of a phase space point for an integrable Hamiltonian system with two degrees of freedom (4.6). (a) Invariant tori in a three dimensional constant energy space $E = \bar{E}$ (after Rasband, 1990). (b) The flow on a two-dimensional torus on \mathcal{M} for $H(P_1, P_2) = E$ (after Lichtenberg & Lieberman, 1992).

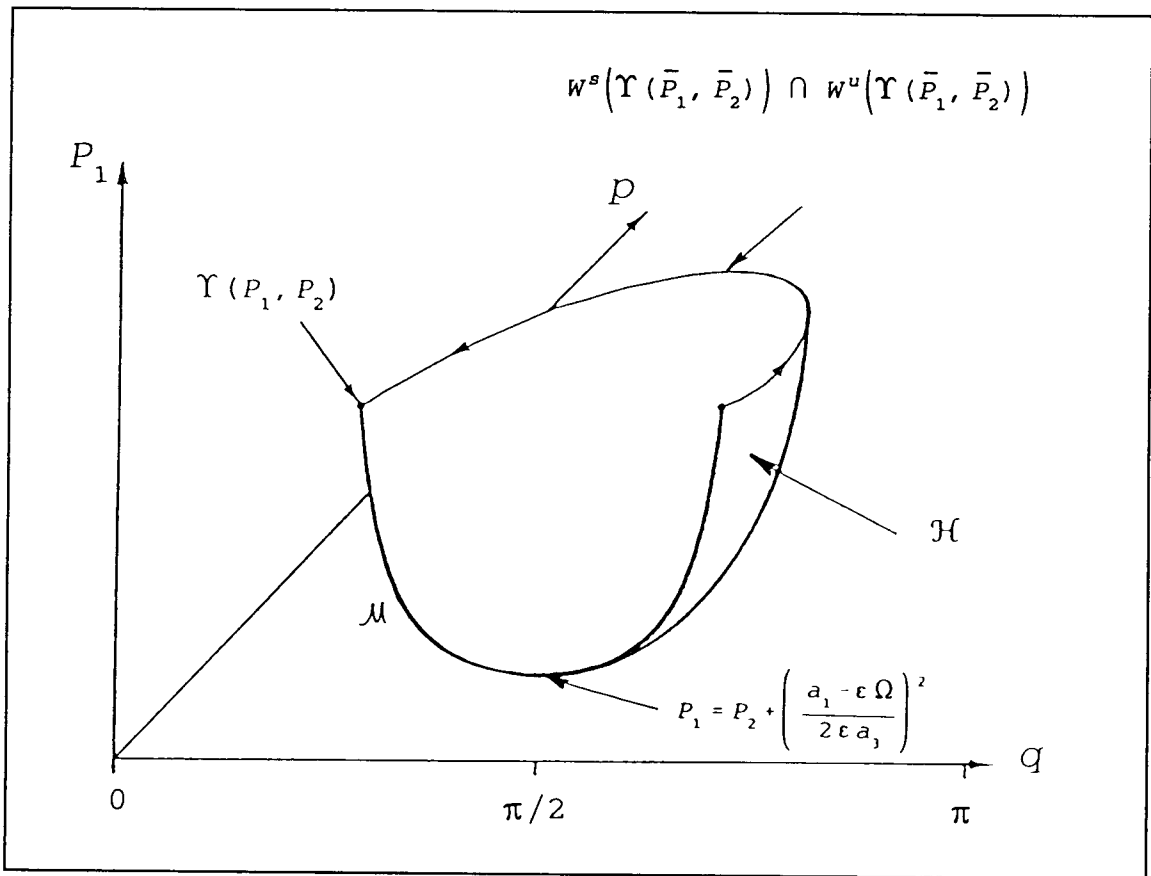


Figure 4. Three-dimensional unperturbed heteroclinic manifold \mathcal{H} (after Bowline et al., in press).

three-dimensional $(\mathbb{R}^1 \times \mathbb{T}^2)$ heteroclinic manifold \mathcal{H} defined in (4.5) for fixed values of $P_1 = \bar{P}_1$ and $P_2 = \bar{P}_2$ as shown in Figure 4. By invariance of manifolds (Wiggins, p.387, 1988), $w^s(\Upsilon(\bar{P}_1, \bar{P}_2)) \subset w^s(\mathcal{M})$ and $w^u(\Upsilon(\bar{P}_1, \bar{P}_2)) \subset w^u(\mathcal{M})$. On a constant level energy surface (4.7), the nonresonant invariant tori $\Upsilon(\bar{P}_1, \bar{P}_2)$ and these stable and unstable manifolds are not isolated. Additionally, the two-dimensional nonresonant invariant torus $\Upsilon(\bar{P}_1, \bar{P}_2) \subset \mathcal{M}$ has a two-dimensional center manifold $w^c(\Upsilon(\bar{P}_1, \bar{P}_2))$ corresponding to non-exponentially expanding or contracting

directions tangent to the normally hyperbolic invariant manifold \mathcal{M} (Wiggins, p.383, 1988).

4.1.3. Heteroclinic orbits

For fixed values of $(P_1, P_2) = (P_1^*, P_2^*) \in \mathbb{R}^2$ the (q, p) components of the unperturbed vector field $\alpha=\gamma=0$ (4.1) possess a one-dimensional heteroclinic orbit connecting the hyperbolic saddle points (q_0, p_0) (4.3e,b). The heteroclinic orbits lie on each of the level energy surfaces defined by (4.7) for fixed values of $P_1 = P_1^*$ and $P_2 = P_2^*$ and are solutions to

$$\langle H \rangle (\gamma=0) - \left(a_1 P_1^* + (a_2 - a_1) P_2^* \right) = 0 \quad (4.12)$$

where the unperturbed Floquet Hamiltonian $\langle H \rangle (\gamma=0)$ is given by (4.2) and (3.38). Values for q on the heteroclinic orbits may be computed from (4.12) and are given by

$$q = \frac{1}{2} \cos^{-1} \left(\frac{a_1 - \epsilon \Omega}{2 \epsilon a_3 \sqrt{P_1^* - p}} \right) \quad (4.13)$$

In the full six-dimensional phase space $(q, p, P_1, P_2, Q_1, Q_2) \in \mathbb{T}^1 \times \mathbb{R}^1 \times \mathbb{R}^2 \times \mathbb{T}^2$, the heteroclinic manifold \mathcal{H} (4.5) may be determined by substituting

$$\cos[2q] = \left(\frac{a_1 - \epsilon \Omega}{2 \epsilon a_3 \sqrt{P_1^* - p}} \right), \quad \sin[2q] = \sqrt{1 - \left(\frac{a_1 - \epsilon \Omega}{2 \epsilon a_3 \sqrt{P_1^* - p}} \right)^2} \quad (4.14a,b)$$

into the RHS of the unperturbed vector field $\alpha=\gamma=0$ (4.1),

and by integrating to obtain the following variables on the heteroclinic manifold:

$$p_h(t) = P_2 + \frac{A}{B} \operatorname{sech}^2[\sqrt{A} t] + p(0) \quad (4.15a)$$

$$q_h(t) = \frac{1}{2} \tan^{-1} \left[-\frac{\sqrt{A}}{a_1 - \varepsilon \Omega} \tanh(\sqrt{A} t) \right] + q(0) \quad (4.15b)$$

$$P_{1h}(t) = P_1(0) \quad (4.15c)$$

$$P_{2h}(t) = P_2(0) \quad (4.15d)$$

$$Q_{1h}(t) = a_1 t - q_h(t) + Q_1(0) + q(0)$$

$$= a_1 t - \frac{1}{2} \tan^{-1} \left[-\frac{\sqrt{A}}{a_1 - \varepsilon \Omega} \tanh(\sqrt{A} t) \right] + Q_1(0) \quad (4.15e)$$

$$Q_{2h}(t) = (a_2 - a_1) t + Q_2(0) \quad (4.15f)$$

where

$$A = \left[- (a_1 - \varepsilon \Omega)^2 + (P_1 - P_2) B \right] > 0 \quad ; \quad B = 4 \varepsilon^2 a_3^2 \quad (4.15g, h)$$

and

$$p(0) = 0 \quad ; \quad q = q_n(0) = (2n+1) \frac{\pi}{2} \quad ; \quad n = 0, 1, 2, \dots \quad (4.15i, j)$$

The trajectories of the unperturbed system $\alpha = \gamma = 0$ along the five-dimensional $(\mathbb{R}^1 \times \mathbb{R}^2 \times \mathbb{T}^2)$ heteroclinic manifold \mathcal{H} (4.5) may be expressed as

$$\Psi^{(P_1, P_2)} = \{ q_h(t), p_h(t), P_1(0), P_2(0), Q_{1h}(t), Q_{2h}(t) \} \quad (4.16)$$

The six-dimensional phase space $(q, p, P_1, P_2, Q_1, Q_2) \in$

$\mathbb{T}^1 \times \mathbb{R}^1 \times \mathbb{R}^2 \times \mathbb{T}^2$ is a direct product of a region in four-

dimensional space with coordinates (q, p, P_1, P_2) and the two-dimensional torus with angular coordinates (Q_1, Q_2) . Because P_1 and P_2 are constants in (4.12), the motion in the six-dimensional phase space is reduced to four dimensions on which four variables (q, p, Q_1, Q_2) flow as shown in Figure 5.

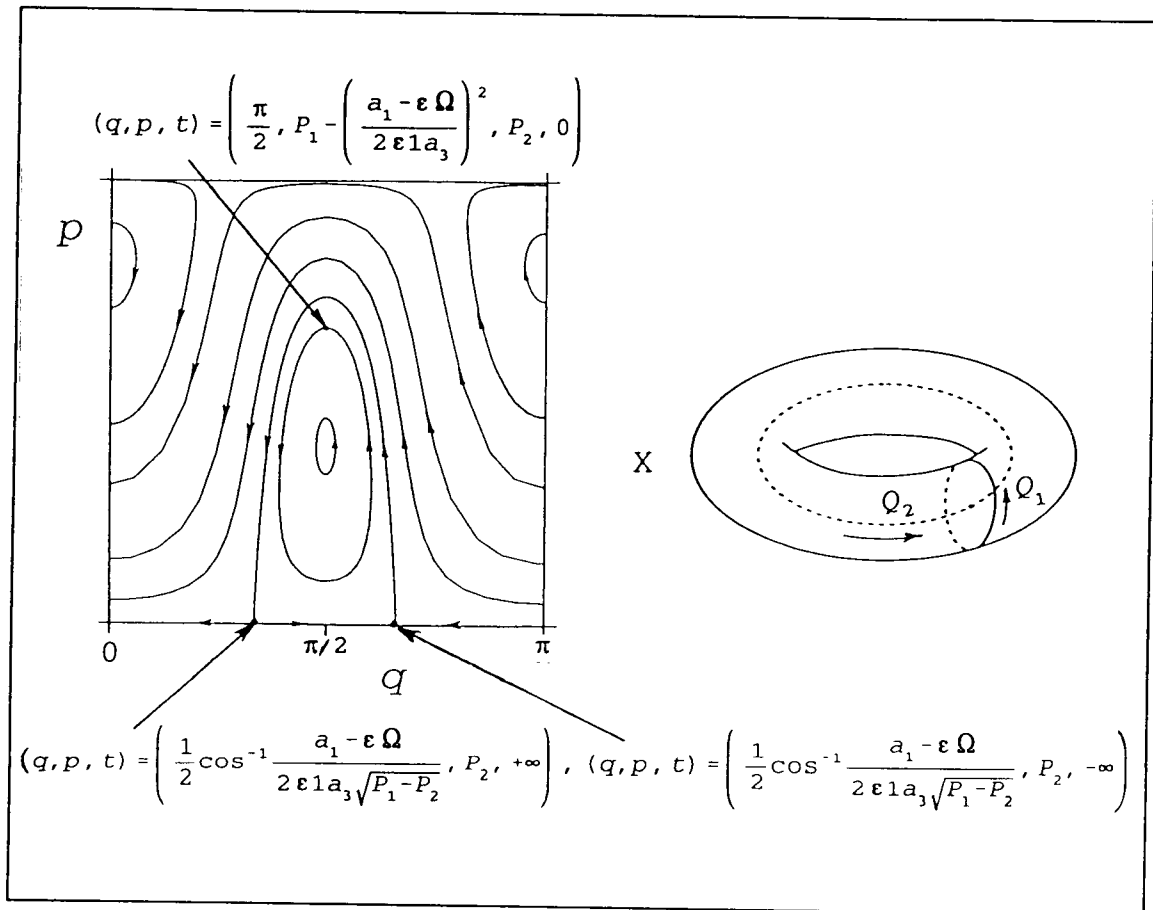


Figure 5. The unperturbed $\alpha=\gamma=0$ reduced four-dimensional phase space $(q, p, Q_1, Q_2) \in T^1 \times \mathbb{R}^1 \times T^2$ (P_1 and P_2 are constants).

Just as in the two-dimensional phase space (Guckenheimer & Holmes, 1983), small perturbations are expected to break up the geometric structure of the

unperturbed system $\alpha=\gamma=0$ and separate the manifolds (Dankowicz, 1996b). The behavior of the perturbed systems $\gamma>0$ and $\alpha>0$ near the unperturbed heteroclinic manifold \mathcal{H} is required for the application of the GMM. The distance between the stable and unstable manifolds of any surviving invariant set in the perturbed system must be computed at a point \mathcal{P} on the unperturbed heteroclinic manifold \mathcal{H} . Two types of perturbed systems will be discussed. First, in §4.2 the perturbed system with perturbation (wavemaker forcing) parameter $\gamma>0$ and with no dissipation $\alpha=0$ is governed by a perturbed vector field that may be derived from the Hamiltonian (3.38). Second, in §4.3 the perturbed system with forcing $\gamma>0$ and dissipation $\alpha>0$ is governed by a perturbed vector field that has a dissipative nature.

4.2. Geometric Structure of Perturbed Hamiltonian Phase Space ($\alpha=0$, $\gamma>0$)

The perturbed vector field $(\dot{\mathbf{q}}, \dot{\mathbf{p}})$ for non-zero perturbation (wavemaker forcing) parameter $\gamma>0$ and no dissipation $\alpha=0$ may be determined by setting $\alpha=0$ in the evolution equations (3.41) and is given by

$$\dot{\mathbf{q}} = -a_1 + \varepsilon \Omega + \varepsilon a_3 \frac{2P_1 + P_2 - 3p}{\sqrt{P_1 - p}} \cos[2q] - \gamma c_1 \frac{\sin[2Q_1]}{\varepsilon \sqrt{P_1 - p}} - \gamma c_2 \sin[2(q + Q_1)] \quad (4.17a)$$

$$\dot{p} = 4 \varepsilon a_3 \sqrt{P_1 - p} (p - P_2) \sin[2q] - 2\gamma c_2 (P_2 - p) \cos[2(q + Q_1)] \quad (4.17b)$$

$$\dot{P}_1 = -\frac{4\gamma}{\varepsilon} c_1 \sqrt{P_1 - p} \cos[2Q_1] - 2\gamma c_2 (P_2 - p) \cos[2(q + Q_1)] \quad (4.17c)$$

$$\dot{P}_2 = 0 \quad (4.17d)$$

$$\dot{Q}_1 = a_1 + \varepsilon a_3 \frac{(p-P_2)}{\sqrt{P_1-p}} \cos[2q] + \gamma c_1 \frac{\sin[2Q_1]}{\varepsilon \sqrt{P_1-p}} \quad (4.17e)$$

$$\dot{Q}_2 = a_2 - \varepsilon \Omega - 2\varepsilon a_3 \sqrt{P_1-p} \cos[2q] + \gamma c_2 \sin[2(q+Q_1)] \quad (4.17f)$$

that is a System III (Wiggins, p.336, 1988) with

$(q, p, P_1, P_2, Q_1, Q_2) \in \mathbb{T}^1 \times \mathbb{R}^1 \times \mathbb{R}^2 \times \mathbb{T}^2$. The condition (3.28d) from the Hamilton-Jacobi canonical transformation (§3.5c) for the canonical variables p is $P_1 > p \geq P_2 > 0$. The entire perturbed vector field $\alpha=0$ and $\gamma>0$ (4.17) is derived from the Hamiltonian (3.38) given by the five-dimensional level energy surfaces

$$\langle H \rangle = H_0(p, P_1, P_2) + H_\varepsilon(q, p, P_1, P_2) + H_\gamma(q, p, P_1, P_2, Q_1) \quad (4.18)$$

Because the perturbation is Hamiltonian with $\alpha=0$, the three-dimensional level energy surfaces (4.7) are preserved. The four-dimensional normally hyperbolic invariant manifold \mathcal{M} (4.4) of the unperturbed system

$\alpha=\gamma=0$, the locally stable $W_{loc}^s(\mathcal{M})$ and unstable $W_{loc}^u(\mathcal{M})$

manifolds §4.1, and the flow on \mathcal{M} (4.9) may be used to describe the geometric structure of the perturbed phase space. In particular, the perturbed normally hyperbolic

locally invariant manifold \mathcal{M}_γ , the locally stable $W_{loc}^s(\mathcal{M}_\gamma)$

and unstable $W_{loc}^u(\mathcal{M}_\gamma)$ manifolds, and the persistence of the

two-dimensional nonresonant invariant tori $\Upsilon_\gamma(P_1, P_2)$ (vide (4.19-21) below).

4.2.1. Persistence of \mathcal{M}

By proposition 4.1.16 (Wiggins, 1988), the perturbed system $\alpha=0$ and $\gamma>0$ possesses a four-dimensional normally hyperbolic locally invariant manifold \mathcal{M}_γ ; i.e., trajectories may leave \mathcal{M}_γ by crossing its boundary because $\dot{P}_1 \neq 0$ by (4.17c). If all trajectories eventually leave \mathcal{M}_γ by crossing its boundary, then there are no recurrent motions on \mathcal{M}_γ . The objective is to locate any recurrent motions in \mathcal{M}_γ in order to apply the GMM. The perturbed normally hyperbolic locally invariant manifold \mathcal{M}_γ is given by

$$\mathcal{M}_\gamma = \left\{ \begin{array}{l} (q, p, P_1, P_2, Q_1, Q_2) \in T^1 \times \mathbb{R}^1 \times \mathbb{R}^2 \times T^2 \ni \\ q = \tilde{q}_0(P_1, P_2, Q_1, Q_2; \gamma) = q_0(P_1, P_2) + O(\gamma); \\ p = \tilde{p}_0(P_1, P_2, Q_1, Q_2; \gamma) = p_0(P_2) + O(\gamma) \end{array} \right\} \quad (4.19)$$

where the hyperbolic saddle points $q_0(P_1, P_2)$ and $p_0(P_2)$ are given by (4.3e,b). Moreover, on \mathcal{M}_γ there are locally stable $W_{loc}^s(\mathcal{M}_\gamma)$ and unstable $W_{loc}^u(\mathcal{M}_\gamma)$ manifolds that are of equal dimensions and are close to the unperturbed locally stable $W_{loc}^s(\mathcal{M})$ and unstable $W_{loc}^u(\mathcal{M})$ manifolds §4.1,

respectively. Although trajectories in $W_{loc}^s(\mathcal{M}_\gamma)$ and

$W_{loc}^u(\mathcal{M}_\gamma)$ approach \mathcal{M}_γ as $t \rightarrow \pm\infty$, they need not terminate on \mathcal{M}_γ because all trajectories on \mathcal{M}_γ may leave \mathcal{M}_γ in finite time. The perturbed normally hyperbolic locally invariant

manifold \mathcal{M}_γ intersects each of the five-dimensional level energy surfaces given by (4.18) in a three-dimensional set of which, by the KAM theorem (Arnold, Appendix 8, 1978), most of a two-parameter family of two-dimensional nonresonant invariant tori persist in (4.6). These two-dimensional tori, now called KAM tori, may be slightly deformed compared to those of the unperturbed system for $\alpha=\gamma=0$; nevertheless, the qualitative motion remains much the same as in the unperturbed system $\alpha=\gamma=0$ that is governed by the unperturbed vector field given in (4.1). The Melnikov integral may be computed to determine if the stable and unstable manifolds of the KAM tori intersect transversely.

4.2.2. KAM theorem

The KAM theorem (Arnold, Appendix 8, 1978) may be applied in order to determine if recurrent motions occur on the perturbed normally hyperbolic locally invariant manifold \mathcal{M}_γ ; and in particular, if any of the two parameter family of two-dimensional nonresonant invariant tori $\Upsilon(\bar{P}_1, \bar{P}_2)$ (4.10) survive the Hamiltonian perturbation $\alpha=0$ and $\gamma>0$. The unperturbed Floquet Hamiltonian $\langle H \rangle (\gamma=0)$ given by (4.2) satisfies the following nondegeneracy (or nonresonance) condition given by (Wiggins, p.386, 1988):

$$\left| \begin{array}{cc} \frac{\partial^2 \langle H \rangle}{\partial P_1^2} & \frac{\partial^2 \langle H \rangle}{\partial P_1 \partial P_2} \\ \frac{\partial^2 \langle H \rangle}{\partial P_2 \partial P_1} & \frac{\partial^2 \langle H \rangle}{\partial P_2^2} \end{array} \right|_{(q=q_0, p=p_0; \gamma=0)} = - \frac{(a_1 - \epsilon \Omega)^2}{4 (P_1 - P_2)^2} < 0 \quad (4.20)$$

where the hyperbolic saddle points (q_0, p_0) are given by (4.3e,b). Consequently, most of the two-dimensional nonresonant invariant tori $\Upsilon(P_1, P_2)$ (4.10) persist; are

only slightly deformed on the perturbed normally hyperbolic locally invariant manifold \mathcal{M}_γ ; and may also be referred to as KAM tori and denoted by $\Upsilon_\gamma(P_1, P_2)$ analogous to (4.10). Accordingly, in the phase space of the perturbed system $\alpha=0$ and $\gamma>0$, there are invariant tori that are densely filled with winding trajectories that are conditionally periodic with two independent frequencies σ_1 and σ_2 (4.8). The resulting conditionally-periodic motions of the perturbed system $\alpha=0$ and $\gamma>0$ with these two fixed frequencies are smooth functions of the perturbation (wavemaker forcing) parameter γ (Arnold, Appendix 8, 1978). A generalization of the KAM theorem states that the KAM tori $\Upsilon_\gamma(P_1, P_2) \subset \mathcal{M}_\gamma$ has three-dimensional stable and unstable manifolds denoted by $W^s(\Upsilon_\gamma(P_1, P_2))$ and $W^u(\Upsilon_\gamma(P_1, P_2))$, respectively (Wiggins, p.387, 1988). By invariance of manifolds (*cf.*, Wiggins, p.387, 1988), $W^s(\Upsilon_\gamma) \subset W^s(\mathcal{M}_\gamma)$ and $W^u(\Upsilon_\gamma) \subset W^u(\mathcal{M}_\gamma)$.

In order to determine if chaos exist, it remains only to determine whether or not $W^s(\Upsilon_\gamma(P_1, P_2))$ and $W^u(\Upsilon_\gamma(P_1, P_2))$ intersect transversely. Because the perturbation $\alpha=0$ and $\gamma>0$ is Hamiltonian in the six-dimensional phase space $(q, p, P_1, P_2, Q_1, Q_2) \in T^1 \times \mathbb{R}^1 \times \mathbb{R}^2 \times T^2$, trajectories are restricted to lie in five-dimensional level energy surfaces given by (4.18). Thus, two measurements are required in order to determine whether or not $W^s(\Upsilon_\gamma)$ and $W^u(\Upsilon_\gamma)$ intersect transversely (Wiggins, Lemma 4.1.18, 1988). Moreover, because $\dot{P}_2 = 0$ (4.17d), only one measurement along a constant unit vector in the P_1 direction denoted as \hat{P}_1 will be required to determine whether or not $W^s(\Upsilon_\gamma)$ and $W^u(\Upsilon_\gamma)$ intersect transversely (*vide* (4.21) below).

4.2.3. Melnikov Integral

The distance between $w^s(\Upsilon_\gamma)$ and $w^u(\Upsilon_\gamma)$ at any point $\mathcal{P} \in \mathcal{H}$ may be computed from (Wiggins, 4.1.85, 1988)

$$\mathbf{M}(Q_1(0)) = - \int_{-\infty}^{\infty} \frac{\partial H^\gamma}{\partial Q_1} \left(\Psi^{(P_1, P_2)} \right) dt \quad (4.21a)$$

where

$$H^\gamma = \frac{2c_1}{\varepsilon} \sqrt{P_1 - p} \sin(2Q_1) + c_2 (P_2 - p) \sin 2(q + Q_1) \quad (4.21b)$$

where $H_\gamma = \gamma H^\gamma$ in (3.38) and where the coefficients c_1, c_2 are defined in Appendix C. The Melnikov integral $\mathbf{M}(Q_1(0))$ (4.21a) represents the leading order term in a Taylor series expansion (with respect to γ) for the distance between $w^s(\Upsilon_\gamma)$ and $w^u(\Upsilon_\gamma)$ at the point $\mathcal{P} \in \mathcal{H}$ along a constant unit vector in the P_1 direction denoted as $\hat{\mathbf{P}}_1$. In order to compute (4.21a), only the perturbed vector field $\alpha=0$ and $\gamma>0$ (4.17) and the trajectories along the unperturbed heteroclinic manifold \mathcal{H} (4.16) are required. Substituting (4.16) and (4.17c) into the RHS of (4.21a) yields

$$\mathbf{M}(Q_1(0)) = \int_{-\infty}^{\infty} \left[-\frac{4c_1}{\varepsilon} \sqrt{P_1 - p_h} \cos[2Q_{1h}] - 2c_2 (P_2 - p_h) \cos[2(q_h + Q_{1h})] \right] dt \quad (4.22a)$$

Substituting (4.15e) into (4.22a) and then expanding by elementary trigonometric identities results in the following two integrals:

$$\begin{aligned}
M(Q_1(0)) = \cos 2(Q_1(0) + q(0)) \int_{-\infty}^{\infty} \left[\begin{aligned} & -\frac{4c_1}{\epsilon} \sqrt{P_1 - p_h} (\cos(2q_h - 2a_1 t)) \\ & - 2c_2 (P_2 - p_h) \cos(2a_1 t) \end{aligned} \right] dt \\
+ \sin 2(Q_1(0) + q(0)) \int_{-\infty}^{\infty} \left[\begin{aligned} & -\frac{4c_1}{\epsilon} \sqrt{P_1 - p_h} (\sin(2q_h - 2a_1 t)) \\ & + 2c_2 (P_2 - p_h) \sin(2a_1 t) \end{aligned} \right] dt
\end{aligned} \tag{4.22b}$$

Substituting $q = q_h$ and $p = p_h$, (4.14a,b) may be transformed to

$$\cos(2q_h) = \left(\frac{a_1 - \epsilon \Omega}{2\epsilon a_3 \sqrt{P_1 - p_h}} \right) \tag{4.23a}$$

$$\sin(2q_h) = \frac{\sqrt{(2\epsilon a_3 \sqrt{P_1 - p_h})^2 - (a_1 - \epsilon \Omega)^2}}{2\epsilon a_3 \sqrt{P_1 - p_h}} = \frac{\sqrt{A + B(P_2 - p_h)}}{2\epsilon a_3 \sqrt{P_1 - p_h}} \tag{4.23b}$$

where A, B are given by (4.15g,h). Substituting (4.15a) and (4.23) into (4.22b) and retaining only the even integrands reduce the Melnikov integral to simply

$$M(Q_1(0)) = \cos 2(Q_1(0) + q(0)) [I_1 + I_2 + I_3] \tag{4.24a}$$

where the integrals I_i are

$$I_1 = \frac{-2c_1(a_1 - \epsilon \Omega)}{\epsilon^2 a_3} \int_{-\infty}^{\infty} \cos(2a_1 t) dt \tag{4.24b}$$

$$I_2 = \frac{2c_2 A}{B} \int_{-\infty}^{\infty} \cos(2a_1 t) \operatorname{sech}^2(\sqrt{A}t) dt \tag{4.24c}$$

$$I_3 = \frac{-2c_1 \sqrt{A}}{\epsilon^2 a_3} \int_{-\infty}^{\infty} \sin(2a_1 t) \tanh(\sqrt{A}t) dt \tag{4.24d}$$

and where the coefficients c_1, c_2, a_1 and a_3 are defined in Appendix C. By Proposition 4.1.29 and Lemma 4.1.27 (Wiggins, p.412 and p.410, 1988), these improper integrals may be evaluated if the limits $\pm\infty$ are approached along sequences of discrete times (*vide* Appendix E). Theorems (4.1.19) and (4.1.20) (Wiggins, p.393, 1988) give sufficient conditions for the transverse intersection of $W^s(\Upsilon_\gamma)$ and $W^u(\Upsilon_\gamma)$ in the five-dimensional level energy surfaces. Because all of the Melnikov components in (4.24) are bounded and do not sum to zero (Appendix E), the Melnikov integral $M(Q_1(0)) = 0$ when

$$Q_1(0) = \bar{Q}_{1n}(0) = (2n+1) \frac{\pi}{4} - q(0) \quad ; \quad n = 0, 1, 2, \dots \quad (4.25)$$

Furthermore, the derivatives

$$\frac{\partial M(\bar{Q}_{1n}(0))}{\partial Q_1(0)} = -2 \sin 2\left(\bar{Q}_{1n}(0) + q(0)\right) \left[I_1 + I_2 + I_3\right] \neq 0 \quad , \quad n = 0, 1, 2, \dots \quad (4.26)$$

are never zeros and (4.25) represent simple zeros of the Melnikov integral. The stable $W^s(\Upsilon_\gamma(P_1, P_2))$ and unstable $W^u(\Upsilon_\gamma(P_1, P_2))$ manifolds of the KAM tori $\Upsilon_\gamma(P_1, P_2)$ intersect transversely yielding Smale horseshoes (Wiggins, 1990) on the appropriate five-dimensional level energy surfaces (4.18); and these imply multiple transverse intersections and the existence of chaotic dynamics in the perturbed system $\alpha=0$ and $\gamma>0$ that is governed by the perturbed vector field given in (4.17).

4.3. Geometric Structure of Perturbed Dissipative Phase Space ($\alpha>0, \gamma>0$)

The following perturbed dissipative vector field $(\dot{\mathbf{q}}, \dot{\mathbf{p}})$ for non-zero perturbation (wavemaker forcing)

parameter $\gamma > 0$ and non-zero dissipation $\alpha > 0$ may be obtained from (3.41) by setting $\alpha = v \gamma$ where $v \ll 1$:

$$\dot{q} = \left[-a_1 + \varepsilon \Omega + \varepsilon a_3 \frac{2P_1 + P_2 - 3p}{\sqrt{P_1 - p}} \cos[2q] \right] + \gamma \left[g^q(q, p, P_1, P_2, Q_1, v; \gamma) \right] \quad (4.27a)$$

$$\dot{p} = \left[4 \varepsilon a_3 \sqrt{P_1 - p} (p - P_2) \sin[2q] \right] + \gamma \left[g^p(q, p, P_1, P_2, Q_1, v) \right] \quad (4.27b)$$

$$\dot{P}_1 = \gamma \left[g^{P_1}(q, p, P_1, P_2, Q_1, v) \right] \quad (4.27c)$$

$$\dot{P}_2 = \gamma \left[g^{P_2}(P_2, v) \right] \quad (4.27d)$$

$$\dot{Q}_1 = \left[a_1 + \varepsilon a_3 \frac{(p - P_2)}{\sqrt{P_1 - p}} \cos[2q] \right] + \gamma \left[g^{Q_1}(q, p, P_1, P_2, Q_1, v; \gamma) \right] \quad (4.27e)$$

$$\dot{Q}_2 = \left[a_2 - \varepsilon \Omega - 2 \varepsilon a_3 \sqrt{P_1 - p} \cos[2q] \right] + \gamma \left[g^{Q_2}(q, p, P_1, Q_1, v; \gamma) \right] \quad (4.27f)$$

where the perturbed components g^i (Wiggins, §4, 1988) are given by

$$\begin{aligned} g^q(q, p, P_1, P_2, Q_1, v; \gamma) = & -c_1 \frac{\sin[2Q_1]}{\varepsilon \sqrt{P_1 - p}} - c_2 \sin[2(q + Q_1)] + v^2 \gamma d_1 \\ & - v \varepsilon \left(\frac{d_2(P_1 - p) + d_3(P_2 - p)}{\sqrt{P_1 - p}} \right) \sin[2q] \end{aligned} \quad (4.27g)$$

$$\begin{aligned}
g^P(q, p, P_1, P_2, Q_1, v) = & -2 c_2 (P_2 - p) \cos [2 (q + Q_1)] + v d_4 P_2 - \frac{v}{\tau_1} p \\
& + 2 v \varepsilon d_2 \sqrt{P_1 - p} (p - P_2) \cos [2 q]
\end{aligned}
\quad (4.27h)$$

$$\begin{aligned}
g^{P_1}(q, p, P_1, P_2, Q_1, v) = & \frac{-4}{\varepsilon} c_1 \sqrt{P_1 - p} \cos [2 Q_1] - 2 c_2 (P_2 - p) \cos [2 (q + Q_1)] \\
& + v \frac{(4 \lambda^2 - 1) (P_2 - p) - P_1}{2 \lambda^2 \tau_1} - v \varepsilon d_5 \sqrt{P_1 - p} (p - P_2) \cos [2 q]
\end{aligned}
\quad (4.27i)$$

$$g^{P_2}(P_2, v) = v P_2 \left(\frac{\tau - \lambda^4 \xi \tau_\lambda}{\lambda^6 \xi \tau_1 \tau_\lambda} \right) \quad (4.27j)$$

$$g^{Q_1}(q, p, P_1, P_2, Q_1, v; \gamma) = c_1 \frac{\sin [2 Q_1]}{\varepsilon \sqrt{P_1 - p}} + v^2 \gamma d_6 + v \varepsilon d_3 \frac{P_2 - p}{\sqrt{P_1 - p}} \sin [2 q]
\quad (4.27k)$$

$$g^{Q_2}(q, p, P_1, v; \gamma) = c_2 \sin [2 (q + Q_1)] + v^2 \gamma d_7 + v \varepsilon d_2 \sqrt{P_1 - p} \sin [2 q]
\quad (4.27l)$$

This perturbed dissipative vector field is a System I

(Wiggins, p.336, 1988) with $(q, p, P_1, P_2, Q_1, Q_2) \in$

$T^1 \times \mathbb{R}^1 \times \mathbb{R}^2 \times T^2$. The condition (3.28d) from the Hamilton-Jacobi canonical transformation (§3.5c) for the canonical variables p is $P_1 > p \geq P_2 > 0$. The four-dimensional normally hyperbolic invariant manifold \mathcal{M} (4.4) of the unperturbed system $\alpha = \gamma = 0$, its locally stable $W_{loc}^s(\mathcal{M})$ and

unstable $W_{loc}^u(\mathcal{M})$ manifolds §4.1 may be used to describe the geometric structure of the perturbed dissipative phase space. In particular, the perturbed normally hyperbolic locally invariant manifold $\mathcal{M}_{\gamma\alpha}$, the locally stable $W_{loc}^s(\mathcal{M}_{\gamma\alpha})$ and unstable $W_{loc}^u(\mathcal{M}_{\gamma\alpha})$ manifolds, and the persistence of the two-dimensional nonresonant invariant tori $\Upsilon_{\gamma\alpha}(P_1, P_2)$.

4.3.1. Persistence of \mathcal{M}

By proposition 4.1.5 (Wiggins, p.354, 1988), the perturbed dissipative system $\alpha > 0$ and $\gamma > 0$ possesses a four-dimensional normally hyperbolic locally invariant manifold $\mathcal{M}_{\gamma\alpha}$; i.e., trajectories may leave $\mathcal{M}_{\gamma\alpha}$ by crossing its boundary because $\dot{P}_1 \neq 0$ and $\dot{P}_2 \neq 0$ by (4.27c,d). If all trajectories eventually leave $\mathcal{M}_{\gamma\alpha}$ by crossing its boundary, then there are no recurrent motions on $\mathcal{M}_{\gamma\alpha}$. The objective is to locate any recurrent motions in $\mathcal{M}_{\gamma\alpha}$ in order to apply the GMM. The perturbed normally hyperbolic locally invariant manifold $\mathcal{M}_{\gamma\alpha}$ is given by

$$\mathcal{M}_{\gamma\alpha} = \left\{ \begin{array}{l} (q, p, P_1, P_2, Q_1, Q_2) \in \mathbb{T}^1 \times \mathbb{R}^1 \times \mathbb{R}^2 \times \mathbb{T}^2 \ni \\ q = \tilde{q}_0(P_1, P_2, Q_1, Q_2; \gamma) = q_0(P_1, P_2) + O(\gamma); \\ p = \tilde{p}_0(P_1, P_2, Q_1, Q_2; \gamma) = p_0(P_2) + O(\gamma) \end{array} \right\} \quad (4.28)$$

where the hyperbolic saddle points $q_0(P_1, P_2)$ and $p_0(P_2)$ are given by (4.3e,b). Moreover, $\mathcal{M}_{\gamma\alpha}$ has locally stable $W_{loc}^s(\mathcal{M}_{\gamma\alpha})$ and unstable $W_{loc}^u(\mathcal{M}_{\gamma\alpha})$ manifolds that are close to the unperturbed locally stable $W_{loc}^s(\mathcal{M})$ and unstable

$W_{loc}^u(\mathcal{M})$ manifolds §4.1, respectively. If $W^s(\mathcal{M}_{\gamma\alpha})$ and $W^u(\mathcal{M}_{\gamma\alpha})$ intersect transversely, then the Smale-Birkhoff homoclinic theorem (Smale, 1963) predicts the existence of horseshoes and their attendant chaotic dynamics in the perturbed dissipative system $\alpha > 0$ and $\gamma > 0$ governed by the perturbed dissipative vector field given in (4.27).

4.3.2. Averaging method

An averaging method (Simiu, 1996) may be applied for the perturbed dissipative vector field $\alpha > 0$ and $\gamma > 0$ (4.27) in order to determine if recurrent motions occur on the perturbed normally hyperbolic locally invariant manifold $\mathcal{M}_{\gamma\alpha}$. If there are any tori on $\mathcal{M}_{\gamma\alpha}$, then the Melnikov integral may be computed to determine whether or not the stable and unstable manifolds of these tori intersect. A two-dimensional hyperbolic invariant torus $\Upsilon_{\gamma\alpha}(P_1, P_2)$ may be located on $\mathcal{M}_{\gamma\alpha}$ by averaging the perturbed dissipative vector field $\alpha > 0$ and $\gamma > 0$ (4.27) restricted to $\mathcal{M}_{\gamma\alpha}$ over the angular variables Q_1 and Q_2 (vide (4.29,30) below). The averaging method requires nonresonance conditions resulting in trajectories densely filling the surface of the torus $\Upsilon_{\gamma\alpha}(P_1, P_2)$. The averaging method is not appropriate for Hamiltonian systems (cf., Wiggins, p.359, 1988). In the case of Hamiltonian perturbation $\alpha=0$ and $\gamma > 0$ (§4.2), two-dimensional invariant tori $\Upsilon_{\gamma}(P_1, P_2)$ were located on the perturbed normally hyperbolic locally invariant manifold \mathcal{M}_{γ} by the KAM theorem. The perturbed dissipative vector field $\alpha > 0$ and $\gamma > 0$ (4.27) restricted to the perturbed hyperbolic locally invariant manifold $\mathcal{M}_{\gamma\alpha}$ (4.28) may be determined from (4.27c-f) and (4.28) and is given by

$$\dot{P}_1 = \gamma \left[g^{P_1}(q=q_0(P_1, P_2), p=p_0(P_2), P_1, P_2, Q_1, v) \right] + O(\gamma^2) \quad (4.29a)$$

$$\dot{P}_2 = \gamma \left[g^{P_2}(P_2, v) \right] + O(\gamma^2) \quad (4.29b)$$

$$\dot{Q}_1 = \dot{Q}_1(q=q_0(P_1, P_2), p=p_0(P_2); \gamma=0) + O(\gamma) = a_1 + O(\gamma) \quad (4.29c)$$

$$\dot{Q}_2 = \dot{Q}_2(q=q_0(P_1, P_2), p=p_0(P_2); \gamma=0) + O(\gamma) = a_2 - a_1 + O(\gamma) \quad (4.29d)$$

where the hyperbolic saddle points $q_0(P_1, P_2)$ and $p_0(P_2)$ are given by (4.3e,b), $g^{P_2}(P_2, v)$ by (4.27j), and where

$$g^{P_1}(q=q_0, p=p_0, P_1, P_2, Q_1, v) = -\frac{4C_1}{\epsilon} \sqrt{P_1 - P_2} \cos[2Q_1] - \frac{v}{2\lambda^2 \tau_1} P_1 \quad (4.29e)$$

The associated averaged equations

$$\langle \dot{P}_1 \rangle = \frac{\gamma}{(2\pi)^2} \int_0^{2\pi} \int_0^{2\pi} g^{P_1}(q_0, p_0, P_1, P_2, Q_1, v) dQ_1 dQ_2 = \frac{-v\gamma}{2\lambda^2 \tau_1} P_1 \quad (4.30a)$$

$$\langle \dot{P}_2 \rangle = \frac{\gamma}{(2\pi)^2} \int_0^{2\pi} \int_0^{2\pi} g^{P_2}(P_2, v) dQ_1 dQ_2 = \frac{v\gamma(\tau - \lambda^4 \xi \tau_\lambda)}{\lambda^6 \xi \tau_1 \tau_\lambda} P_2 \quad (4.30b)$$

have a unique stable hyperbolic fixed point at

$(P_1, P_2) = (0, 0)$ with two negative eigenvalues provided that the determinant

$$\left| \begin{array}{cc} \frac{\partial \langle \dot{P}_1 \rangle}{\partial P_1} & \frac{\partial \langle \dot{P}_1 \rangle}{\partial P_2} \\ \frac{\partial \langle \dot{P}_2 \rangle}{\partial P_1} & \frac{\partial \langle \dot{P}_2 \rangle}{\partial P_2} \end{array} \right| = \frac{v^2 \gamma^2 (\lambda^4 \xi \tau_\lambda - \tau)}{2 \lambda^8 \xi \tau_1^2 \tau_\lambda} > 0 \quad (4.31)$$

is positive (viz, $\lambda^4 \xi \tau_\lambda > \tau$). This fixed point of the averaged equations (4.30) corresponds to a two-dimensional torus denoted as $\Upsilon_{\gamma\alpha}(0,0)$ on the perturbed hyperbolic locally invariant manifold $\mathcal{M}_{\gamma\alpha}$ (4.28). By proposition 4.1.6 (Wiggins, p.358, 1988) and in the context of the full six-dimensional phase space $(q, p, P_1, P_2, Q_1, Q_2) \in T^1 \times \mathbb{R}^1 \times \mathbb{R}^2 \times T^2$; the perturbed dissipative vector field $\alpha > 0$ and $\gamma > 0$ (4.27) restricted to the hyperbolic locally invariant manifold $\mathcal{M}_{\gamma\alpha}$ (4.29) has a two-dimensional normally hyperbolic invariant torus $\Upsilon_{\gamma\alpha}(0,0) \subset \mathcal{M}_{\gamma\alpha}$ that has a five-dimensional stable manifold $W^s(\Upsilon_{\gamma\alpha}(0,0))$ and three-dimensional unstable manifold $W^u(\Upsilon_{\gamma\alpha}(0,0))$. By invariance of manifolds (cf., Wiggins, p.359, 1988), $W^s(\Upsilon_{\gamma\alpha}(0,0)) \subset W^s(\mathcal{M}_{\gamma\alpha})$ and $W^u(\Upsilon_{\gamma\alpha}(0,0)) \subset W^u(\mathcal{M}_{\gamma\alpha})$. The normal hyperbolicity of $\Upsilon_{\gamma\alpha}(0,0)$ insures that the dynamics normal to the invariant torus dominate the dynamics on the invariant torus under the action of the perturbed dissipative flow (Wiggins, p.319, 1988). The dissipative perturbation $\alpha > 0$ and $\gamma > 0$ creates two new independent vectors in the tangent space of the stable manifold $W^s(\Upsilon_{\gamma\alpha}(0,0))$ that comes from the breakup of the two-dimensional center manifold $W^c(\Upsilon(\bar{P}_1, \bar{P}_2))$ of the unperturbed system $\alpha = \gamma = 0$ in §4.1 following (4.11) (Wiggins, p.369, 1988).

In order for chaos to exist, the five-dimensional stable manifold $W^s(\Upsilon_{\gamma\alpha}(0,0))$ and the three-dimensional unstable manifold $W^u(\Upsilon_{\gamma\alpha}(0,0))$ must intersect transversely.

For any point $\mathcal{P} \in W^s(\mathcal{M})$, the tangent space of $W^s(\mathcal{M})$ at \mathcal{P} denoted as $T_{\mathcal{P}}W^s(\mathcal{M})$ is a five-dimensional linear vector space. By proposition 4.1.2 (Wiggins, p.342, 1988), a one-dimensional vector space in $(T^1 \times \mathbb{R}^1 \times \mathbb{R}^2 \times T^2)$ complementary to $T_{\mathcal{P}}W^s(\mathcal{M})$ is given by

$$N_{\mathcal{P}} = \text{span} \left\{ \frac{\partial \langle H \rangle(\gamma=0)}{\partial q}, \frac{\partial \langle H \rangle(\gamma=0)}{\partial p}, 0, 0, 0, 0 \right\} \quad (4.32)$$

where $\langle H \rangle(\gamma=0)$ is the unperturbed Floquet Hamiltonian (4.2) and where its derivatives in (4.32) are evaluated at \mathcal{P} . Due to the normal hyperbolicity of $\Upsilon_{\gamma\alpha}(0,0)$, the angle between the local stable and unstable manifolds, $W_{loc}^s(\mathcal{M}_{\gamma\alpha})$ and $W_{loc}^u(\mathcal{M}_{\gamma\alpha})$, respectively, is bounded away from zero independently of perturbation (wavemaker forcing) parameter γ (Wiggins, p.364, 1988). Lemma 4.1.8 (Wiggins, p.361, 1988) assures that the components of the distance between the stable manifold $W^s(\Upsilon_{\gamma\alpha}(0,0))$ and the unstable manifold $W^u(\Upsilon_{\gamma\alpha}(0,0))$ may be set equal to zero in the directions along constant unit vectors in the P_1 and the P_2 directions denoted as \hat{P}_1 and \hat{P}_2 , respectively. Therefore, only one measurement along the one-dimensional vector space $N_{\mathcal{P}}$ defined by (4.32) will be required to determine whether or not $W^s(\Upsilon_{\gamma\alpha}(0,0))$ and $W^u(\Upsilon_{\gamma\alpha}(0,0))$ intersect transversely.

For the case of Hamiltonian perturbation $\alpha=0$ and $\gamma>0$ in §4.2, trajectories are restricted to lie in five-dimensional level energy surfaces given by (4.18). Because the one-dimensional vector space $N_{\mathcal{P}}$ is complementary to these level energy surfaces, there is no need to measure

along N_p and only measurements along the constant unit vectors \hat{P}_1 and \hat{P}_2 are required to determine whether or not $W^s(\Upsilon_\gamma)$ and $W^u(\Upsilon_\gamma)$ intersect transversely (vide (4.21)). The interested reader is referred to Figure 4.1.6 in Wiggins (1988) that illustrates the intersection of $W^s(\mathcal{M}_{\gamma\alpha})$ and $W^u(\mathcal{M}_{\gamma\alpha})$ with the so called homoclinic plane that is spanned by N_p (4.32) and the constant unit vectors in the P_1 and the P_2 directions denoted as \hat{P}_1 and \hat{P}_2 , respectively. It is impossible to sketch an analogous figure for our perturbed dissipative system $\alpha > 0$ and $\gamma > 0$ because of the dimensionality of this system $n=1, m=2, \ell=2, j=2$ (cf., Wiggins, $\mathbb{R}^{2n} \times \mathbb{R}^m \times \mathbb{T}^\ell$, p.362, 1988).

4.3.3. Melnikov Integral

The distance between $W^s(\Upsilon_{\gamma\alpha}(0,0))$ and $W^u(\Upsilon_{\gamma\alpha}(0,0))$ at any point $\mathcal{P} \in \mathcal{H}$ may be computed from (Wiggins, 4.1.47, 1988)

$$\begin{aligned} M(Q_1(0)) &= \int_{-\infty}^{\infty} \left[\dot{q} g^q - \dot{p} g^p + \dot{Q}_1 g^{P_1} + \dot{Q}_2 g^{P_2} \right] \left(\Psi^{(0,0)}(t); \gamma=0 \right) dt \\ &\quad - \dot{Q}_1 \left(q_0(P_1, P_2), p_0(P_2); \gamma=0 \right) \int_{-\infty}^{\infty} g^{P_1} \left(\Psi^{(0,0)}(t); \gamma=0 \right) dt \\ &\quad - \dot{Q}_2 \left(q_0(P_1, P_2), p_0(P_2); \gamma=0 \right) \int_{-\infty}^{\infty} g^{P_2} \left(\Psi^{(0,0)}(t); \gamma=0 \right) dt \end{aligned} \quad (4.33a)$$

where the hyperbolic saddle points $q_0(P_1, P_2)$ and $p_0(P_2)$ are given by (4.3e,b) and where

$$\Psi^{(0,0)}(t) = \{ q_h(t), p_h(t), Q_{1h}(t), Q_{2h}(t) \}_{(P_1=0, P_2=0)} \quad (4.33b)$$

is a heteroclinic trajectory of the unperturbed system $\alpha=\gamma=0$ in (4.16) on the $P_1=P_2=0$ level corresponding to the hyperbolic fixed point of the averaged vector field on the perturbed hyperbolic locally invariant manifold $\mathcal{M}_{\gamma\alpha}$

(4.30). Because $P_1 \geq P_2 + \left(\frac{a_1 - \varepsilon \Omega}{2\varepsilon a_3} \right)^2$ in (4.3f) on the

unperturbed normally hyperbolic invariant manifold \mathcal{M} (4.4), then $P_1=P_2=0$ is a point on \mathcal{M} provided that

$$a_1 = \varepsilon \Omega \quad (4.34a)$$

that is the lowest point on the unperturbed heteroclinic manifold shown in Figure 4. Bowline et al. (p.39, in press) identified this fixed point as a point of weak chaos for cross waves without surface tension or dissipation. Substituting (3.30d) and the definition for a_1 in Appendix C into (4.34a) and solving for β yields

$$\beta_- = \frac{1}{\Lambda} - \frac{1}{\Lambda} \left[1 - \Lambda \left(1 - \frac{1}{4\xi} \right) \right]^{\frac{1}{2}} \quad (4.34b)$$

where

$$\Lambda = \frac{\tau}{\xi \lambda^6 \tau_1^2} \quad (4.34b)$$

Expanding β by the binomial expansion gives, approximately,

$$\beta \approx \frac{1}{2} \left(1 - \frac{1}{4\xi} \right) \quad (4.34c)$$

The Melnikov integral $\mathbf{M}(Q_1(0))$ (4.33) represents (to $O(\gamma^2)$) the distance between $W^s(\Upsilon_{\gamma\alpha}(0,0))$ and $W^u(\Upsilon_{\gamma\alpha}(0,0))$ at any

point $\mathcal{P} \in \mathcal{H}$ along the one-dimensional vector space N_p defined by (4.32). In order to compute (4.33a), only the perturbed dissipative vector field $\alpha > 0$ and $\gamma > 0$ (4.27) and the trajectories along the unperturbed heteroclinic manifold \mathcal{H} (4.16) are required. The computation of the Melnikov integral (4.33a) on the $P_1 = P_2 = 0$ level and considering the improper integrals as limit of discrete time sequences (vide Appendix E) leads to $M(Q_1(0))$ being identically zero. This implies that the Melnikov method fails to provide the necessary condition for the occurrence of chaos in this particular dissipative system.

4.3.4. *Liapunov characteristic exponents*

In contrast to Hamiltonian (conservative $\alpha = 0$) systems in which the phase-space volume is conserved, by Liouville theorem (Verhulst, 1990), dissipative systems are characterized by continued contraction of the phase-space volume with time t . Hamiltonian systems may be chaotic (§4.2), but they cannot possess phase-space attractors (Lichtenberg & Lieberman, p.460, 1992). Dissipative systems are characterized by the attraction of all trajectories passing through a certain domain towards an invariant surface or an attractor of lower dimensionality than the original space. The basin of attraction is defined as the set of initial conditions from which originate trajectories that converge to the attractor as $t \rightarrow \infty$. If the dissipative system parameter is changed, then, the motion on the attractor may also change from regular (i.e., sink or limit cycle) to chaotic (i.e., strange attractor). A strange attractor is an attractor on which nearby trajectories diverge exponentially (Lichtenberg & Lieberman, p.63, 1992). Rates of divergence or convergence of trajectories, called Liapunov characteristic exponents,

are of fundamental importance in studying chaos. These exponents measure the sensitivity of the system to changes in initial conditions. One positive Liapunov characteristic exponent is a strong indicator of chaotic motions (Rasband, 1990). For a completely integrable Hamiltonian system the Liapunov characteristic exponents are all zero. A strange attractor must have at least one negative, one zero, and one positive Liapunov characteristic exponents (Parker & Chua, 1989). A negative exponent indicates that the phase space contains an attractor. A zero exponent indicates a divergence rate that is slower than exponential divergence along an orbit. A positive exponent indicates chaos within the attractor. For the six-dimensional phase space $(q, p, P_1, P_2, Q_1, Q_2) \in T^1 \times \mathbb{R}^1 \times \mathbb{R}^2 \times T^2$; there are six real exponents that may be ordered as

$$\mu_1 \geq \mu_2 \geq \mu_3 \geq \mu_4 \geq \mu_5 \geq \mu_6 \quad (4.35)$$

with μ_1 being the largest Liapunov characteristic exponent, and one of the remaining five exponents that represents the direction along the perturbed dissipative flow, being zero. The sum of the Liapunov characteristic exponents $\sum_i \mu_i$ represents the average contraction rate of the phase-space volume (Wolf, 1986). There is a set or spectrum of Liapunov characteristic exponents with each one characterizing divergence of trajectories in a particular direction. For the six-dimensional phase space $(q, p, P_1, P_2, Q_1, Q_2) \in T^1 \times \mathbb{R}^1 \times \mathbb{R}^2 \times T^2$; there are ten distinct strange attractors with the following spectral signs of Liapunov characteristic exponents:

$$\begin{aligned}
& (+, +, +, +, 0, -) , \quad (+, +, +, 0, 0, -) , \quad (+, +, +, 0, -, -) \\
& (+, +, 0, 0, 0, -) , \quad (+, +, 0, 0, -, -) , \quad (+, +, 0, -, -, -) \\
& (+, 0, 0, 0, 0, -) , \quad (+, 0, 0, 0, -, -) , \quad (+, 0, 0, -, -, -) \\
& (+, 0, -, -, -, -)
\end{aligned} \tag{4.36}$$

Numerical calculation of μ_1 . For a criterion to determine chaos, only the largest Liapunov characteristic exponent μ_1 is required to determine whether nearby trajectories diverge ($\mu_1 > 0$) or converge ($\mu_1 \leq 0$) on the average (Moon, 1992). The perturbed dissipative vector field $\alpha > 0$ and $\gamma > 0$ (4.27) is numerically integrated by the fourth-order Runge-Kutta method with a time step $\Delta t = 0.02$ to determine a reference trajectory $\psi(t)$ in the six-dimensional phase space $(q, p, P_1, P_2, Q_1, Q_2) \in \mathbb{T}^1 \times \mathbb{R}^1 \times \mathbb{R}^2 \times \mathbb{T}^2$ using a Mathematica program (vide Appendix F). The largest Liapunov characteristic exponent μ_1 is calculated by solving the first variation of the perturbed dissipative vector field $\alpha > 0$ and $\gamma > 0$ (4.27) according to

$$\begin{pmatrix} \delta \dot{q} \\ \delta \dot{p} \\ \delta \dot{P}_1 \\ \delta \dot{P}_2 \\ \delta \dot{Q}_1 \\ \delta \dot{Q}_2 \end{pmatrix} = \begin{vmatrix} \frac{\partial \dot{q}}{\partial q} & \frac{\partial \dot{q}}{\partial p} & \frac{\partial \dot{q}}{\partial P_1} & \frac{\partial \dot{q}}{\partial P_2} & \frac{\partial \dot{q}}{\partial Q_1} & \frac{\partial \dot{q}}{\partial Q_2} \\ \frac{\partial \dot{p}}{\partial q} & \frac{\partial \dot{p}}{\partial p} & \frac{\partial \dot{p}}{\partial P_1} & \frac{\partial \dot{p}}{\partial P_2} & \frac{\partial \dot{p}}{\partial Q_1} & \frac{\partial \dot{p}}{\partial Q_2} \\ \frac{\partial \dot{P}_1}{\partial q} & \frac{\partial \dot{P}_1}{\partial p} & \frac{\partial \dot{P}_1}{\partial P_1} & \frac{\partial \dot{P}_1}{\partial P_2} & \frac{\partial \dot{P}_1}{\partial Q_1} & \frac{\partial \dot{P}_1}{\partial Q_2} \\ \frac{\partial \dot{P}_2}{\partial q} & \frac{\partial \dot{P}_2}{\partial p} & \frac{\partial \dot{P}_2}{\partial P_1} & \frac{\partial \dot{P}_2}{\partial P_2} & \frac{\partial \dot{P}_2}{\partial Q_1} & \frac{\partial \dot{P}_2}{\partial Q_2} \\ \frac{\partial \dot{Q}_1}{\partial q} & \frac{\partial \dot{Q}_1}{\partial p} & \frac{\partial \dot{Q}_1}{\partial P_1} & \frac{\partial \dot{Q}_1}{\partial P_2} & \frac{\partial \dot{Q}_1}{\partial Q_1} & \frac{\partial \dot{Q}_1}{\partial Q_2} \\ \frac{\partial \dot{Q}_2}{\partial q} & \frac{\partial \dot{Q}_2}{\partial p} & \frac{\partial \dot{Q}_2}{\partial P_1} & \frac{\partial \dot{Q}_2}{\partial P_2} & \frac{\partial \dot{Q}_2}{\partial Q_1} & \frac{\partial \dot{Q}_2}{\partial Q_2} \end{vmatrix} \begin{pmatrix} \delta q \\ \delta p \\ \delta P_1 \\ \delta P_2 \\ \delta Q_1 \\ \delta Q_2 \end{pmatrix} \tag{4.37}$$

Figure 6 illustrates a reference trajectory $\psi(t)$ and a nearby trajectory $\psi(t) + \delta\psi(t)$ with initial conditions ψ_0 and $\psi_0 + \delta\psi_0$, respectively, that evolve with time yielding the tangent vector $\delta\psi(\psi_0, t)$ in the six-dimensional phase space $(q, p, P_1, P_2, Q_1, Q_2) \in T^1 \times \mathbb{R}^1 \times \mathbb{R}^2 \times T^2$ with its Euclidean norm

$$d(t) = \|\delta\psi(\psi_0, t)\| \quad (4.38)$$

A renormalization procedure due to Benettin, *et al.* (1976) and used by Umeki & Kambi (1989) for parametrically excited surface waves is adopted to avoid overflows and other computation errors that come from the exponential growth of $d(t)$. For computational convenience, the initial norm is chosen to be unity and $\delta\psi$ is renormalized to a norm of unity every $T = 0.1$ seconds. The values for $d(t)$ (4.38) are determined iteratively with a total number of time steps $N = 500$. The Liapunov restart time step is $NT = 50$ seconds. The largest Liapunov exponent is (Lichtenberg & Lieberman, p.315, 1992)

$$\mu_1(\psi, \delta\psi) = \lim_{N \rightarrow \infty} \frac{1}{NT} \sum_{i=1}^N \ln d_i \quad (4.38)$$

The results were obtained for the following initial conditions:

$$\psi_0 = \{0, 0, 0.1, 0, 0, 0\} \quad (4.39a)$$

$$\delta\psi_0 = \{0, 1, 0, 0, 0, 0\} \quad (4.39b)$$

and the following numerical values for the dimensionless parameters: $\gamma = 0.25$, $\lambda = 0.5$, $\xi = 24\pi$, $f_1 = 1$, $\beta = 0.45$, $\tau = 0.016$, $b = \pi$. For twenty different values of the new dimensionless damping parameter $0 < \nu \leq 1$ and twenty different values of the dimensionless Floquet parametric forcing parameter $0 < \varepsilon < 1$,

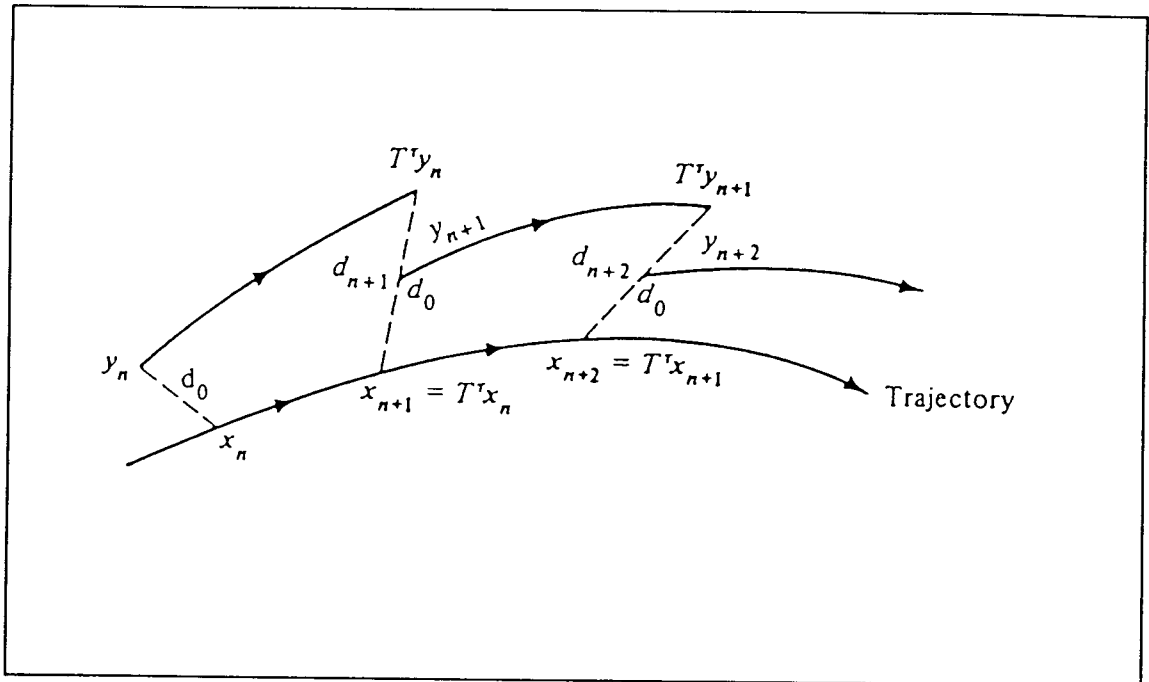


Figure 6. Numerical calculation of the largest Liapunov characteristic exponent (after Benettin et al., 1976). Where $d_0=1$, $x=\psi$, $y=\psi+\delta\psi$, $\tau = 0.1$ seconds.

the largest Liapunov characteristic exponents are calculated and a chaos diagram for the positive values of the largest Liapunov exponents is given in Figure 7. This chaos diagram is useful to search for possible regions of parameters space where chaotic motions may exist. In the parameter space in Figure 7 defined by v as the abscissa and ε as the ordinate, the region in which chaotic motion may occur is wedge-shaped. Inside this wedge, regular motion exists and outside the wedge chaotic motion exists.

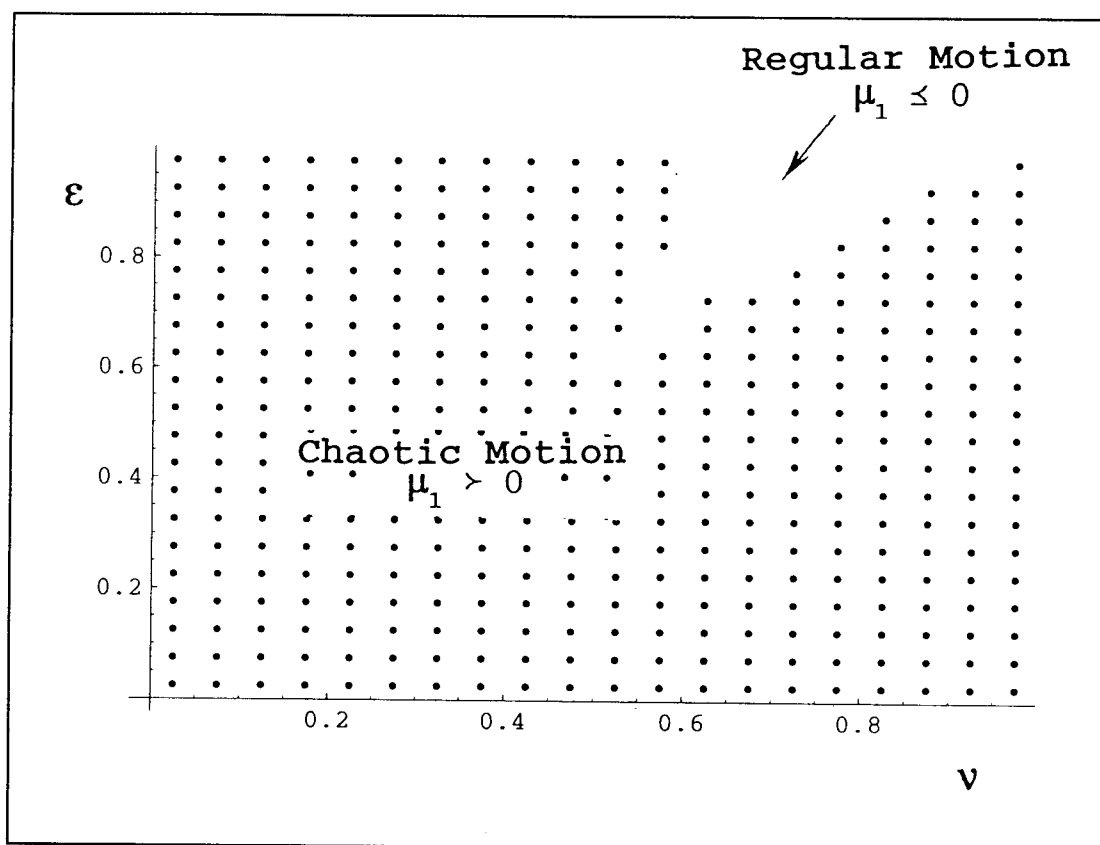


Figure 7. Chaos diagram for the regions in the parameter space (v, ε) where chaotic motion may exist.

4.4. Comparison with Data

Bowline *et al.*, (in press) analyzed parametrically excited cross waves without surface tension or dissipation both theoretically and experimentally. Their mathematical model of cross waves in a rectangular wave channel was based on Luke's Lagrangian formulation (1967). They applied the GMM and found chaos. In order to obtain a suspended system for the application of the GMM, seven canonical transformations were required. In contrast, the application of the generalized Herglotz algorithm (GHA) required only three canonical transformations as a consequence of the

extension of the Herglotz algorithm to nonautonomous dynamical systems that is given in §3.3.

Cross wave experiments were performed by Bowline et al., (in press) at the O.H. Hinsdale Wave Research Laboratory at Oregon State University. The channel is 12 ft wide, 12 ft deep, and approximately 300 ft long. Forty experimental runs were recorded and stability diagrams were obtained for modes 1, 2, and 4 that are illustrated in Figures 8, 9, and 10, respectively, where $f_{wm} (= \omega'_p / 2\pi)$ and $S (= a'_w)$ = wavemaker forcing frequency and stroke, respectively. The dotted lines in the stability diagrams (Figures 8, 9, and 10) represent an estimation of the neutral stability curves for each mode; and the number

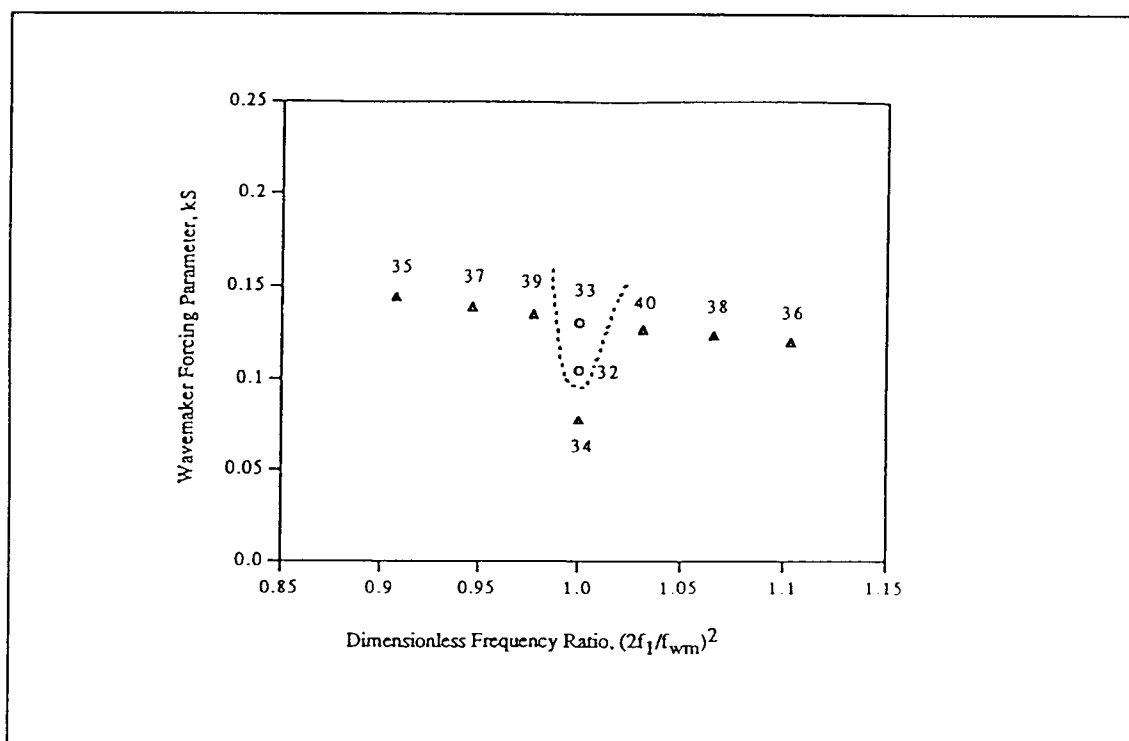


Figure 8. Stability diagram for mode 1 cross waves. Numbers refer to the experiment run numbers for mode 1 cross waves (circles) and no cross waves (triangles) (after Bowline et al., in press).

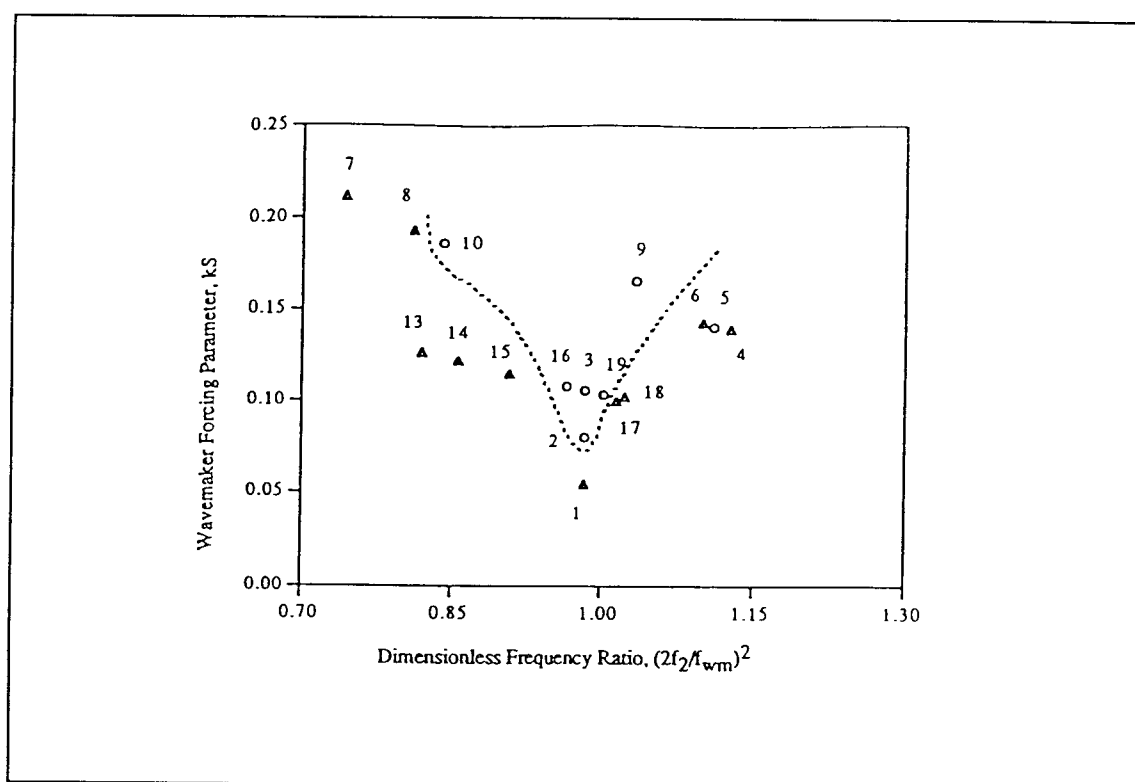


Figure 9. Stability diagram for mode 2 cross waves. Numbers refer to the experiment run numbers for mode 2 cross waves (circles) and no cross waves (triangles) (after Bowline et al., in press).

beside each data point indicates the run number of the experiment. The uncertainty in the location of the neutral stability curve that was reported by Underhill, et al., (1991) may also be observed in these experimental data. These experiments show that the radiation stress of the progressive waves will generate parametrically cross waves if the following two conditions are met: (1) some minimum amplitude of the wavemaker forcing a'_w is exceeded, and (2) the wavemaker frequency ω'_p is in some narrow bandwidth about $2\omega'_c$.

The vertices of the neutral stability curves in Figures 8, 9, and 10 are elevated above the horizontal axis of zero perturbation (wavemaker forcing) parameter γ that is

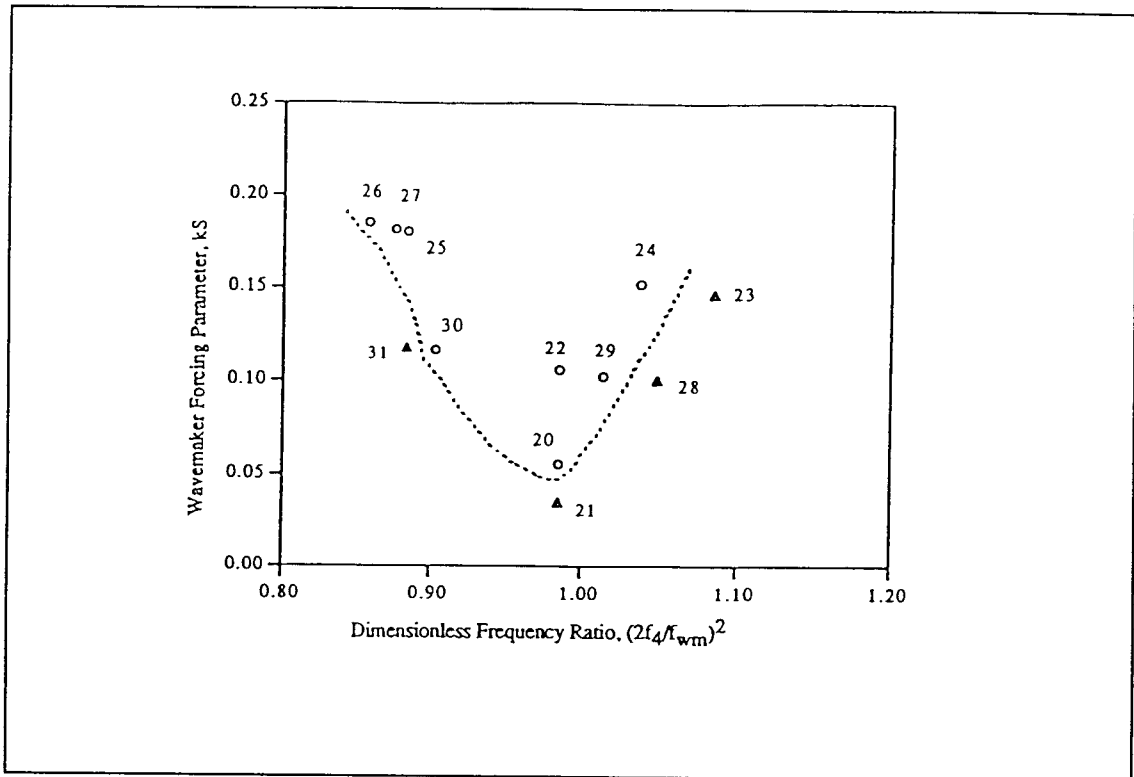


Figure 10. Stability diagram for mode 4 cross waves. Numbers refer to the experiment run numbers for mode 4 cross waves (circles) and no cross waves (triangles) (after Bowline et al., in press).

proportional to the Floquet parametric forcing parameter ε (vide §1). This elevation motivated the inclusion of dissipation effects in the mathematical model of parametrically excited cross waves in a rectangular wave channel (vide §2.1). The experiments performed by Bowline et al., (in press) tested the hypothesis that parametrically excited cross waves by Floquet parametric forcing are chaotic. Experimental evidence of chaos may be obtained by identifying certain characteristics of chaotic motion; viz., sensitivity to initial conditions and increasing complexity of regular motions as some parameter is changed (Moon, 1992). These two characteristics of

chaotic motion may be evaluated analytically by computing the largest Liapunov exponent (*vide* §4.3.4).

The sensitivity to initial conditions that could not be evaluated in the wave channel has been evaluated by finding positive Liapunov exponents of the perturbed dissipative system with surface tension. Increasing complexity of regular motions as the Floquet parametric forcing parameter is changed could be evaluated experimentally by Bowline *et al.*, (*in press*). Outside the neutral stability curves shown in Figures 8, 9, and 10, the motion is a regular progressive wave with no cross wave. Crossing the neutral stability curves either by slightly varying the wavemaker amplitude or frequency results in a more complex system when the cross wave is parametrically excited. Increasing complexity of regular motions as the Floquet parametric forcing parameter ϵ and the new dimensionless damping parameter ν are changed has been evaluated by finding positive Liapunov exponents for some range of ϵ and ν of the perturbed dissipative system with surface tension. The chaos diagram in Figure 7 is useful to search for regions in the $(\nu-\epsilon)$ parameter space at which the motion may be chaotic.

4.5. Conclusions

Conclusions for the application of the GMM to the perturbed Hamiltonian system $\alpha=0$ and $\gamma>0$ with surface tension (§4.2) and the perturbed dissipative system $\alpha>0$ and $\gamma>0$ with surface tension (§4.3) are summarized below.

(1) The dimensionless parameter Γ defined in (2.14f) as the ratio of the progressive wave amplitude to the cross wave amplitude is completely eliminated from the Hamiltonian following the action/angle transformation (3.18) in §3.5b.

Accordingly, the GMM does not depend on the relative amplitudes of the cross waves and the progressive waves.

(2) In the application of the GMM to the perturbed Hamiltonian system $\alpha=0$ and $\gamma>0$ with surface tension (§4.2), the Melnikov integral (4.21) has an infinite number of zeros provided that

$$P_1 > P_2 + \left(\frac{a_1 - \epsilon \Omega}{2 \epsilon a_3} \right)^2 \quad (4.40a)$$

However, at the so-called fixed point of weak chaos

$$P_1 = P_2 + \left(\frac{a_1 - \epsilon \Omega}{2 \epsilon a_3} \right)^2 \quad (4.40b)$$

that is the lowest point on the unperturbed heteroclinic manifold \mathcal{H} shown in Figure 4, the coefficient A (4.15g) that is a function of the long channel parameter ξ (2.13f), of the frequency ratio parameter β (2.14b), of the surface tension parameter τ (2.14d), of the wave-length ratio parameter λ (2.14e), and of the detuning parameter Ω , vanishes. Consequently, the Melnikov integral (4.21a) is identically zero implying that a higher dimensional GMM is necessary in order to demonstrate by the GMM that the motion is chaotic.

(3) At exactly primary resonance (*i.e.*, $\Omega=0$, $\beta=1/2$) chaotic behavior of the cross waves may be detected at any point on the unperturbed heteroclinic manifold \mathcal{H} (Figure 4) except at the fixed point of weak chaos (4.40b) at which the Melnikov integral (4.21a) is identically zero. Consequently, a higher dimensional GMM is necessary in order to demonstrate by the GMM that the motion is chaotic.

(4) For the perturbed Hamiltonian system $\alpha=0$ and $\gamma>0$ with surface tension, the Melnikov integral (4.24) predicts chaotic behavior for any nonzero perturbation (wavemaker forcing) parameter γ because there is no dissipation in the perturbed Hamiltonian system.

(5) With the inclusion of surface tension in Bowline's mathematical model of undamped parametrically excited cross waves in a rectangular wave channel the chaotic motion may still be detected by the GMM.

(6) The elevation of the vertices of the cross waves neutral stability curves estimated by Bowline *et al.*, (in press) (Figures 8, 9, and 10) above the horizontal axis of zero perturbation (wavemaker forcing) parameter γ that is proportional to the Floquet parametric forcing parameter ϵ ; motivated the inclusion of dissipation effects in the mathematical model of parametrically excited cross waves in a rectangular wave channel (*vide* §1 and §2.1).

(7) The application of the GMM to Wiggins' perturbed dissipative System I (Wiggins, 1988) provides a range of the Floquet parametric forcing parameter ϵ and the damping parameter α at which chaos may exist. Although the damping effects are taken into account in the analysis of the perturbed dissipative system $\alpha>0$ and $\gamma>0$ with surface tension, the GMM fails to provide such a range for the system parameters. This is because the fixed point of weak chaos; *i.e.*, the lowest point on the unperturbed heteroclinic manifold \mathcal{H} (Figure 4) is not connected by a homoclinic orbit and it is the only hyperbolic fixed point that survives the averaged equations (4.30) that are restricted to the perturbed hyperbolic invariant manifold $\mathcal{M}_{\gamma\alpha}$. Consequently, the Melnikov integral (4.33) is

identically zero implying that a higher dimensional GMM is necessary in order to demonstrate by the GMM that the motion is chaotic.

5. Recommendations for Further Study

The following are a few directions that future research could take in further theoretical study of the chaotic dynamics of weakly damped parametrically excited cross-waves with surface tension:

(1) *Higher order analysis.* An higher order GMM is necessary for the perturbed dissipative system $\alpha > 0$ and $\gamma > 0$ in §4.3 due to the identically vanishing first order Melnikov integral (4.33). This higher-order analysis will involve more calculus and will require the $O(\epsilon^2)$ terms to be retained in the Taylor series expansion of the wavemaker integral (2.17b) and the free-surface integral (2.17d) in §2.3. Several difficulties are expected with the inclusion of higher order terms. Firstly, including the higher order terms will violate the assumption that the forcing (perturbation) parameter γ is smaller than the Floquet parametric forcing parameter ϵ . Using different scales from the ones used in §2.3. may resolve this difficulty. Secondly, Jones' assumption §1,2 that all $O(\epsilon)$ progressive-wave self-interaction terms may be ignored because they do not contribute to cross wave instability. However, Jones expands to $O(\epsilon^2)$ in his analysis and some $O(\epsilon^2)$ progressive-wave self-interaction result in cross wave instability.

(2) *Dankowicz alternative approach to GMM.* Apply an alternative approach to the GMM due to Dankowicz (1996a,b) that may reduce the amount of calculus involved in higher order calculations. With proper choice for the initial conditions, the variational equations may be solved to obtain analytical expressions for trajectories on the

perturbed manifolds in the form of expansions in the perturbation parameter γ . The distance between the perturbed manifolds may be uniquely defined; and thus provides an alternative approach to the traditional higher dimensional GMM.

(3) *Slow down-wave cross-wave modulation.* There is no x -dependence in the assumed form of the cross wave velocity potential ϕ_c in (2.22a). Several experimental investigations exhibited a down-wave amplitude modulation of the cross wave (Underhill, et al., 1991, and Bowline, et al., in press). Equation (2.22a) may be modified to include a stream-wise modulation. This modification will add more terms to the Lagrangian and the Hamiltonian will probably require a new sequence of canonical transformations.

(4) *Developing more sophisticated techniques.* The KAM theorem and the averaging method that were used for determining the resulting motion on the perturbed normally hyperbolic locally invariant manifold \mathcal{M}_γ and $\mathcal{M}_{\gamma\alpha}$, respectively allow us to find only certain nonresonant motions resulting in trajectories densely filling the surface of the tori $\Upsilon_\gamma(P_1, P_2)$, and $\Upsilon_{\gamma\alpha}(P_1, P_2)$, respectively. If more sophisticated techniques could be developed and applied in the present study this would reveal interesting dynamics that were missed with these two techniques.

Bibliography

- ABRAHAM, R.H. & MARSDEN, J.E. 1978 *Foundation of Mechanics*. Benjamin/Cummings: Reading, MA.
- ABRAHAM, R.H. & SHAW, C.D. 1992 *Dynamics: The Geometry of Behavior*. Second Edition. Addison-Wesley.
- ALLEN, J.S., SAMELSON, R.M., & NEWBERGER, P.A. 1991 Chaos in a model of forced quasi-geostrophic flow over topography: an application of Melnikov's method. *J. Fluid Mech.* 226, 511-547.
- ARNOLD, V.I. 1978 *Mathematical Methods of Classical Mechanics*. Second Edition. Springer-Verlag.
- ARNOLD, V.I. 1983 *Geometrical Methods in the Theory of Ordinary Differential Equations*. Springer-Verlag.
- BARNARD, B.J.S., MAHONEY, J.J. & PRITCHARD, W.G. 1977 The excitation of surface waves near a cut-off frequency. *Phil. Trans. R. Soc. Lond. A* 286, 87-123
- BARNARD, B.J.S. & PRITCHARD, W.G. 1972 Cross-waves. Part 2. Experiments. *J. Fluid Mech.* 55, 245-255.
- BECKER, J.M. & MILES, J.W. 1992 Progressive radial cross-waves. *J. Fluid Mech.* 245, 29-46.
- BENETTIN, G.L., GALGANI, L. & STRELCYN, J.M. 1976 Lyapunov characteristic exponents for smooth dynamical systems and for Hamiltonian systems; A method for computing all of them. Part 2: Numerical application. *Phys. Rev. A* 14, 2338-2347
- BENJAMIN, T.B. & SCOTT, J.C. 1979 Gravity-capillary waves with edge constraints. *J. Fluid Mech.* 92 part 2, 241-267.

BERGE, P., POMEAU, Y. & VIDAL, C. 1984 *Order within Chaos Towards a deterministic approach to turbulence*. John Wiley & Sons.

BL-HAO 1990 *Chaos II*. World Scientific.

BOGOLIUBOV, N.N. & MITROPOLSKY, Y.A. 1961 *Asymptotic Methods in the Theory of Non-Linear Oscillations*. Gordon and Breach Science Publishers.

BOWLINE, C.M., HUDSPETH, R.T. & GUENTHER, R.B. Are cross waves chaotic?. In press.

DANKOWICZ, H. 1996a Looking for chaos. An extension and alternative to Melnikov method. *International Journal of Bifurcation and Chaos*. 6(3), 485-496.

DANKOWICZ, H. 1996b Analytical expressions for stable and unstable manifolds in higher degree of freedom Hamiltonian systems. *International Journal of Bifurcation and Chaos*. 6(11), 1997-2013.

DEAN, R.G. & DARYMPLE, R.A. 1991 *Water Wave Mechanics for Engineers and Scientists*. World Scientific.

DESLOGE, E.A. 1982 *Classical Mechanics*. Volume 2. John Wiley & Sons.

EAGLESON, P.S. & DEAN, R.G. 1966 Small amplitude wave theory. *Estuary and Coastline Hydrodynamics*. Edited by A.T. Ippen. McGraw-Hill Book Co., 1-92.

GARRETT, C.J.R. 1976 On cross-waves. *J. Fluid Mech.* 41, 837-849.

GOLDSTEIN, H. 1980 *Classical Mechanics*. Second Edition. Addison-Wesley.

GRADSHTEYN, I.S. and RYZHIK, I.M. 1980 *Table of Integrals, Series, and Products*. Academic Press.

- GUCKENHEIMER, J. & HOLMES, P. 1983 *Nonlinear Oscillations, Dynamical Systems, and Bifurcations of Vector Fields*. Springer-Verlag.
- GUENTHER, R.B., GOTTSCH, J.A. & KRAMER, D.B. 1996 The Herglotz algorithm for constructing canonical transformations. *SIAM Review*. 38(2), 287-293.
- GUENTHER, R.B. & SCHWERDTFEGGER 1985 *Herglotz. Vorlesungen über die Mechanik der Kontinua*. BSB B.G. Teubner Verlagsgesellschaft, Leipzig.
- HALE, J.K. 1969 *Ordinary Differential Equations*. John Wiley & Sons.
- HELLEMAN, R.H.G. 1980 Self-generated chaotic behavior in nonlinear mechanics. Reprinted in *Universality in Chaos*. Second Edition. Edited by P. Cvitanovic. Institute of Physics Publishing, Bristol and Philadelphia, 1989, 420-488.
- HILDEBRAND, F.B. 1976 *Advanced Calculus for Applications*. Second Edition. Prentice-Hall.
- HOLMES, P. 1986 Chaotic motions in a weakly nonlinear model for surface waves. *J. Fluid Mech.* 162, 365-388.
- HUDSPETH, R.T. & SULISZ, W. 1992 Stokes drift in two-dimensional wave flumes. *J. Fluid Mech.* 230, 209-221.
- JONES, A.F. 1984 The generation of cross-waves in a long deep channel by parametric resonance. *J. Fluid Mech.* 138, 53-74.
- JORDAN, D.W. & SMITH, P. 1987 *Nonlinear Ordinary Differential Equations*. Second Edition. Clarendon Press, Oxford.
- Kambe, T. & Umeki, M. 1990 Nonlinear dynamics of two-mode interactions in parametric excitation of surface waves. *J. Fluid Mech.* 212, 373-393.

- KIT, E. & SHEMER, L. 1989 On neutral stability of cross waves. *Phys. Fluids*. A1 (7), 1128-1132.
- KIT, E. & SHEMER, L. & MILOH, T. 1987 Experimental and theoretical investigation of nonlinear sloshing waves in a rectangular channel. *J. Fluid Mech.* 181, 265-291.
- LANDAU, L.D. & LIFSHITZ, E.M. 1987 *Fluid Mechanics*. Pergamon Press.
- LICHTENBERG, A.J. & LIEBERMAN, M.A. 1983 *Regular and Chaotic Dynamics*. Second Edition. Springer-Verlag.
- LICHTER, S. 1987 Viscous effects on cross-waves, bifurcation, and coupling between modes. *Nonlinear Interactions in Fluids*. Edited by Miksad, Akeylas & Herbert. ASME, New York, AMD-87, 151-156.
- LICHTER, S. & CHEN, J. 1987 Subharmonic resonance of nonlinear cross-waves. *J. Fluid Mech.* 183, 451-465.
- LICHTER, S. & SHEMER, L. 1986 Experiments on nonlinear cross waves. *Phys. Fluids*. 29 (12), 3971-3975.
- LUKE, J.C. 1967 A variational principle for a fluid with a free surface. *J. Fluid Mech.* 27, 395-397.
- MAHONEY, J.J. 1972 Cross-waves. Part 1. Theory. *J. Fluid Mech.* 55, 229-244.
- MELNIKOV, V.K. 1963 On the stability of the center for time-periodic perturbations. *Trans. Moscow Math. Soc.* 12, 1-57.
- MILES, J.W. 1984 Strange attractors in fluid dynamics. *Advanced in Applied Mechanics*, 24, 189-214.
- MILES, J.W. 1988 Parametrically excited standing cross-waves. *J. Fluid Mech.* 186, 119-127.

- MILES, J.W. & BECKER, J. 1988 Parametrically excited, progressive cross-waves. *J. Fluid Mech.* 186, 129-146.
- MILES, J.W. & HENDERSON, D. 1990 Parametrically forced surface waves. *Annu. Rev. Fluid Mech.* 22, 143-165.
- MOON, F.C. 1992 *Chaotic and Fractal Dynamics. An introduction for applied scientists and engineers.* John Wiley & Sons.
- Norris, J.W. 1994 The nonlinear Mathieu equation. *International Journal of Bifurcation and Chaos.* 4, 71-86.
- PARKER, T.S. & CHUA, L.O. 1989 *Practical Numerical Algorithms for Chaotic Systems.* Springer-Verlag.
- RASBAND, S.N. 1990 *Chaotic Dynamics of Nonlinear Systems.* John Wiley & Sons.
- SCHECK, F. 1990 *Mechanics.* Springer-Verlag.
- SHEMER, L. & KIT, E. 1988 Study of the role of dissipation in evolution of nonlinear sloshing waves in a rectangular channel. *Fluid Dynamics Research* 4, 89-105
- SHEMER, L. & KIT, E. 1989 Long-time evolution and regions of existence of parametrically excited nonlinear cross-waves in a tank. *J. Fluid Mech.* 209, 249-263.
- SHEMER, L. & LICHTER, S. 1987 Identification of cross-wave regimes in the vicinity of a cut-off frequency. *Phys. Fluids* 30(11), 3427-3433.
- SMALE, S. 1963 Diffeomorphisms with many periodic points. *In Differential and Combinatorial Topology.* Edited by S. S. Cairns. Princeton University Press. 63-80.

- TSAI, W.T., YUE, D.K.P. & YIP, K.M.K. 1990 Resonantly excited regular and chaotic motions in a rectangular wave tank. *J. Fluid Mech.* 216, 343-380.
- UMEKI, M. & KAMBE, T. 1989 Nonlinear dynamics and chaos in parametrically excited surface waves. *Journal of Physical Society of Japan. Fluid Mech.* 212, 140-154.
- UNDERHILL, W.B., LICHTER, S. & BERNOFF, A.J. 1991 Modulated, frequency-locked, and chaotic cross-waves. *J. Fluid Mech.* 225, 371-394.
- VERHULST, F. 1990 *Nonlinear Differential Equations and Dynamical Systems*. Springer-Verlag.
- WEHAUSEN, J.V. & LAITONE E.V. 1960 Surface Waves. *Encyclopedia of Physics*. Volume IX. Edited by S. Flugge. Springer-Verlag.
- WHITHAM, G.B. 1974 *Linear and Nonlinear Waves*. John Wiley & Sons.
- WIGGINS, S. 1988 *Global Bifurcations and Chaos*. Springer-Verlag.
- WIGGINS, S. 1990 *Introduction to Applied Nonlinear Dynamical Systems and Chaos*. Springer-Verlag.
- WIGGINS, S. & HOLMES, P. 1987 Homoclinic orbits in slowly varying oscillators. *SIAM J. Math Anal.* 18(3), 612-629.
- WOLF, A. 1986 Quantifying chaos with Lyapunov exponents. *Chaos*. Edited by A.V. Holden. Princeton University Press. 273-290.

Appendices

APPENDIX A.

Dimensional Wavemaker Boundary-Value Problem.

Requiring that the independent variation of ϕ' and η' vanish at the arbitrary temporal values t_1' and t_2' in the Hamilton's principle (2.4a) yields the following dimensional boundary value problem with (2.1 and 2.2):

Laplace equation:

$$\bar{\nabla}'^2 \phi' = 0 \quad ; \quad \chi' \leq x' \leq \ell', \quad -b' \leq y' \leq b', \quad -h' \leq z' \leq \eta' \quad (\text{A1})$$

Kinematic free surface boundary condition:

$$\phi'_{z'} = -\eta'_{t'} + \bar{\nabla}' \phi' \cdot \bar{\nabla}' \eta' \quad ; \quad z' = \eta', \quad \chi' \leq x' \leq \ell', \quad -b' \leq y' \leq b' \quad (\text{A2})$$

Dynamical free surface boundary condition:

$$\frac{1}{2} |\bar{\nabla}' \phi'|^2 - \phi'_{t'} + g' \eta' = T' \bar{\nabla}' \cdot (\zeta'^{(-1)} \bar{\nabla}' \eta') + \alpha \sqrt{\frac{g'}{\kappa'}} \frac{D\eta'}{Dt'} \quad ; \quad \begin{cases} z' = \eta', \chi' \leq x' \leq \ell', \\ -b' \leq y' \leq b' \end{cases} \quad (\text{A3})$$

Kinematic fixed-boundary conditions:

$$\bar{\nabla}' \phi' \cdot \hat{n} = 0 \quad ; \quad \begin{cases} y' = |b'|, \quad -h' \leq z' \leq \eta', \quad \chi' \leq x' \leq \ell' \\ z' = -h', \quad -b' \leq y' \leq b', \quad \chi' \leq x' \leq \ell' \end{cases} \quad (\text{A4a,b})$$

Wavemaker kinematic boundary condition:

$$\chi'_{t'} = -\phi'_{x'} + \chi'_{z'} \phi'_{z'} \quad ; \quad x' = \chi', \quad -b' \leq y' \leq b', \quad -h' \leq z' \leq \eta' \quad (\text{A5})$$

Contact line boundary conditions:

$$\bar{\nabla}' \eta' \cdot \hat{n} = 0 \quad ; \quad \begin{cases} x' = \chi', \quad -b' \leq y' \leq b', \quad -h' \leq z' \leq \eta' \\ y' = |b'|, \quad \chi' \leq x' \leq \ell', \quad -h' \leq z' \leq \eta' \end{cases} \quad (\text{A6a,b})$$

APPENDIX B.

Dimensional Linearized Boundary-Value Problem.

The dimensionless boundary-value problem defined by (2.16) may be linearized by expanding the variables in a perturbation series with a perturbation parameter $\epsilon = \kappa' a_c'$. The free-surface and the wavemaker boundary conditions may be expanded in a Taylor series about their mean positions ($x=0, z=0$). Dropping the primes for simplicity, and with (2.1 and 2.2), the dimensional linearized wavemaker boundary-value problem correct to $O(\epsilon)$ is

$$\bar{\nabla}^2 \phi = 0 \quad ; \quad 0 \leq x \leq \ell, y \leq |b|, -h \leq z \leq 0 \quad (\text{B1a})$$

$$\phi_z = -\eta_t \quad ; \quad z = 0, 0 \leq x \leq \ell, y \leq |b| \quad (\text{B1b})$$

$$-\phi_t + g\eta = T(\eta_{xx} + \eta_{yy}) - \alpha \sqrt{\frac{g}{\kappa}} \phi_z \quad ; \quad z = 0, 0 \leq x \leq \ell, y \leq |b| \quad (\text{B1c})$$

$$\phi_y = 0 \quad ; \quad y = |b|, -h \leq z \leq 0, 0 \leq x \leq \ell \quad (\text{B1d})$$

$$\phi_z = 0 \quad ; \quad z = -h, y \leq |b|, 0 \leq x \leq \ell \quad (\text{B1e})$$

$$\phi_x = -\chi_t \quad ; \quad x = 0, y \leq |b|, -h \leq z \leq 0 \quad (\text{B1f})$$

$$\eta_x = 0 \quad ; \quad x = 0, y \leq |b|, -h \leq z \leq 0 \quad (\text{B1g})$$

$$\eta_y = 0 \quad ; \quad y = |b|, 0 \leq x \leq \ell, -h \leq z \leq 0 \quad (\text{B1h})$$

The combined free-surface boundary condition may be determined by eliminating η from the kinematic free-surface boundary condition (B1b) and from the dynamic free-surface boundary condition (B1c) according to

$$\phi_{tt} + g\phi_z = T(\phi_{zxx} + \phi_{zyy}) + \alpha \sqrt{\frac{g}{\kappa}} \phi_{zt} ; \quad z=0, 0 \leq x \leq \ell, y \leq |b| \quad (\text{B2})$$

In addition, a kinematic radiation condition is required at infinity as $x \rightarrow +\ell$ in order to insure that progressive waves be only right progressing or that evanescent eigenmodes be bounded.

The velocity potential ϕ is assumed to be a linear sum of a progressive wave component (subscript p) that is independent of y and a cross wave component (subscript c) that is independent of x given by

$$\phi(x, y, z; t) = \phi_p(x, z; t) + \phi_c(y, z; t) \quad (\text{B3})$$

Substituting (B3) into Laplace equation (B1a) gives the following boundary-value problems for the progressive wave potential ϕ_p and for the cross wave potential ϕ_c :

$$\mathcal{L}^\phi \phi = \mathcal{L}_p^\phi \phi_p + \mathcal{L}_c^\phi \phi_c \equiv 0 \quad (\text{B4a})$$

$$\mathcal{L}_p^\phi \phi_p = 0 ; \quad \mathcal{L}_c^\phi \phi_c = 0 \quad (\text{B4b, c})$$

where the linear operators $\mathcal{L}^\phi \phi, \mathcal{L}_p^\phi \phi_p, \mathcal{L}_c^\phi \phi_c$ are given by

$$\mathcal{L}^\phi \phi = \bar{\nabla}^2 \phi ; \quad \mathcal{L}_p^\phi \phi_p = \phi_{p_{xx}} + \phi_{p_{zz}} ; \quad \mathcal{L}_c^\phi \phi_c = \phi_{c_{yy}} + \phi_{c_{zz}} \quad (\text{B4d-f})$$

The dimensional linearized boundary value problems that govern the progressive wave potential and the cross wave

potential are given by (recall that the primes have been dropped for simplicity)

$$\mathcal{L}_p^\phi \phi_p = 0 \qquad \mathcal{L}_c^\phi \phi_c = 0 \qquad (\text{B5a,b})$$

$$\phi_{p_z} = 0 \quad ; \quad z = -h \qquad \phi_{c_z} = 0 \quad ; \quad z = -h \qquad (\text{B5c,d})$$

$$\phi_{p_x} = -\chi_t \quad ; \quad x=0 \qquad \phi_{c_y} = 0 \quad ; \quad y=|b| \qquad (\text{B5e,f})$$

with the following combined free surface boundary conditions

$$\phi_{p_{tt}} + g\phi_{p_z} - T\phi_{p_{zxx}} - \alpha \sqrt{\frac{g}{\kappa}} \phi_{p_{zt}} = 0 \quad ; \quad z=0 \qquad (\text{B5g})$$

$$\phi_{c_{tt}} + g\phi_{c_z} - T\phi_{c_{zyy}} - \alpha \sqrt{\frac{g}{\kappa}} \phi_{c_{zt}} = 0 \quad ; \quad z=0 \qquad (\text{B5h})$$

Because the boundary conditions are now prescribed at constant values of the independent variables (x,y,z) a solution by separation of variables is suggested according to

$$\phi_p(x, z; t) = X(x) \cdot Z_p(z) \cdot \mathbf{T}_p(t) \qquad (\text{B6a})$$

$$\phi_c(y, z; t) = Y(y) \cdot Z_c(z) \cdot \mathbf{T}_c(t) \qquad (\text{B6b})$$

For the following temporal dependencies for the potentials:

$$\mathbf{T}_p(t) = \exp[-i \omega_p t] \quad ; \quad \mathbf{T}_c(t) = \exp[-i \beta \omega_p t] \quad ; \quad (\text{B7a,b})$$

where $i = \sqrt{-1}$, a kinematic radiation condition may be written as:

$$\lim_{x \rightarrow \pm \infty} \left\{ \frac{\partial}{\partial x} - i k_n \right\} \phi_p = 0 \qquad (\text{B8})$$

A solution for (B6a) that represents all possible values of the separation constant K_p on the real line; viz., $K_p^2 < 0$,

$K_p^2 = 0$, $K_p^2 > 0$ is

$$X = (a_1 x + a_2) + (a_3 \exp[K_e x] + a_4 \exp[-K_e x]) + (a_5 \exp[i K_p x] + a_6 \exp[-i K_p x]) \quad (\text{B9a})$$

$$Z_p = (a_7 z + a_8) + (a_9 \cos[K_e (z+h)] + a_{10} \sin[K_e (z+h)]) + (a_{11} \cosh[K_p (z+h)] + a_{12} \sinh[K_p (z+h)]) \quad (\text{B9b})$$

For no steady flow through the wavemaker the coefficient a_1 in (B9a) must be zero and a_2 may be set to zero without affecting the velocity field (Dean and Darymple, 1991). For a bounded solution as $x \rightarrow +\ell$, $a_3 = 0$. Applying the kinematic radiation condition (B8) $k_n = K_p$ and $a_6 = 0$. Applying the bottom boundary condition (B5c) for (B9b) yields $a_7 = a_{10} = 0$. Combining these results, (B6a) becomes the real part of

$$\begin{aligned} \phi_p(x, z; t) = & A_1 \exp[i(i K_e x - \omega_p t)] \cos[K_e (z+h)] \\ & + A_2 \exp[i(K_p x - \omega_p t)] \cosh[K_p (z+h)] \end{aligned} \quad (\text{B10})$$

The first term in (B10) represents an evanescent eigenmode that decreases exponentially with distance from the wavemaker. The second term in (B10) represents the right-propagating progressive wave.

A solution for (B6b) that represents all possible values of the separation constant K_c on the real line; viz., $K_c^2 < 0$, $K_c^2 = 0$, $K_c^2 > 0$ is

$$Y = (c_1 y + c_2) + (c_3 \cosh[K_c(y-b)] + c_4 \sinh[K_c(y-b)]) + (c_5 \cos[K_c(y-b)] + c_6 \sin[K_c(y-b)]) \quad (B11a)$$

$$Z_c = (c_7 z + c_8) + (c_9 \cos[K_c z] + c_{10} \sin[K_c z]) + (c_{11} \cosh[K_c(z+h)] + c_{12} \sinh[K_c(z+h)]) \quad (B11b)$$

Applying the homogeneous contact line boundary conditions (B5f) for (B11a) gives $c_1 = c_3 = c_4 = c_6 = 0$ and

$$K_{c_n} = n\pi/2b \quad (B11c)$$

Applying the homogeneous boundary condition (B5d) for (B11b) gives $c_7 = c_{12} = 0$. Combining these results, (B6b) becomes the real part of

$$\phi_c(y, z; t) = C_n \exp[-i\beta\omega_p t] \cos[K_{c_n}(y-b)] \cosh[K_{c_n}(z+h)] \quad (B12)$$

Dispersion relationships. Substituting (B7), (B10) and (B12) into the combined free-surface boundary conditions (B5g,h) yields the following dispersion equations:

$$\omega_p^2 = gK_p \left(1 + \frac{TK_p^2}{g}\right) \tanh[K_p h] + i\alpha \sqrt{\frac{g}{\kappa}} K_p \omega_p \tanh[K_p h] \quad (B13a)$$

$$\omega_p^2 = -gK_e \left(1 - \frac{TK_e^2}{g}\right) \tan[K_e h] - i\alpha \sqrt{\frac{g}{\kappa}} K_e \omega_p \tan[K_e h] \quad (B13b)$$

$$\beta^2 \omega_p^2 = gK_{c_n} \left(1 + \frac{TK_{c_n}^2}{g}\right) \tanh[K_{c_n} h] + i\alpha \sqrt{\frac{g}{\kappa}} K_{c_n} \omega_c \tanh[K_{c_n} h] \quad (B13c)$$

The progressive wave wavenumber $k = K_p$ is determined from the progressive wave frequency ω_p using the dispersion relationship (B13a). The evanescent-wave wavenumber $k = K_e$ is determined from the progressive wave frequency ω_p using the dispersion relationship (B13b). The cross wave

wavenumber $\kappa = K_{c_n}$ is determined by the width of the tank (2b) using (B11c) and the nondimensional parameter β may be computed from the dispersion relationship (B13c).

As chaos is assumed to be temporal rather than spatial, the time dependencies of the potentials will be the unknown variables. Consequently, for the case of deep water, the dimensional progressive wave potential (B10) far from the wavemaker may be written as:

$$\phi_p(x, z; t) = [Q_1(t) \cos[K_p x] + Q_2(t) \sin[K_p x]] \exp[K_p z] \quad (\text{B14})$$

and the dimensional cross wave potential (B12) may be written as:

$$\phi_c(y, z; t) = q_n(t) \cos[K_{c_n}(y-b)] \exp[K_{c_n} z] \quad (\text{B15})$$

APPENDIX C.

Coefficients used in (2.13), (2.16), (2.26), and (3.41).

$\tau_1 = \sqrt{1+\tau}$, $\kappa_\tau = \kappa(1+\tau)$	$\tau_\lambda = 1 + (\tau/\lambda^4)$
$f_1 = \int_{-h}^0 f(z) \exp\left[\frac{z}{\lambda^2}\right] dz = \begin{cases} \lambda^2 \left(1 - \exp\left[-\frac{h}{\lambda^2}\right]\right) ; & \text{for a full draft piston,} \\ \frac{\lambda^4}{h} \left(\frac{h}{\lambda^2} - 1 + \exp\left[-\frac{h}{\lambda^2}\right]\right) ; & \text{for a full draft hinge} \end{cases}$	
$a_1 = \left(-\frac{1}{8\beta\xi} + \frac{\beta\tau}{2\xi\lambda^6\tau_1^2}\right)$	$a_2 = \left(-\frac{1}{\beta} + \frac{1}{8\beta\xi} - \frac{\beta\tau}{2\xi\lambda^6\tau_1^2}\right)$
$a_3 = \left(\frac{2\beta\tau^2 - \xi\lambda^4\tau_\lambda(\lambda^2 - \beta\tau)}{8\sqrt{2}b\beta\xi^5\lambda^9\tau_1\tau_\lambda}\right)$	$c_1 = \left(\frac{\sqrt{b}f_1\lambda\tau_1}{4\sqrt{2}\xi\beta^3}\right)$
$c_2 = \left(\frac{2\beta - 1}{4\beta\xi}\right)$	$d_1 = \frac{1}{4} \left(\frac{2}{\tau_1^2} + \frac{\tau - \lambda^4\xi\tau_\lambda}{\beta\lambda^6\xi\tau_\lambda^2}\right)$
$d_2 = \frac{1}{8\sqrt{2}b\beta\xi^3\lambda^3\tau_1^2}$	$d_3 = \frac{\tau(2\tau + \lambda^4\xi\tau_\lambda)}{8\sqrt{2}b\beta\xi^5\lambda^9\tau_\lambda^2}$
$d_4 = \frac{(\tau + \lambda^4\xi\tau_\lambda(\lambda^2 - 1))}{\lambda^6\xi\tau_1\tau_\lambda}$	$d_5 = \frac{(\tau\tau_1^2 - \lambda^2\tau_\lambda)}{2\sqrt{2}b\beta\xi^3\lambda^5\tau_\lambda\tau_1^2}$
$d_6 = \frac{(-\tau + \lambda^4\xi\tau_\lambda)}{4\beta\lambda^6\xi\tau_\lambda^2}$	$d_7 = \frac{1}{4} \left(\frac{-2}{\tau_1^2} + \frac{\tau + \lambda^4\xi\tau_\lambda}{\beta\lambda^6\xi\tau_\lambda^2}\right)$

Appendix D.

Nonautonomous Hamiltonian Components.

The nonautonomous components of the Hamiltonian (3.32a) following the Hamilton-Jacobi transformation in §3.5.c. are

$$H_0(t) = \left[\frac{\beta \tau}{2 \xi \lambda^6 \tau_1^2} + \frac{1}{8 \beta \xi} \right] (P_1 - p) \cos \left(4 Q_1 + \frac{2 t}{\beta} \right) \\ - \left[\frac{\beta \tau}{2 \xi \lambda^6 \tau_1^2} + \frac{1}{8 \beta \xi} \right] P_2 \cos \left(4 (q + Q_1 + Q_2) + \frac{6 t}{\beta} \right) \quad (D1)$$

$$H_e(t) = \frac{\varepsilon (p - P_2) \sqrt{P_1 - p}}{4 \sqrt{2 b \beta \xi^5 \lambda^9 \tau_1 \tau_\lambda}} \left[\begin{aligned} & \left(2 \beta \tau^2 + \xi \lambda^4 \tau_\lambda (\lambda^2 + \beta \tau) \right) \cos \left(2 q + 4 Q_1 + \frac{2 t}{\beta} \right) \\ & - 2 \beta \tau (2 \tau + \xi \lambda^4 \tau_\lambda) \cos \left(2 Q_1 + \frac{t}{\beta} \right) \end{aligned} \right] \\ + \frac{\varepsilon (p - P_2) \sqrt{P_2}}{4 \sqrt{2 b \beta \xi^5 \lambda^9 \tau_1 \tau_\lambda}} \left[\begin{aligned} & 4 \beta \tau (-2 \tau + \xi \lambda^4 \tau_\lambda) \cos \left(2 (q + Q_1 + Q_2) + \frac{3 t}{\beta} \right) \sin^2 \left(q + Q_1 + \frac{t}{2 \beta} \right) \\ & + 2 \lambda^6 \xi \tau_\lambda \sin \left(2 (q + Q_1) + \frac{t}{\beta} \right) \sin \left(2 (q + Q_1 + Q_2) + \frac{3 t}{\beta} \right) \end{aligned} \right] \quad (D2)$$

$$\begin{aligned}
H_Y(t) = & \frac{\gamma \cos\left(\frac{t}{\beta}\right)}{2\beta\lambda^6\xi^2\tau_\lambda} \left[\left(\sqrt{P_1-p} \sin\left(2Q_1 + \frac{t}{\beta}\right) + \sqrt{P_2} \sin\left(2(q+Q_1+Q_2) + \frac{3t}{\beta}\right) \right) \right. \\
& \left((\lambda^2 - \sqrt{\tau}) (2\tau + \xi\lambda^4\tau_\lambda) \sqrt{P_1-p} \cos\left(2Q_1 + \frac{t}{\beta}\right) + \right. \\
& \left. \left. (\lambda^2 + \sqrt{\tau}) (-2\tau + \xi\lambda^4\tau_\lambda) \sqrt{P_2} \cos\left(2(q+Q_1+Q_2) + \frac{3t}{\beta}\right) \right) \right] \\
& - \frac{\gamma}{2\beta\xi} \sin\left(\frac{t}{\beta}\right) \left[\frac{-\beta^2}{\lambda^6\tau_1^2} \left[\begin{aligned} & (\lambda^2 - \sqrt{\tau}) \sqrt{P_1-p} \cos\left(2Q_1 + \frac{t}{\beta}\right) + \\ & (\lambda^2 + \sqrt{\tau}) \sqrt{P_2} \cos\left(2(q+Q_1+Q_2) + \frac{3t}{\beta}\right) \end{aligned} \right]^2 + \right. \\
& \left. \left[\sqrt{P_1-p} \sin\left(2Q_1 + \frac{t}{\beta}\right) + \sqrt{P_2} \sin\left(2(q+Q_1+Q_2) + \frac{3t}{\beta}\right) \right]^2 \right] \\
& + \frac{\gamma\sqrt{B}f_1\tau_1\lambda}{2\varepsilon\sqrt{2\xi\beta^3}} \left[\sqrt{P_2} \left(\sin\left(2(q+Q_1+Q_2) + \frac{4t}{\beta}\right) + \sin\left(2(q+Q_1+Q_2) + \frac{2t}{\beta}\right) \right) \right. \\
& \left. + \sqrt{P_1-p} \sin\left(2Q_1 + \frac{2t}{\beta}\right) \right] \\
& + \left(\frac{\gamma\tau_1^2(1+2\beta)}{4\xi\beta\tau_1^2} \right) (p-P_2) \sin\left(2(q+Q_1) + \frac{2t}{\beta}\right)
\end{aligned}$$

(D3)

Appendix E.

Calculation of the Melnikov Integral.

The Melnikov integral (4.24) in §4.2 is given by

$$M(Q_1(0)) = \cos 2(Q_1(0) + q(0)) [I_1 + I_2 + I_3] \quad (\text{E1a})$$

where the integrals I_i are

$$I_1 = \frac{-2c_1(a_1 - \varepsilon \Omega)}{\varepsilon^2 a_3} \int_{-\infty}^{\infty} \cos(2a_1 t) dt \quad (\text{E1b})$$

$$I_2 = \frac{2c_2 A}{B} \int_{-\infty}^{\infty} \cos(2a_1 t) \operatorname{sech}^2(\sqrt{A}t) dt \quad (\text{E1c})$$

$$I_3 = \frac{-2c_1 \sqrt{A}}{\varepsilon^2 a_3} \int_{-\infty}^{\infty} \sin(2a_1 t) \tanh(\sqrt{A}t) dt \quad (\text{E1d})$$

Each integral component will be discussed separately below.

Component I_1 . The improper integral (E1b) may be evaluated as a limit of sequence of times $T_n = 2\pi n/2a_1$ (Wiggins, p.447, 1988)

$$\begin{aligned} I_1 &= \frac{-2c_1(a_1 - \varepsilon \Omega)}{\varepsilon^2 a_3} \int_{-\infty}^{\infty} \cos(2a_1 t) dt \\ &= \frac{-2c_1(a_1 - \varepsilon \Omega)}{\varepsilon^2 a_3} \lim_{n \rightarrow \infty} \left[\int_{-\frac{\pi n}{a_1}}^{\frac{\pi n}{a_1}} \cos(2a_1 t) dt \right] = 0 \end{aligned} \quad (\text{E2})$$

Component I_2 . The integrand in the improper integral (E1c) is even and I_2 may be written as

$$I_2 = \frac{4 C_2 A}{B} \int_0^{\infty} \cos(2 a_1 t) \operatorname{sech}^2(\sqrt{A} t) dt \quad (\text{E3a})$$

and may be evaluated from Gradshteyn and Ryzhik (p.505, #3.982(1), 1980) to obtain

$$\int_0^{\infty} \cos(2 a_1 t) \operatorname{sech}^2(\sqrt{A} t) dt = \frac{a_1 \pi}{A \sinh \frac{a_1 \pi}{\sqrt{A}}} \quad (\text{E3b})$$

Component I_3 . The integrand in the improper integral (E1d) is even and may be integrated by parts according to

$$\begin{aligned} I_3 &= \frac{-4 C_1 \sqrt{A}}{2 \epsilon^2 a_3} \int_{-\infty}^{\infty} \sin(2 a_1 t) \tanh(\sqrt{A} t) dt \\ &= \frac{-4 C_1 \sqrt{A}}{\epsilon^2 a_3} \int_0^{\infty} \sin(2 a_1 t) \tanh(\sqrt{A} t) dt \\ &= \left[\frac{4 C_1 \sqrt{A}}{\epsilon^2 a_3} \frac{\cos(2 a_1 t)}{2 a_1} \tanh(\sqrt{A} t) \right]_0^{\infty} \\ &\quad - \frac{4 C_1 A}{2 a_1 \epsilon^2 a_3} \int_0^{\infty} \cos(2 a_1 t) \operatorname{sech}^2(\sqrt{A} t) dt \end{aligned} \quad (\text{E4a})$$

The integral in (E4a) may be evaluated from Gradshteyn and Ryzhik (p.505, #3.982(1), 1980) to obtain

$$\int_0^{\infty} \cos(2 a_1 t) \operatorname{sech}^2(\sqrt{A} t) dt = \frac{a_1 \pi}{A \sinh \frac{a_1 \pi}{\sqrt{A}}} \quad (\text{E4b})$$

Consequently, the summation expression in the Melnikov integral (E1a) is bounded and the Melnikov integral

$M(Q_1(0))$ is zero when

$$\cos 2 \left(Q_1(0) + q(0) \right) = 0 \quad (\text{E5a})$$

so that

$$Q_1(0) = \bar{Q}_1(0) = (2n+1) \frac{\pi}{4} - q(0) \quad ; \quad n = 0, 1, 2, \dots \quad (\text{E5b})$$

Appendix F

A Mathematica Program for Calculating the Largest Liapunov Exponent.

```

ve = Table[{i, j}, {i, 0.025, 1, 0.05}, {j, 0.025, 1, 0.05}];
ve[[1]]
n2 = Length[ve[[1]]]
n3 = Length[ve]
ve[[n3]]

n1 = 500 ; q0 = 0 ; p0 = 0 ; P10 = 0.1 ; P20 = 0 ; Q10 = 0 ; Q20 = 0 ;
parameter = {{, }} ; colk = {};
Do[{ collectj = {} ;
Do[{ eqns = { q'[t] == q /. {v -> ve[[k, j, 1]], e -> ve[[k, j, 2]] },
p'[t] == p /. {v -> ve[[k, j, 1]], e -> ve[[k, j, 2]] },
P1'[t] == P1 /. {v -> ve[[k, j, 1]], e -> ve[[k, j, 2]] },
P2'[t] == P2 /. {v -> ve[[k, j, 1]], e -> ve[[k, j, 2]] },
Q1'[t] == Q1 /. {v -> ve[[k, j, 1]], e -> ve[[k, j, 2]] },
Q2'[t] == Q2 /. {v -> ve[[k, j, 1]], e -> ve[[k, j, 2]] },
q[0] == q0, p[0] == p0, P1[0] == P10, P2[0] == P20, Q1[0] == Q10, Q2[0] == Q20 } ;

sol = NDSolve[ eqns , {q, p, P1, P2, Q1, Q2}, {t, 0, 0.1} ] ;

EV = Evaluate[ {q[t], p[t], P1[t], P2[t], Q1[t], Q2[t]} /. sol ] ;
EV1 = EV[[1, 1]] ; EV2 = EV[[1, 2]] ; EV3 = EV[[1, 3]] ;
EV4 = EV[[1, 4]] ; EV5 = EV[[1, 5]] ; EV6 = EV[[1, 6]] ;

in1 = {0} ; in2 = {1} ;
in3 = {0} ; in4 = {0} ; in5 = {0} ; in6 = {0} ; (* norm = 1 *)
out = {} ; Logdsum = 0 ;

Do[ { DE = { w1'[t] == (w1dot /. {v -> ve[[k, j, 1]], e -> ve[[k, j, 2]] }) /.
{q -> EV1,
p -> EV2, P1 -> EV3, P2 -> EV4, Q1 -> EV5, Q2 -> EV6 } ,
w2'[t] == (w2dot /. {v -> ve[[k, j, 1]], e -> ve[[k, j, 2]] }) /.
{q -> EV1,
p -> EV2, P1 -> EV3, P2 -> EV4, Q1 -> EV5, Q2 -> EV6 } ,
w3'[t] == (w3dot /. {v -> ve[[k, j, 1]], e -> ve[[k, j, 2]] }) /.
{q -> EV1,
p -> EV2, P1 -> EV3, P2 -> EV4, Q1 -> EV5, Q2 -> EV6 } ,
w4'[t] == (w4dot /. {v -> ve[[k, j, 1]], e -> ve[[k, j, 2]] }) /.
{q -> EV1,
p -> EV2, P1 -> EV3, P2 -> EV4, Q1 -> EV5, Q2 -> EV6 } ,
w5'[t] == (w5dot /. {v -> ve[[k, j, 1]], e -> ve[[k, j, 2]] }) /.
{q -> EV1,
p -> EV2, P1 -> EV3, P2 -> EV4, Q1 -> EV5, Q2 -> EV6 } ,
w6'[t] == (w6dot /. {v -> ve[[k, j, 1]], e -> ve[[k, j, 2]] }) /.
{q -> EV1,
p -> EV2, P1 -> EV3, P2 -> EV4, Q1 -> EV5, Q2 -> EV6 } ,

```



```

w1[0] == in1[[i]], w2[0] == in2[[i]], w3[0] == in3[[i]],
w4[0] == in4[[i]], w5[0] == in5[[i]], w6[0] == in6[[i]]    };

S  = NDSolve[DE,
            {w1, w2, w3, w4, w5, w6}, {t, 0, 0.1}, StartingStepSize->0.02 ];

W  = Evaluate[{w1[0.1], w2[0.1], w3[0.1], w4[0.1], w5[0.1], w6[0.1]} /. S];

d  = Sqrt[(W[[1, 1]])^2 + (W[[1, 2]])^2 + (W[[1, 3]])^2 +
          (W[[1, 4]])^2 + (W[[1, 5]])^2 + (W[[1, 6]])^2];

w10 = W[[1, 1]]/d ; w20 = W[[1, 2]]/d ; w30 = W[[1, 3]]/d ;
w40 = W[[1, 4]]/d ; w50 = W[[1, 5]]/d ; w60 = W[[1, 6]]/d ;

in1 = Join[in1, {w10}]; in2 = Join[in2, {w20}]; in3 = Join[in3, {w30}];
in4 = Join[in4, {w40}]; in5 = Join[in5, {w50}]; in6 = Join[in6, {w60}];

out = Join[out, {Log[d]}]; Logdsum = Logdsum + out[[i]];
(* Print[in1] *)
(* Print[out] *) , {i, 1, n1}]

LE = (Logdsum)/(n1 (0.1)); (* Print[LE] *)

If[ LE > 0, parameter = Join[parameter, {{ve[[k, j, 1]], ve[[k, j, 2]]}},
(Print["FOUND", " ",
      LE, " ", ve[[k, j, 1]], " ", ve[[k, j, 2]] )]

collectj = Join[collectj, {LE}] ;
(* Print[collectj] *) , {j, 1, n2}]
colk      = Join[colk, {collectj}] ;
(* Print[colk] *) , {k, 1, n3}]

```

Appendix G

Nomenclature

a'_c	Dimensional cross-wave amplitude.
a'_p	Dimensional progressive-wave amplitude.
a'_w	Dimensional amplitude of the wavemaker motion.
A, B	Coefficients defined in (4.15g,h).
b, b'	Dimensionless and dimensional half-width of the wave channel.
dS'	Differential volume or surface.
$d\mathcal{S}'$	Differential surface or line.
$d(t)$	Euclidean norm of the tangent vector $\delta\psi$.
D_1, D_2, D_3	Damping forces.
$\tilde{D}_1, \tilde{D}_2, \tilde{D}_3$	Transformed damping forces.
e	Exponential function.
$f(z)$	Wavemaker shape function.
$F(D\eta/Dt)$	Generalized dissipation function per unit mass density.
f_1	Integral over depth of the wavemaker shape function defined in Appendix C.
F	Generating function of the canonical transformation.
$\bar{\mathbf{F}}', G'$	Vector and scalar functions used in (2.6).
g'	Gravitational acceleration.
g^i	Perturbed components in (4.27).
h, h'	Dimensionless and dimensional still water depth.
h	A small parameter in (1.1).

H	The Hamiltonian following the Legendre transformation, the same notation is also used for the final Hamiltonian.
$H_0, H_\epsilon, H_\gamma$	The free oscillations, nonlinear Floquet parametric forcing, and the perturbed (forced) components of the Hamiltonian, the same notation is also used for the final Hamiltonian.
\tilde{H}	The transformed Hamiltonian following the rotation of axes canonical transformation.
$\tilde{H}_0, \tilde{H}_\epsilon, \tilde{H}_\gamma$	The Hamiltonian components following the rotation of axes canonical transformation.
\hat{H}	The transformed Hamiltonian following the action/angle canonical transformation.
$\hat{H}_0, \hat{H}_\epsilon, \hat{H}_\gamma$	The Hamiltonian components following the action/angle canonical transformation.
\mathcal{H}	Five-dimensional unperturbed homoclinic manifold.
H^γ	Perturbed part of the final Hamiltonian.
i, j, k	Indices.
i	Imaginary unit $\sqrt{-1}$.
I_1, I_2, I_3	Components of the Melnikov integral.
k'	Dimensional wavenumber for the progressive wave.
K	Transformed Hamiltonian (3.7c).
K_{c_n}	Separation constants.
ℓ'	Dimensional length of the wave channel.
L'_c, L'_p	Wavelength for the cross and progressive waves.
\mathcal{L}'	The Lagrangian for a free surface wave with surface tension (2.3a).
L'	The Lagrangian without the zero variation parts.
$L'_{V'}$	The component of L' integrated over the volume.
$L'_{\chi'}, L_\chi$	The dimensional and dimensionless component of L' integrated over the wavemaker surface.

L'_ℓ, L_ξ	The dimensional and dimensionless component of L' integrated over the cross section down the channel.
L'_η, L_η	The dimensional and dimensionless component of L' integrated over the free surface.
L'_T, L_τ	The dimensional and dimensionless component of L' from the surface tension term in \mathcal{L}' (2.3a).
$L_0, L_\varepsilon, L_\gamma$	The free oscillations, nonlinear Floquet parametric forcing, and the perturbed (forced) components of the Lagrangian.
\mathcal{M}	Unperturbed normally hyperbolic invariant manifold.
$\mathcal{M}_\gamma, \mathcal{M}_{\gamma\alpha}$	Perturbed normally hyperbolic invariant manifolds in (4.19), (4.28).
$\mathbf{M}(\mathcal{Q}_1(0))$	Melnikov integral.
$\hat{\mathbf{n}}$	Outward unit normal of the fluid boundary.
N	Integer.
n	mode number of the cross wave.
$\mathbf{p} = p, P_1, P_2$	Conjugate momenta in the original (untransformed) variables and the final variables.
$\tilde{\mathbf{p}} = \tilde{p}, \tilde{P}_1, \tilde{P}_2$	Conjugate momenta following the rotation of axes canonical transformation.
$\hat{\mathbf{p}} = \hat{p}, \hat{P}_1, \hat{P}_2$	Conjugate momenta following the action/angle canonical transformation.
\bar{P}_1, \bar{P}_2	Fixed value for (P_1, P_2)
P_1^*, P_2^*	Fixed value for (P_1, P_2)
\mathbf{p}_{orig}	Original (untransformed) generalized momenta $p_{orig}, P_{1_{orig}}, P_{2_{orig}}$, denoted this way to avoid confusion with the final variables in §3.5.d.
p_h, P_{1h}, P_{2h}	Variables on the homoclinic manifold.
P'	Dimensional total pressure in the fluid.
\mathcal{P}	A point on the unperturbed homoclinic manifold \mathcal{H} .

\hat{P}_1, \hat{P}_2	Constant unit vectors in the P_1, P_2 directions.
(p_0, q_0)	Hyperbolic saddle points (4.3b,d).
$(\mathbf{p}, \mathbf{q}) \Rightarrow (\mathbf{P}, \mathbf{Q})$	A canonical transformation.
$\mathbf{q} = q, Q_1, Q_2$	Generalized coordinates in the original (untransformed) variables and the final variables
$\tilde{\mathbf{q}} = \tilde{q}, \tilde{Q}_1, \tilde{Q}_2$	Generalized coordinates following the rotation of axes canonical transformation.
$\hat{\mathbf{q}} = \hat{q}, \hat{Q}_1, \hat{Q}_2$	Generalized coordinates following the action/angle canonical transformation.
\mathbf{q}_{orig}	Original (untransformed) generalized coordinates $q_{orig}, Q_{1_{orig}}, Q_{2_{orig}}$, denoted this way to avoid confusion with the final variables in §3.5.d.
q_h, Q_{1h}, Q_{2h}	Variables on the homoclinic manifold.
R	Member of the transformed set of variables (§3.2)
$S'_{\pm b}, S'_{-h}, S'_t, S'_\chi, S'_\eta$	Six surface boundaries of the fluid domain.
T'	Positive-definite kinematic surface tension.
T'_c, T'_p	Cross wave and progressive wave periods.
t, t'	Dimensionless and Dimensional time.
t'_1, t'_2	Arbitrary temporal values.
\mathbf{u}'	Dimensional fluid particle velocities.
u, U	N old, new variables (§3.1).
V'_1, V'_2	System configurations at t'_1, t'_2 .
v, V	N old, new variables (§3.1).
W^s, W^u, W^c	Stable, unstable, and center manifolds.
W^s_{loc}, W^u_{loc}	Locally stable and unstable manifolds.
x, x'	Dimensionless and dimensional position down the wave channel, with $x=0$ and $x'=0$ at the equilibrium position of the wavemaker

X_1, X_2, X_3	Herglotz auxiliary functions.
y', y	Dimensionless and dimensional position across the wave channel, with $y=0$ and $y'=0$ at the centerline of the wave channel.
z', z	Dimensionless and dimensional position at depth, with $z=0$ and $z'=0$ at the still water level.
α	Dimensionless dissipation parameter.
β	Dimensionless frequency ratio parameter.
γ	Dimensionless perturbation (forcing) parameter.
Γ	Dimensionless ratio of progressive-wave amplitude to cross-wave amplitude.
δ	Weak dissipation in (1.2).
δ_{ij}	Kronecker delta function.
ε	Dimensionless Floquet parametric forcing parameter
ζ'	Function of the gradient of the free-surface elevation, $\bar{\nabla}'\eta'$ in (2.3c).
η, η'	Dimensionless and dimensional free surface elevation, measured from the still water level.
η_c, η'_c	Dimensionless and dimensional cross-wave free surface elevation.
η_p, η'_p	Dimensionless and dimensional progressive-wave free surface elevation.
η_h^c, η_h^p	Homogeneous solutions.
η_i^c, η_i^p	Inhomogeneous particular solutions.
θ	Rotation angle for the rotation of axes canonical transformation.
κ'	Dimensional wavenumber for the cross wave.
Λ	Coefficient defined in (4.34b).
λ	Dimensionless wavelength ratio parameter.
μ_i	Liapunov characteristic exponents.

ν	Dimensionless parameter relating the dissipation parameter α and the perturbation parameter γ .
ξ	Dimensionless length parameter down the wave channel, $k'\ell'$.
ρ'	Fluid mass density.
σ_1, σ_2	Two independent frequencies of motion on the surface of a two-dimensional torus.
$\sum_{\partial p_i}, \sum_{\partial q_i}$	Summation expressions on the RHS of (3.36).
τ	Dimensionless surface tension parameter.
Υ	Two-dimensional nonresonant invariant torus of the unperturbed system ($\alpha=\gamma=0$).
Υ_γ	KAM two-dimensional torus of the perturbed Hamiltonian system $\alpha=0, \gamma>0$.
$\Upsilon_{\gamma\alpha}$	Two-dimensional torus of the perturbed dissipative system $\alpha>0, \gamma>0$.
ϕ, ϕ'	Dimensionless and dimensional velocity potential.
ϕ_c, ϕ'_c	Dimensionless and dimensional cross-wave velocity potential.
ϕ_p, ϕ'_p	Dimensionless and dimensional progressive-wave velocity potential.
χ, χ'	Dimensionless and dimensional wavemaker position measured from the equilibrium vertical position.
ψ, ψ_0	Reference trajectory and initial conditions.
ψ'	Scalar functions used in (2.6).
$\Psi^{(p_1, p_2)}$	Trajectories along the homoclinic manifold \mathcal{H} .
Ω	Detuning parameter.
ω'_c, ω'_p	Dimensional cross-wave and progressive-wave frequencies.
ω_0	Natural frequency of the pendulum in (1.1).
ω	Half-frequency of the parametric excitation in (1.1).

$O(\cdot)$	Order of magnitude.
$\delta(\cdot)$	The first variation, a derivative of a functional.
$\bar{\nabla}', \bar{\nabla}^{\prime 2}$	Three-dimensional gradient operators.
$D(\cdot)/Dt$	Stokes material derivative.
$T^1 \times \mathbb{R}^1 \times \mathbb{R}^2 \times T^2$	The full six-dimensional phase space.
$N_{\mathcal{P}}$	One-dimensional vector space defined by (4.32).
$ \cdot $	Absolute value of a scalar.
$ \mathcal{A} $	Determinant of any matrix \mathcal{A} .
$ \bar{\mathbf{v}} ^2$	The Dot product $\bar{\mathbf{v}} \cdot \bar{\mathbf{v}}$.
$\ \cdot\ $	Euclidean norm of a vector.
$[\cdot, \cdot]$	Poisson bracket.
$\langle \cdot \rangle$	Average over the dimensionless cross wave period.
\in	a member of.
\ni	such that.
\subset	contained in.
\cap	intersection.